

NOVEL DETECTION APPROACHES FOR  
CAPILLARY ELECTROPHORESIS OF  
POLLUTANTS AND TOXICANTS

By

ARRON KARCHER

Bachelor of Science

University of Central Oklahoma

Edmond, Oklahoma

1994

Submitted to the Faculty of the  
Graduate College of the  
Oklahoma State University  
in partial fulfillment of  
the requirements for  
the Degree of  
DOCTOR OF PHILOSOPHY  
May, 2000

NOVEL DETECTION APPROACHES FOR  
CAPILLARY ELECTROPHORESIS OF  
POLLUTANTS AND TOXICANTS


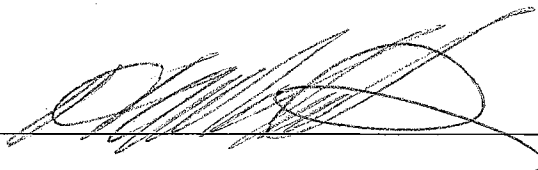
Thesis Approved:



Thesis Advisor



Richard A. Bruce



Wayne B. Powell  
Dean of the Graduate College

## ACKNOWLEDGMENTS

I am very thankful for the many individuals who contributed vast amounts of time towards the completion of this dissertation. First of all, I would like to thank my research advisor, Dr. Ziad El Rassi for his many helpful discussions and professional opinions on a host of complicated issues that compose this thesis. I truly believe that Dr. El Rassi has prepared me for a great career in the separation sciences.

I would like to also acknowledge the members of my graduate committee, Dr. Richard Bunce, Dr. Hassan Melouk, and Dr. Neil Purdie. They have helped foster a great learning experience for me at Oklahoma State University and have greatly contributed to the advancement of my career.

My sincere appreciation is also directed to the members of Dr. El Rassi's research group. I wish the best of luck for the newcomers Eric Wall and Darin Allen, and a special thank you to Tony Tegeler for his patience with me in learning all there practically is to know about computers. As a group, I will never forget all those amusing and fun times on the golf course. I wish all of you continued success and a life of happiness.

Personally, I would like to extend my fullest gratitude to my wife, Becky. I am truly blessed to have someone that has the patience to stay with me during these last four years. Not only have you been there with me from practically the beginning, but you have also graduated from OSU and matured into a wonderful kindergarten teacher. I love

you, and I am very optimistic about our future together with our son and daughter, Colby and Natalee.

To my brother Jeff, I sincerely hope that you finish your undergraduate studies at OSU and attain all of your professional goals. I appreciate all the time we hung out together and the many attempts at hunting. Those were instrumental to me for relief from the rigors of graduate school.

Finally, I would like to dedicate this thesis to my parents Jerry and Carol Karcher. Through your efforts and encouragement, I have been able to fulfill every goal that I have set for myself. You both have been shining examples of the qualities of life that Becky and I strive to obtain. I hope that God will bless our lives as much as he has blessed yours. Thank you very much.

## TABLE OF CONTENTS

Chapter	Page
<b>I. INTRODUCTION TO HIGH PERFORMANCE CAPILLARY ELECTROPHORESIS</b>	
Introduction .....	1
Historical Background and Development .....	3
Basic Principles .....	7
Electrophoretic Migration .....	7
Electroosmotic Flow .....	9
Analytical Parameters .....	14
Migration Time and Apparent Mobility .....	14
Separation Efficiency .....	15
Resolution and Selectivity .....	17
Factors Affecting the Efficiency of Separation in CZE .....	18
Modes of Operation .....	19
General Instrumentation and Capillary .....	23
Sample Injection .....	24
Detection in HPCE .....	26
Conclusions .....	28
References .....	30
<b>II. SUMMARY OF HPCE OF GLUCOSINOLATES AND PESTICIDES- RATIONALE AND SIGNIFICANCE</b>	
Background and Rationale .....	32
Recent Advancements in the CE of Pesticides and Glucosinolates .....	34
CE of Pesticides .....	34
CE of Glucosinolates .....	35
Detection of Pesticides and Glucosinolates in CE .....	35
Conclusion .....	37
References .....	38
<b>III. ANALYSIS OF PYRETHROID INSECTICIDES VIA THEIR HYDROLYSIS PRODUCTS LABELED WITH A FLUORESCING AND UV ABSORBING TAG FOR LIF AND UV DETECTION</b>	
Introduction .....	42

Materials and Methods .....	46
Reagents and Materials .....	46
Capillary Electrophoresis Instruments .....	46
Procedures .....	47
Pyrethroid Hydrolysis .....	47
Precolumn Derivatization .....	48
Results and Discussion .....	50
Hydrolysis .....	50
Precolumn Derivatizaion .....	51
Limit of Detection .....	52
Capillary Electrophoresis with Neutral Surfactant Systems .....	53
Conclusion .....	59
References .....	62

#### IV. EFFECTS OF THE NATURE OF FLUORESCENT LABELS ON THE ENANTIO- SEPARATION OF PESTICIDES AND THEIR DEGRADATION PRODUCTS BY CAPILLARY ZONE ELECTROPHORESIS WITH UV AND LASER INDUCED FLUORESCENCE DETECTION

Introduction .....	64
Materials and Methods .....	66
Reagents and Materials .....	66
Capillary Electrophoresis Instruments .....	67
Procedures .....	68
Pyrethroid Hydrolysis .....	68
Precolumn Derivatization .....	68
Results and Discussion .....	69
OG Micellar System .....	69
Nature of the Fluorescent Tag .....	69
Ionic Strength .....	73
OG Concentration .....	75
OM Micellar System .....	75
Nature of the Fluorescent Tag .....	75
Ionic Strength .....	77
OM Concentration .....	80
Conclusions .....	80
References .....	83

#### V. CAPILLARY ELECTROPHORESIS OF THE FLUORESCENTLY LABELED ACID HYDROLYSIS PRODUCTS OF GLUCOSINOLATES-PROFILING OF GLUCOSINOLATES IN WHITE AND RED CABBAGES

Introduction .....	84
Materials and Methods .....	87
Reagents and Materials .....	87
Capillary Electrophoresis Instruments .....	89
Procedures .....	90
Extraction and Acid Hydrolysis of Glucosinolates from Red and White Cabbages .....	90
Precolumn Derivatization of the Acid Hydrolysis Products of Glucosinolates .....	91
Results and Discussion .....	92
Precolumn Derivatization, Fluorescence Properties and Limits of Detection .....	92
Capillary Electrophoresis with a Neutral Surfactant System .....	97
Capillary Electrophoresis with In-Situ Charged Surfactant System .....	100
Profiling of Glucosinolates in Cabbages .....	103
References .....	109

## VI. DETERMINATION OF INDIVIDUAL GLUCOSINOLATES AND RAPESEED BY LASER INDUCED FLUORESCENCE-CAPILLARY ELECTROPHORESIS VIA THE ENZYMATICALLY RELEASED ISOTHIOCYANATE AGLYCONES

Introduction .....	112
Materials and Methods .....	116
Reagents and Materials .....	116
Capillary Electrophoresis Instrument and Capillary Column .....	117
Sources of GS's .....	117
Extraction of the Intact GS's and Their Isothiocyanate Degradation Products After Treatment with Myrosinase .....	118
Conversion of the Isothiocyanates to Amines by Reaction with 1,2-Benzendithiol .....	118
Conversion of the Isothiocyanates to Amines by Base Hydrolysis .....	119
Labeling of Amines with Dansyl Chloride .....	119
Labeling of Amines with Fluorescein Isothiocyanate .....	120
Results and Discussion .....	120
CE of Isothiocyanates .....	120
Profiling of Isothiocyanates in Fresh Rapeseed Leaves, Roots, and in Fresh White Cabbage .....	122
Comparison of the Two Conversion Schemes of Isothiocyanates to Amines .....	125
Comparison of Two Labeling Procedures .....	127
Quantitative Analysis of the GS Content in the Rapeseed Leaves, Roots, and White Cabbage .....	131
Conclusions .....	135
References .....	137

VII. DETERMINATION OF TOTAL GLUCOSINOLATES IN CABBAGE  
AND RAPESEED BY CAPILLARY ELECTROPHORESIS VIA THE  
ENZYMATICALLY RELEASED GLUCOSE

Introduction .....	139
Experimental .....	144
Reagents and Materials .....	144
Capillary Electrophoresis Instrument and Capillaries .....	144
Sources of GS's .....	145
Procedures .....	145
Extraction of Intact GS's from White Cabbage .....	145
Extraction of Intact GS's from Rapeseed .....	146
Strategy for Determining Total GS Content Via Enzymatically Released Gluconic Acid Labeled with ANDSA .....	146
Results and Discussion .....	148
Profiling of Intact GS's in White Cabbage .....	148
Profiling of Intact GS's in Fresh Rapeseed Leaves and Roots .....	150
Determination of Total GS Concentration Via Enzymatically Released Glucose .....	154
References .....	160



## LIST OF FIGURES

Figure		Page
Chapter I		
1.	Schematics of the Electric Double-Layer at the Surface of the Fused-Silica Capillary and an Illustration of the Electric Double-Layer Potential Gradient .....	11
2.	Schematic Illustrations of EOF Flow Profile, the Ideal CZE Separation Before and After Applying an Electric Field, and a Hypothetical Electropherogram .....	13
3.	Illustration of the Separation of Zones in a Capillary and the Detected Electropherogram for a Single Component in MECC .....	21
4.	Instrumentation Set-up of a Typical Manual Electrophoresis Instrument .....	25
5.	Full and Cross-Sectional View of a Fused-Silica Capillary .....	27
6.	Different Modes of Hydrodynamic Injection in CE .....	29
Chapter III		
1.	Structures of Some Typical Pyrethroids and Their Hydrolytic Reactions Under Basic Conditions .....	49
2.	Electropherograms of the Hydrolytic Products of Pyrethroids Derivatized with ANDSA .....	56
3.	Structures of the Enantiomers of DCA-ANDSA and CA-ANDSA .....	58
4.	Plots of the Effective Electrophoretic Mobility of the ANDSA Derivatives of the Hydrolytic Products Versus OG Concentration .....	60
5.	Electropherograms of the ANDSA Derivatives of the Hydrolytic Products Obtained by LIF Detection .....	61

## Chapter IV

Figure		Page
1.	Electropherograms of the Chiral Separation of the ANSA and ANDSA Derivatives .....	71
2.	Plots of the Alpha and Resolution of the ANSA Derivatized Analytes Versus Sodium Phosphate Concentration at Constant OG Concentration .....	74
3.	Plots of the Alpha and Resolution of ANDSA Derivatized Analytes Versus Sodium Phosphate Concentration at Constant OG Concentration .....	76
4.	Plots of the Alpha and Resolution of ANSA Derivatized Analytes Versus Sodium Phosphate Concentration at Constant OM Concentration .....	78
5.	Plots of the Alpha and Resolution of ANDSA Derivatized Analytes Versus Sodium Phosphate Concentration at Constant OM Concentration .....	79
6.	Electropherograms of ANSA and ANDSA Derivatives .....	81
7.	Electropherogram of 2-PPA Labeled with ANTS .....	82

## Chapter V

1.	General Structure of Glucosinolates and Structures of the Standard Acid Hydrolysis Products .....	85
2.	Reaction Scheme Depicting the Products from the Acid Hydrolysis of a Glucosinolate .....	88
3.	ANDSA Derivatives of the Acid Hydrolysis Products of a Glucosinolate.....	94
4.	Electropherograms of IAA Before and After Derivatization with ANDSA .....	95
5.	Excitation and Emission Spectra for Four ANDSA Derivatized Acid Hydrolysis Products .....	96

Figure	Page
6. Electropherogram of the ANDSA Derivatives of the Acid Hydrolysis Product Standards .....	98
7. Electropherogram of the ANDSA Derivatives of the Acid Hydrolysis Product Standards Obtained by LIF Detection .....	101
8. Plots of the Effective Electrophoretic Mobility of the ANDSA Derivatives as a Function of OG Concentration .....	102
9. Electropherograms of the Extract of White Cabbage Before and After Treatment with Myrosinase .....	105
10. Electropherograms of the ANDSA Derivatives of the Acid Hydrolysis Products from White Cabbage .....	107

#### Chapter VI

1. Degradation of Glucosinolates to Isothiocyanates by Myrosinase and Their Transformation of the Isothiocyanates to Amines Upon Base Hydrolysis .....	113
2. Reaction Schemes for the Conversion of Isothiocyanates to Amines Via Base Hydrolysis or 1,2-Benzenedithiol .....	115
3. Electropherogram of the Separation of the Standard Isothiocyanates .....	121
4. Profiling of the Isothiocyanates in Rapeseed Leaves, Roots and in White Cabbage .....	123
5. Electropherograms of the Standard Amines Labeled With Dns-Cl or FITC .....	129
6. Electropherograms of the FITC Labeled Amines from the Glucosinolates in Rapeseed Leaves, Roots and in White Cabbage .....	132

#### Chapter VII

1. General Structure and Enzymatic Degradation of Glucosinolates and the Derivatization of Gluconic Acid .....	140
2. Electropherograms of Glucosinolates in White Cabbage Before and After Myrosinase Treatment .....	149

Figure	Page
3. Electropherograms of Glucosinolates in Rapeseed Leaves Before and After Myrosinase Treatment .....	151
4. Electropherograms of Glucosinolates in Rapeseed Roots Before and After Myrosinase Treatment .....	152
5. Electropherograms of the ANDSA Derivatives of Sinigrin, Glucose and Gluconic Acid Obtained by LIF Detection .....	155
6. Electropherogram of GA-ANDSA from Rapeseed Leaves After Treatment with Glucose Oxidase .....	157
7. Electropherogram of GA-ANDSA from Rapeseed Leaves After Treatment with Myrosinase and Glucose Oxidase .....	158

## LIST OF TABLES

Table	Page
Chapter I	
I. Sources of Zone Broadening in HPCE .....	20
Chapter III	
I. Limits of Detection of the ANDSA Derivatives of the Hydrolytic Products of the Pyrethroids .....	53
Chapter IV	
I. Resolution Values of the ANSA and ANDSA Derivatives .....	72
Chapter V	
I. Percent Derivatized and Limits of Detection of the Acid Hydrolysis Product Standards of the Glucosinolates .....	93
II. Charge-to-Mass Ratios for the ANDSA Derivatives of the Acid Hydrolysis Product Standards .....	97
Chapter VI	
I. Percent Conversion of Isothiocyanates to Amines via Base Hydrolysis and 1,2-Benzenedithiol .....	126
II. Percent Derivatization of the Amines with Dns-Cl and FITC .....	128
III. Amounts of Some Individual GS's in Extracts from White Cabbage, Rapeseed Roots and Rapeseed Leaves Determined Via Their Corresponding Amine Compounds .....	135
Chapter VII	

I. Total Glucosinolate Content in the Sample Matrices in this Study .....	159
---	-----

## LIST OF SYMBOLS AND ABBREVIATIONS

$\alpha$	selectivity
$\delta$	thickness of the double layer
$\varepsilon$	dielectric constant
$\eta$	viscosity of the electrolyte solution
$\kappa$	Debye-Hückel constant
$\mu_{app}$	apparent analyte mobility
$\mu_{eo}$	electroosmotic mobility
$\mu_{ep}$	electrophoretic mobility
$\rho$	surface charge density of the capillary surface
$\sigma_l$	standard deviation of the peak in unit length
$\zeta$	zeta potential
$a$	radius of the ionic species
$D$	diffusion coefficient of the solute
$E$	electrical field strength
$f$	translational resistance
$F_d$	drag force
$F_e$	electrical field force
$I$	ionic strength of the medium
$k'$	retention factor

$l$	length of the separation capillary from the inlet to the detection point
$L$	total length of the separation capillary
$N$	number of theoretical plates
$q$	net charge of a species
$r$	radius of the species
$R_s$	resolution
$t_M$	migration time
$t_{mc}$	migration time of the micelle
$t_0$	migration time of a neutral solute
$V$	external applied voltage
$v_{ep}$	electrophoretic velocity
$w_b$	peak width at the base
$w_h$	peak width at the half-height
$w_i$	peak width at the inflection point
ANDSA	7-amino-1,3-disulfonic acid
ANSA	5-amino-1-naphthalenesulfonic acid
ANTS	8-aminonaphthalene-1,3,6-trisulfonic acid
CA	chrysanthemic acid
CGE	capillary gel electrophoresis
CIEF	capillary isoelectric focusing
CITP	capillary isotachopheresis
CMBA	2-(4-chlorophenyl)-3-methylbutanoic acid
CMC	critical micellar concentration



2,4-CPPA	2-(4-chlorophenoxy)propionic acid
CZE	capillary zone electrophoresis
DCA	dichlorochrysanthemic acid
DCC	dicyclohexylcarbodiimide
Dichlor	2-(2,4-dichlorophenoxy)propionic acid
Dns-Cl	5-dimethylamino-1-naphthalenesulfonyl chloride
EDAC	1-ethyl-3-(3-dimethylaminopropyl) carbodiimide
FITC	fluorescein isothiocyanate
GA	gluconic acid
GC	gas chromatography
GOD	glucose oxidase
GS's	glucosinolates
HCA	hydrocinnamic acid
3-HPA	3-hydroxyphenylacetic acid
4-HPA	4-hydroxyphenylacetic acid
HPCE	high performance capillary electrophoresis
HPLC	high performance liquid chromatography
IAA	indole acetic acid
LIF	laser-induced fluorescence
LOD	limit of detection
MECC	micellar electrokinetic capillary chromatography
3-MPA	3-methoxyphenylacetic acid
4-MPA	4-methoxyphenylacetic acid

MS	mass spectrometry
NANA	<i>N</i> -acetylneuraminic acid
NCS	isothiocyanate
NG	nonylglucoside
OG	octylglucoside
OM	octylmaltoside
4-PA	4-pentenoic acid
PAA	phenylacetic acid
3-PBA	3-phenoxybenzoic acid
3-PBAL	3-phenoxybenzyl alcohol
2-PPA	2-phenoxypropionic acid
SFC	supercritical fluid chromatography
TCCA	2,2,3,3-tetramethylcyclopropanecarboxylic acid
VAA	vinylacetic acid

## CHAPTER 1

### INTRODUCTION TO HIGH PERFORMANCE

### CAPILLARY ELECTROPHORESIS

#### Introduction

Capillary electrophoresis (CE) also known as high-performance capillary electrophoresis (HPCE), is the instrumental version of electrophoresis. This draws similarity to comparing the sophisticated instrumentation of high performance liquid chromatography (HPLC) to that of thin layer chromatography. HPCE is a micro-separation technique combining the high resolving power of electrophoresis and the automation of today's modern chromatographic instrumentation, such as HPLC. In HPCE, the separation of solutes is based on the differential migration of electrically charged molecules or ions by attraction or repulsion in the presence of an applied electric field.

The introduction of HPCE was facilitated by the research trends associated with miniaturizing traditional chromatographic techniques. For instance, the most significant example is that of gas chromatography (GC). Here, the advantages of open-tubular capillaries have virtually eliminated the use of packed columns. Thus, by performing electrophoresis in capillaries (i.e., HPCE), the traditional set up of electrophoresis is

improved and the scope of typical applications has been extended to include small ions and molecules.

During electrophoretic separations, there are two major transport processes that are occurring, separative and dispersive. Separative transports are caused by the free-energy transport experienced by compounds in their physico-chemical environment. The basic separation mechanisms may be dependent on equilibria processes such as adsorption, extraction or ion exchange, or kinetic processes such as electrophoresis and dialysis. The dispersive transport, or bandbroadening, is the sum of processes that contribute and cause the dispersion of the analyte zones about their center of gravity. These processes include but are not limited to diffusion, convection and restricted mass transfer. Therefore, dispersive transport must be controlled in order to prevent the co-migration of peaks even under optimal separative conditions. In this regard, modern HPCE is perhaps the finest example of optimizing both transport mechanisms to yield highly efficient separations.

It should be noted that this dissertation consists of three parts. The first part includes chapters 1 and 2. These chapters provide, (i) an introduction to HPCE, (ii) background on method development for HPCE of pesticides and glucosinolates, and (iii) rationale and significance of the research themes of this dissertation. Chapters 3 and 4 constitute the second part of this dissertation. They introduce novel methods for the chiral and achiral CZE analysis of environmentally important solutes, the pesticides. The third part of the thesis (Chapters 5-7) entails the introduction of HPCE methods for the analysis and quantitation of important naturally occurring compounds, the glucosinolates.

The goal of this chapter is to provide (i) a historical background of the introduction of electrophoresis and its development into today's high performance capillary electrophoresis, and (ii) review the fundamental concepts of electrophoretic separations in fused-silica capillaries, instrumentation, and modes of operation.

### Historical Background and Development

The development of electrophoresis can be traced back to more than a century ago(1). These electrophoretic separations were attempted in solutions as well as various gels. These fundamental investigations led to more complex electrophoresis designs to reduce the amount of convective mixing which was encountered in electrophoretic separation performed in free solutions. These improvements included the addition of stabilizing media such as, agar(2), cellulose powder(3), glass wool(4), paper(5), silica gel(6) and acrylamide(7). Though these investigations provided more insight to electrophoretic processes, they only had moderate success.

The direct forerunner of today's HPCE was developed as an alternative approach to previously applied free solution electrophoresis. Its main emphasis was to alleviate the problems associated with convection in free solution by the use of tubes with small internal diameters. The use of small tubes or capillaries allowed for better dissipation of heat and a more uniform thermal cross-section of the sample within the tube. One of the earliest publications using such tubes or capillaries dates back to 1953 when Edstrom(8) used fine silk fibers of 15  $\mu\text{m}$  internal diameter for the determination of RNA contained within a single cell. This facilitated the development of free zone electrophoresis in open tubes which was first demonstrated by Hjertèn(7) in 1967. Hjertèn's approach involved

rotating tubes with 3 mm internal diameters (i.d.) using high electrical field strength and on-column UV detection for sensing the solutes as they passed across the detection point. Other significant contributions to the development of CE involved using tubes with smaller i.d. such as, Pyrex glass columns combined with potentiometric detection of alkali cations by Virtanen(9) in 1974. Later, Mikkers et al.(10) used a small diameter PTFE column (i.d. 200  $\mu\text{m}$ ) with both UV and conductometric detection for the determination of inorganic and organic anions. Despite the giant strides that were taken during this time, CE was still not recognized as a powerful analytical technique until major improvements in detection schemes and sample loading techniques occurred during the 1980s.

These complicating and challenging issues were solved in 1981 when Jorgenson and Lukacs(11) solved the intricate problems of injection and detection in CE by using 75  $\mu\text{m}$  i.d. fused-silica capillaries for the separation of amino acids and peptides with on-column fluorescence detection. This was a major advancement in CE in terms of separation efficiency and sensitivity, and marked the commencement of the modern era of HPCE.

Soon after, several other modes of CE were introduced. Gel electrophoresis was adapted to the capillary format(12) as well as isoelectric focusing(13). However, Cohen and Karger(14) are credited as the first researchers to demonstrate highly efficient separations by capillary gel electrophoresis. In 1984, Terabe *et al.*(15) described a new form of electrophoresis called micellar electrokinetic capillary chromatography (MECC). This new technique allowed the chromatographic separation of neutral as well as charged molecules *via* their differential partitioning into a charged micelle acting as a “pseudo-

stationary” phase. As a result of the introduction of this technique as well as other electrokinetic capillary techniques, such as ligand exchange(16), ion exchange(17) and use of cyclodextrins(18), a wide variety of molecules, previously inseparable by electrophoresis, could be analyzed.

Solute detection was one final major concern of HPCE that was also addressed in the 1980's. Walbroehl and Jorgenson(19) introduced an improved UV detector that helped overcome some of the serious limitations of the short path length as dictated by the i.d. of the capillary. The detector developed had a “slit” width of only 100  $\mu\text{m}$ , thus providing a very good spatial resolution. It was linear over four orders of magnitude with detection limits as low as 15 pg for isoquinoline. Detection limits could be further lowered to attomole levels by employing laser-induced fluorescence (LIF) detection schemes(20). Interfacing HPCE with the mass spectrometer for on-line detection again proved to be another powerful addition(21), while Wallingford and Ewing(22) developed a sensitive electrochemical detector, permitting the measurement of catecholamines in a single snail neuron. Finally, the adaption of an indirect detection scheme to CE allowed for the monitoring of solutes that neither absorbed nor fluoresced(23). More recently, detection of solutes have been improved through the use of specially designed capillaries that are used to extend the optical pathway without increasing overall capillary area. These advancements brought forth improved detection of solutes without increasing the generated current and subsequent heating within the capillary. Of particular interest is the bubble cell design, which offers a unique method to extend the pathway with nearly no degradation of separation efficiency. It is made by forming an expanded region, a bubble, directly within the capillary. This capillary is commercially available from

Hewlett-Packard with a three times expansion. Furthermore, up to 15 times radial expansion has been demonstrated by glass-blowing(24). One of the latest improvements in detection through increasing the path length in CE is the use of a Z-shaped capillary cell(25), with measurement along the long axis of the capillary. However, unlike the bubble cell, band broadening in the “Z” capillary is a significant problem, since the absorbance is integrated along the long axis of the capillary. If a second band enters the long axis before the first band leaves, the peaks will overlap, thus degrading the separation efficiency.

One significant problem that restricted the applicability of CE in its early days was that of protein interaction with the capillary wall. This was addressed through several means. Early on, researchers developed the use of treated capillaries(26) in 1985. Other approached the problem by adjusting the buffer conditions and compositions that reduce the electrostatic interactions between the solute and capillary wall. This allowed the separation of proteins on untreated capillaries(27). Based on these and later related developments(28-31), solute-wall interactions have been drastically reduced allowing for highly efficient separation of charged proteins.

Through successful efforts of the 1980's, an increased interest has grown in HPCE with the first commercial instrument available in 1988. Since then, over six companies now market automated HPCE instruments. Thus, HPCE has been transformed into a powerful new microseparation (or nanoseparation) technique for the analysis of neutral and ionic species of varying sizes. HPCE methodologies are now evident more than ever by the increasing number of national and international meetings dedicated to HPCE.



## Basic Principles

### Electrophoretic Migration

In the presence of an applied electric field, ions in solution will migrate to the electrode of opposite charge. In other words, anions will migrate towards the anode and cations will migrate towards the cathode. In order to maintain electroneutrality, the ionization of water corrects for the loss of the migrating cations and anions. Therefore, in a fluid solution current is carried by cations and anions. The molecular weight of the charge bearing ions ranges from one for a single proton to tens of thousands for large complex ions such as proteins, thus the mobility of the ions is dependent on the charge-to-mass ratios of the ionized solutes. Not only does the mass of the molecules contribute to mobility, but the size and shape of the ions must also be considered. It is dependent on several parameters including molecular weight, three dimensional structure, and sphere of hydration.

Under the influence of an applied external electric field, a charged species experiences a force  $F_e$  which is equal to the product of its net charge  $q$  and the electrical field strength  $E$ :

$$F_e = q \times E \quad (1)$$

$E$  is given by:

$$E = \frac{V}{L} \quad (2)$$

where  $L$  is the total length of the separation capillary and  $V$  is the external applied voltage.  $F_e$  is positive for positively charged ions such that this force pushes them in the

direction of the more negative electrode; the opposite applies to negative ions. Although the electrical force acting on a charged species is supposed to accelerate it, the species are not only affected by this force alone. A drag force opposite to the electrical force is experienced by the species as a result of their movement through the electrolytic buffer. This drag force  $F_d$  is directly proportional to the species electrophoretic velocity  $v_{ep}$ , and is given by:

$$F_d = -f \times v_{ep} \quad (3)$$

where  $f$  is the translational resistance. The frictional resistance for small spherical ions can be expressed by Stoke's Law:

$$f = 6\pi\eta r \quad (4)$$

where  $\eta$  is the viscosity of the electrolyte through which the species are migrating and  $r$  is the radius of the species. The frictional drag is directly proportional to viscosity, size, and electrophoretic velocity. Due to the presence of the frictional drag a charged species is accelerated to a limiting velocity, which is dependent on both  $F_e$  and  $F_d$ . This limiting velocity is called drift velocity, steady-state velocity, or electrophoretic velocity ( $v_{ep}$ ) and is achieved when the acceleration force is balanced by the retarding forces as follows:

$$v_{ep} = \frac{qE}{f} \quad (5)$$

Since the electrophoretic mobility,  $\mu_{ep}$ , is defined as the electrophoretic mobility of the solute per unit field strength, a combination of equation (4) and (5) will give the following mathematical expression for electrophoretic mobility:

$$\mu_{ep} = \frac{v_{ep}}{E} = \frac{q}{6\pi\eta r} \quad (6)$$

Through inspection of equation (6), it is evident that small highly charged species have high mobilities whereas large minimally charged species will experience low mobilities. The magnitude of  $\mu_{ep}$  depends on the net charge on a molecule and its frictional properties (size and shape) as well as the dielectric constant  $\varepsilon$  and the viscosity of the running buffer. The relationship for large molecules or colloids is given by(32):

$$\mu_{ep} = \frac{2\varepsilon\zeta}{3\eta} f(\kappa a) \quad (7)$$

where  $\zeta$  is the zeta potential of the charged species,  $\kappa$  is the Debye-Hückel constant and  $a$  is the radius of the ionic species. The parameter  $f(\kappa a)$  is a constant whose value varies between 1 and 1.5 depending on the shape of the migrating species.

### Electroosmotic Flow

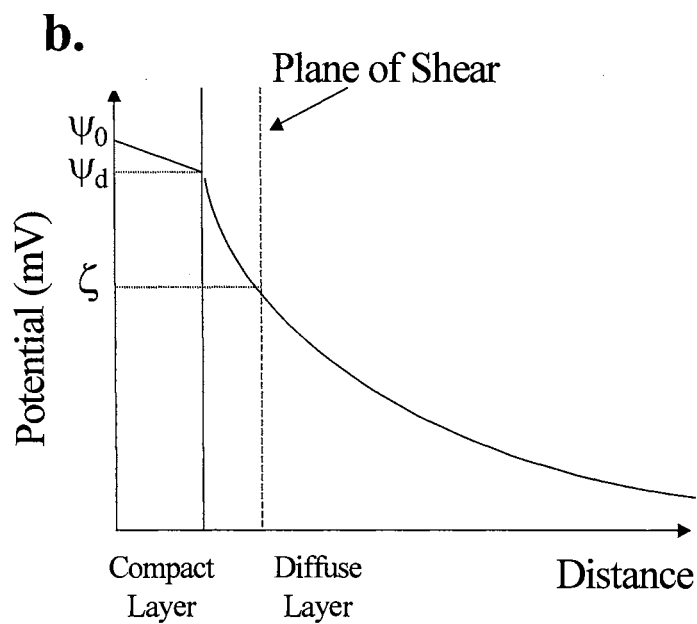
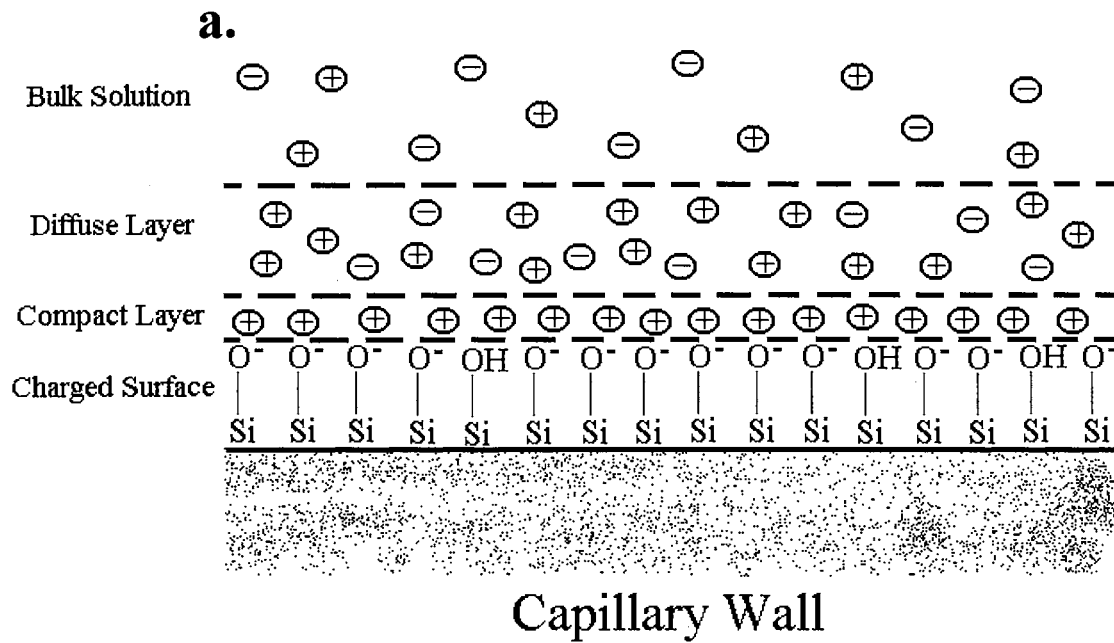
Separations that are performed in HPCE are most often done in capillaries composed of bare fused-silica. The chemistry of fused-silica is widely known and understood. It consists of silanol groups which ionize under most conditions leaving a negatively charged surface. As a result, anionic species will be repelled by the surface and cationic species will be attracted to this surface. Therefore, this repulsion and attraction forms a distribution of charge, which creates a potential gradient inside the capillary. The resulting distribution is shown in Figure 1a. The ions (mostly cations) closest to the capillary surface are tightly bound in a layer that is immobile, called the compact layer. Further towards the interior of the capillary is the diffuse region of the electric double layer. It consists mainly of cationic species and some anionic species. While far from the capillary surface, is the bulk of solution that contains equal amounts of both cationic and anionic species. This overall spatial distribution of ions within the

electrical double-layer, produces an electrical potential gradient originating from the theory according to Stern-Gouy-Chapman(32) and is illustrated in Fig. 1b. From inspection of Fig. 1b, it is noticeable, that the greatest electric potential ( $\psi$ ) is at  $\psi_0$  which is located at the surface of the capillary. From there, a linear decrease in potential is observed when moving across the compact layer, an exponential decay occurs in the diffuse region, and then the potential is drastically reduced in the bulk of the solution. There are certain areas along this potential gradient that are intangible planes that are used to describe the electric double layer.  $\psi_d$  is the electric potential at the interface between the compact layer and the diffuse layer, or the interface between the stagnant layer and the mobile layer.  $\zeta$  is the zeta potential, which is another characteristic used to define the potential at the plane of shear occurring when the liquid is forced to move by an applied external electric field. When an external voltage is applied, the cations forming the diffuse layer are attracted towards the cathode. These cations are solvated, and their movement towards the cathode drags the bulk of the solution towards the cathode. Even though this diffuse layer is approximately only 100-300 Å thick, the flow is transmitted throughout the radial section of the capillary. This is the fundamental electroosmotic flow (EOF) in HPCE. The magnitude of the EOF can be expressed in terms of velocity or mobility(33):

$$v_{eo} = \mu_{eo} E = \frac{\varepsilon \zeta}{4\pi\eta} E \quad (8)$$

where  $\mu_{eo}$  is the electroosmotic mobility. The zeta potential is governed by the surface charge on the capillary wall and is expressed as(34):

$$\zeta = \frac{4\pi\delta\rho}{\varepsilon} \quad (9)$$



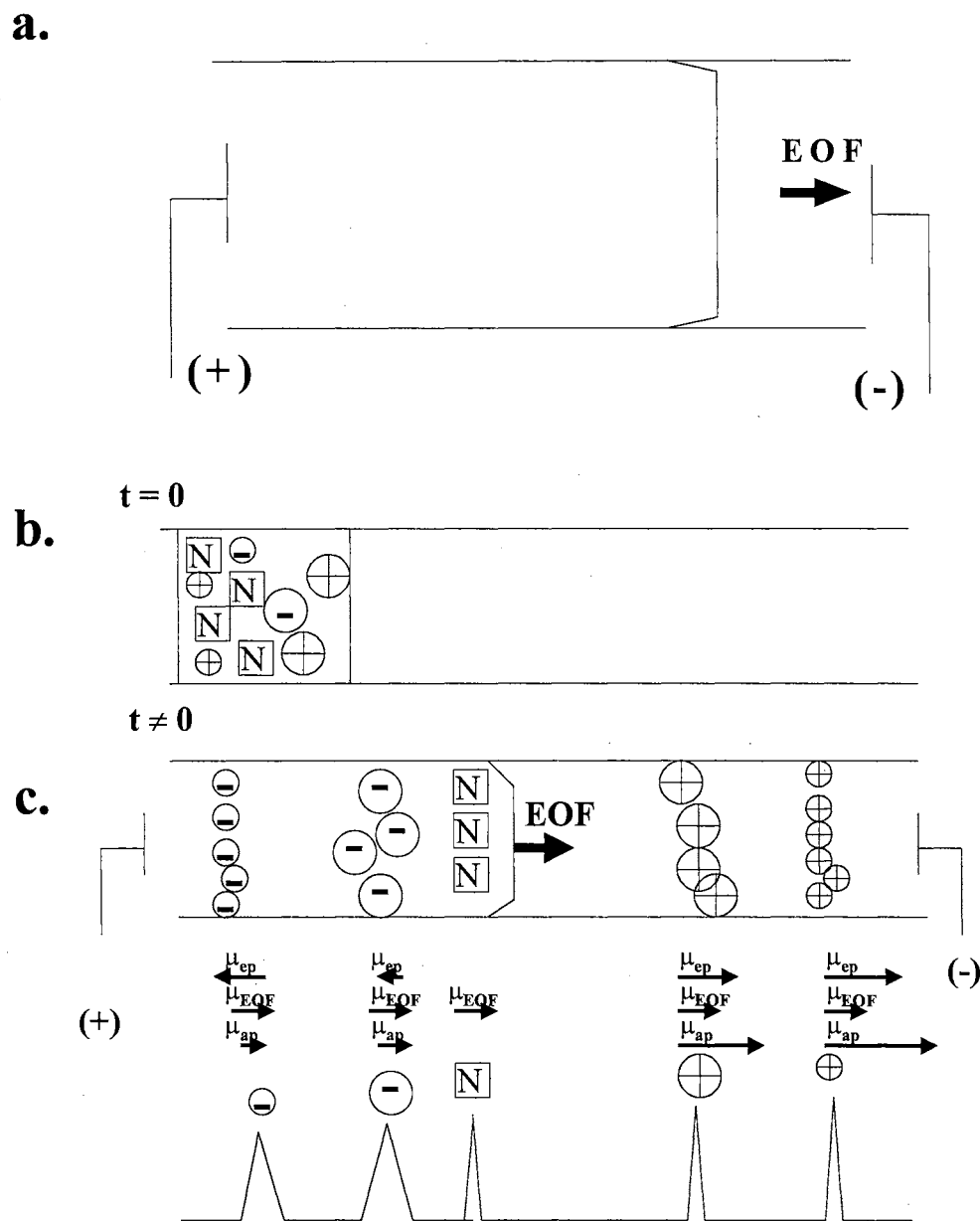
**Figure 1.** Schematic of (a) the electric double-layer at the surface of the fused-silica capillary, (b) the electric double-layer potential gradient

where  $\rho$  is the surface charge density of the capillary surface and  $\delta$  is the thickness of the double layer. By implementing modern electrolyte theory which states that  $\delta$  equals  $1/\kappa$  equation (9) can be arranged to:

$$\zeta = \frac{4\pi\rho}{\kappa\epsilon} \propto \frac{1}{\sqrt{I}} \quad (10)$$

where  $\kappa$  is the Debye-Hückel parameter and  $I$  is the ionic strength of the medium. Therefore,  $\zeta$  which is governed by the surface charge on the capillary wall, is strongly dependent on pH. Therefore, the magnitude of the EOF is pH dependent. At high pH, where the silanol groups are ionized, EOF is significantly greater than at low pH where silanol groups are less ionized. Furthermore,  $\zeta$  is inversely proportional to  $I$  of the electrolyte as proposed in the double-layer theory. An increase in  $I$  compresses the double layer, decreases the zeta potential, and therefore, reduces the EOF.

A unique feature of the EOF is its flat profile. In other chromatographic techniques this is a laminar or parabolic flow profile. The cartoon in Figure 2a depicts the flow of the EOF inside a capillary. Figure 2b and 2c show an ideal CZE separation of positive and negative molecules, as well as the co-migration of all neutral solutes. The cationic species elute passed the detector first, since both the EOF and their effective electrophoretic mobility are in the same direction. Being void of a charge, the neutral analytes co-migrate with the EOF. Finally, the negative solutes whose effective electrophoretic mobility is opposite of the EOF migrate to the detection point. Therefore, cations, anions, and neutrals can be electrophoresed in a single run. The force of the EOF in electrophoretic separations is for the most part beneficial, but it must be controlled. Too strong of an EOF can cause the co-migration of two charged analytes, because the



**Figure 2.** Schematic illustration of EOF flow profile (a) and the ideal CZE separation before (b) and after (c) applying an electric field, and a hypothetical electropherogram.

analytes are pushed off the column before baseline resolution is obtained. Furthermore, other electrophoretic separation methods such as capillary gel electrophoresis, isoelectric focusing, and isotachopheresis will often require a large reduction or elimination of the EOF, and the techniques for reducing the EOF are discussed later in this dissertation.

## Analytical Parameters

### Migration Time and Apparent Mobility

In order for the idealized separation in Fig. 2c to occur, each of the solutes must have a unique apparent mobility ( $\mu_{app}$ ) which is given by:

$$\mu_{app} = \mu_{ep} + \mu_{eo} \quad (11)$$

where  $\mu_{eo}$  is the electroosmotic mobility. Likewise, the apparent velocity ( $v_{app}$ ) of a solute is explained by:

$$v_{app} = v_{ep} + v_{eo} = (\mu_{ep} + \mu_{eo})E = (\mu_{ep} + \mu_{eo})\frac{V}{L} \quad (12)$$

where  $V$  is the applied voltage,  $E$  is the applied electric field and  $L$  is the total length of the capillary. The amount of time the analyte spends in the capillary from the moment of injection to the time of detection is considered the migration time ( $t_M$ ), which is given by:

$$t_M = \frac{l}{v_{app}} = \frac{l}{(v_{ep} + v_{eo})} = \frac{lL}{(\mu_{ep} + \mu_{eo})V} \quad (13)$$

where  $l$  is the length of the capillary from the inlet to the detection point. The difference between  $l$  and  $L$  are illustrated later in this chapter in Figure 5. The migration time,  $t_o$ , of a



neutral solute (i.e., EOF marker) can be expressed in terms of mobility through the following relationship of mobilities and velocities:

$$\mu_{eo} = \frac{v_{eo}}{E} = \frac{IL}{t_o V} \quad (14)$$

Some commonly employed neutral markers are dimethyl sulfoxide, acetone, or mesityl oxide. Therefore, the electrophoretic mobility,  $\mu_{ep}$ , is given by:

$$\mu_{ep} = \mu_{app} - \mu_{eo} = \frac{v_{ep}}{E} = \frac{IL}{V} \left( \frac{1}{t_M} - \frac{1}{t_o} \right) \quad (15)$$

where  $\mu_{app}$  is calculated using the observed migration time of the solute:

$$\mu_{app} = \frac{IL}{t_M V} \quad (16)$$

The direction ( $\pm$  sign) of  $\mu_{ep}$  can be either positive or negative in sign depending on the solutes charge . It is positive for cations and negative for anions.

### Separation Efficiency

The high separation efficiency of HPCE is the consequence of several unrelated factors. First, there is no stationary phase in HPCE. One of the largest sources of band broadening in liquid chromatography (LC) is resistance to mass transfer between the stationary and mobile phases. This mechanism does not operate in HPCE. Likewise, other mechanisms of dispersion (i.e., eddy diffusion and stagnant mobile phase) are unimportant. Secondly, HPCE is not a pressure driven technique. The frictional forces

of the mobile phase in LC interacting at the walls of the capillary result in radial velocity gradients throughout the capillary. This yields the characteristic laminar or parabolic flow pattern. These forces together with the previously mentioned stationary phase considerations result in a substantial pressure drop across the column, causing large amounts of band broadening.

In techniques such as HPCE where electrically driven systems are employed, the EOF is generated uniformly down the entire length of the capillary. Unlike LC, there is no pressure drop across the capillary in HPCE, and the radial flow profile is uniform except very close to the walls where the flow rate approaches zero. Therefore, the separation efficiency in HPCE can be expressed in the number of theoretical plates,  $N$ , which is given by:

$$N = \left( \frac{l}{\sigma_l} \right)^2 \quad (17)$$

where  $\sigma_l$  is the standard deviation of the peak in unit of length. Under ideal conditions, longitudinal diffusion (along the capillary) can be considered to be the only contributor to solute-zone broadening. Thus, through the use of Einstein's law, the efficiency can be related to molecular diffusion:

$$\sigma_l^2 = 2Dt_M = \frac{2DlL}{\mu_{ep}V} \quad (18)$$

where  $D$  is the diffusion coefficient of the solute. By substituting equation (18) into equation (17), the expression of separation efficiency becomes:

$$N = \frac{\mu_{ep}Vl}{2DL} = \frac{\mu_{ep}El}{2D} \quad (19)$$

Usually,  $N$  can be calculated directly from the electropherogram by using the same mathematical equation used in liquid chromatography(35):

$$N = 4\left(\frac{t_M}{w_i}\right)^2 = 5.54\left(\frac{t_M}{w_h}\right)^2 = 16\left(\frac{t_M}{w_b}\right)^2 \quad (20)$$

where  $w_i$ ,  $w_h$ , and  $w_b$  are the peak widths at the inflection point, half-height, and base, respectively.

From these equations (17-20), several trends can be predicted. First, it can be seen that the use of high voltages gives the greatest number of theoretical plates, since the separation is rapid. A rapid separation, minimizes the amount of diffusion until the point where heat dissipation becomes inadequate. Secondly, solutes that are highly mobile produce high plate counts because their rapid velocity through the capillary. Finally, solutes with low diffusion coefficients (e.g., large proteins, DNA, polysaccharides, etc.) give high separation efficiency because of slow diffusional band broadening.

### Resolution and Selectivity

The selectivity,  $\alpha$ , and resolution,  $R_s$ , for two adjacent zones is given by the following expressions:

$$\alpha = \frac{\Delta\mu_{ep}}{\bar{\mu}} = \frac{\Delta\mu_{ep}}{\bar{\mu}_{ep} + \mu_{eo}} \quad (21)$$

and

$$R_s = \frac{1}{4}\sqrt{N}\frac{\Delta\mu_{ep}}{\bar{\mu}} = \frac{1}{4\sqrt{2}}\Delta\mu_{ep}\sqrt{\frac{Vl}{DL(\bar{\mu}_{ep} - \mu_{eo})}} \quad (22)$$

respectively. When  $l = L$ , equation (22) can be simplified to:

$$R_s = \frac{1}{4\sqrt{2}} \Delta\mu_{ep} \sqrt{\frac{V}{D(\bar{\mu}_{ep} - \mu_{eo})}} \quad (23)$$

In the last three equations,  $\Delta\mu_{ep}$  is the difference in the electrophoretic mobilities of the two adjacent zones, and  $\bar{\mu}_{ep}$  is the average electrophoretic mobility of the same adjacent zones. While  $\bar{\mu}$  is the average apparent mobilities of the two adjacent zones. Again, a slight inspection of equation (23) reveals that  $R_s$  approaches infinity when the average electrophoretic mobility becomes equal but opposite in sign to the electroosmotic mobility. Consequently, when this condition is met, the analysis time will also approach infinity. The applied voltage is also another important parameter. The separation efficiency was shown to increase linearly with voltage (see eq. 19), but resolution increases with the square root of voltage.

#### Factors Affecting the Efficiency of Separation in HPCE

It was previously mentioned that in order to derive the equations that yield separation efficiency,  $N$ , it was assumed that only longitudinal diffusion is occurring. Thus, equation (19) does not account for other factors affecting band broadening. Therefore, when calculating  $N$ , equation (20) will yield lower values than what is predicted through theory, since the magnitude of equation (20) is reflective of all band broadening processes that can occur simultaneously during solute migration. Thus, the total variance,  $\sigma_T^2$ , of the observed peak is predicted by:

$$\sigma_T^2 = \sigma_D^2 + \sigma_{\Delta T}^2 + \sigma_i^2 + \sigma_{\Delta ke}^2 + \sigma_w^2 \quad (24)$$

where the variances  $\sigma_D^2$ ,  $\sigma_{\Delta T}^2$ ,  $\sigma_i^2$ ,  $\sigma_{\Delta ke}^2$ ,  $\sigma_w^2$  are the contributions to the total variance from molecular diffusion, Joule heating, injection volume, conductivity differences, and

solute-wall interaction, respectively. Table 1 lists the important contributors to solute-zone broadening in HPCE.

### Modes of Operation

In capillary electrophoresis, there are several modes of operation. Each mode has been developed for specific solutes, thus optimizing the electrophoretic separations. These various modes are (i) capillary zone electrophoresis (CZE), (ii) micellar electrokinetic capillary chromatography (MECC), (iii) capillary gel electrophoresis (CGE), (iv) capillary isoelectric focusing (CIEF), and (v) capillary isotachopheresis (CITP).

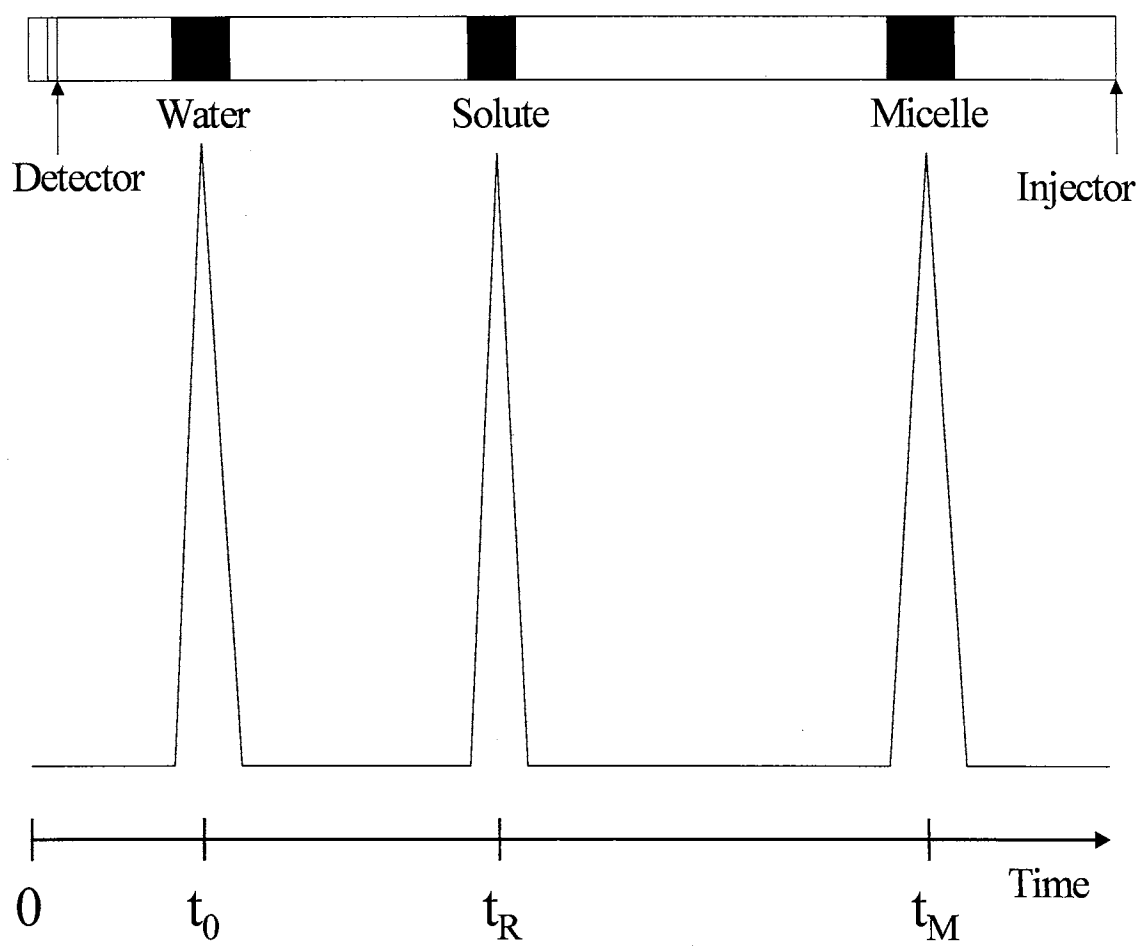
Capillary zone electrophoresis separations are performed in a homogeneous carrier buffer. The basis of the separation lies in the phenomena of discrete solute mobilities originating from their size and charge-to-mass ratios. Using CZE, many separations have been performed for analytes such as small ions, small molecules, peptides, proteins, viruses, bacteria, and colloidal particles.

In MECC, in which the EOF is directed towards the cathode, a negatively charged micelle (i.e., sodium dodecyl sulfate ) is added to the separation buffer, creating a pseudo-stationary phase. These MECC separations are based on the interaction of the solutes with a pseudo-stationary micellar phase. Any ionic surfactants above their critical micellar concentration (CMC) can serve as pseudo-stationary phases. This generates a phase equilibria for a solute, thus separations are based on the solutes differential partitioning into the micelle. Hydrophobic analytes interact stronger with the micelle than do less hydrophobic analytes.

TABLE I.

Sources of Zone Broadening in HPCE.

Source of zone band broadening	Comments
Longitudinal diffusion	<ul style="list-style-type: none"> <li>• Defines the fundamental limit of efficiency. Solutes with lower diffusion coefficients form narrower migration zones</li> </ul>
Joule heating	<ul style="list-style-type: none"> <li>• Leads to temperature gradient and laminar flow</li> </ul>
Injection plug length	<ul style="list-style-type: none"> <li>• Injection length should be less than the diffusion controlled zone lengths</li> <li>• Dilute samples often necessitate longer than ideal injection lengths</li> </ul>
Sample adsorption	<ul style="list-style-type: none"> <li>• Interaction of solutes with capillary walls cause severe peak tailing</li> </ul>
Conductivity differences	<ul style="list-style-type: none"> <li>• Solutes with higher conductivities than the running buffer result in fronted peaks</li> <li>• Solutes with lower conductivities than the running buffer result in tailed peaks</li> </ul>



**Figure 3.** Illustration of the separation of zones in a capillary (upper trace) and the detected electropherogram (lower trace) for a single component in MECC.

In the case of charged solutes, the separation is obtained through incorporation of both the interactions with the micelle and through the solutes own mobility (charge-to-mass ratios). An illustration of a single-component separation is shown in Figure 3. The fundamental equation for the retention factor ( $k'$ ) accounts for the presence of the mobile pseudo-stationary micellar phase. It is a modification of the equation for  $k'$  used in liquid chromatography:

$$k' = \frac{t_R - t_0}{t_0(1 - t_R/t_{mc})} \quad (25)$$

where  $t_{mc}$  is the time of the micelle. As the velocity of the micelle approaches zero,  $t_{mc}$  approaches infinity, thus this equation simplifies to the classical chromatographic expression for the retention factor,  $k'$ . The resolution between two adjacent solutes in MECC is defined by:

$$R_s = \frac{\sqrt{N}}{4} \left( \frac{\alpha - 1}{\alpha} \right) \left( \frac{k'_2}{1 + k'_2} \right) \left( \frac{1 - t_0/t_{mc}}{1 + (t_0/t_{mc})k'_1} \right) \quad (26)$$

like the MECC expression for  $k'$ , the expression for resolution simplifies to the classical chromatographic equation when  $t_{mc}$  approaches infinity.

CGE, has been extremely successful in the analysis of large molecular weight biopolymers. In this CE mode, the solutes are separated on the basis of differences in size as they migrate through the maze of pores in gel-filled capillaries. Since the gel (i.e., polyacrylamide) provides an anticonvective medium, the amount of solute diffusion is drastically reduced and up to 30 million theoretical plates per meter(14) have been reported in CGE type separations.



In CIEF, solutes are separated on the basis of their isoelectric points or pI values(13) in a capillary filled with a pH gradient buffer. Briefly, a sample is mixed with a series of ampholytes known as carrier electrolytes. These carrier electrolytes generate a pH gradient. When an external voltage is applied, the molecules will migrate so long as it is charged. When it becomes neutral in the capillary due to the pH gradient of the carrier electrolyte equaling the pI value of the molecule, it will remain stationary (focused) until a mobilization step is performed which passes the focused molecules in front of a detector.

CITP provides another powerful separation based on distribution of the solutes into continuous but discrete sharp zones in a discontinuous buffer medium. Usually, the solutes are introduced between a leading and terminating electrolyte. The leading buffer is selected so that it has a mobility higher than that of any solutes in the sample. The terminating electrolyte has a mobility less than that of any of the components in the sample. Sample components condense between the leading and terminating electrolytes, producing a steady-state migrating configuration composed of consecutive sample zones. An isotachophergram contains a series of steps, with each step representing an analyte zone where the amount of sample present can be determined from the zone length.

### General Instrumentation and Capillary

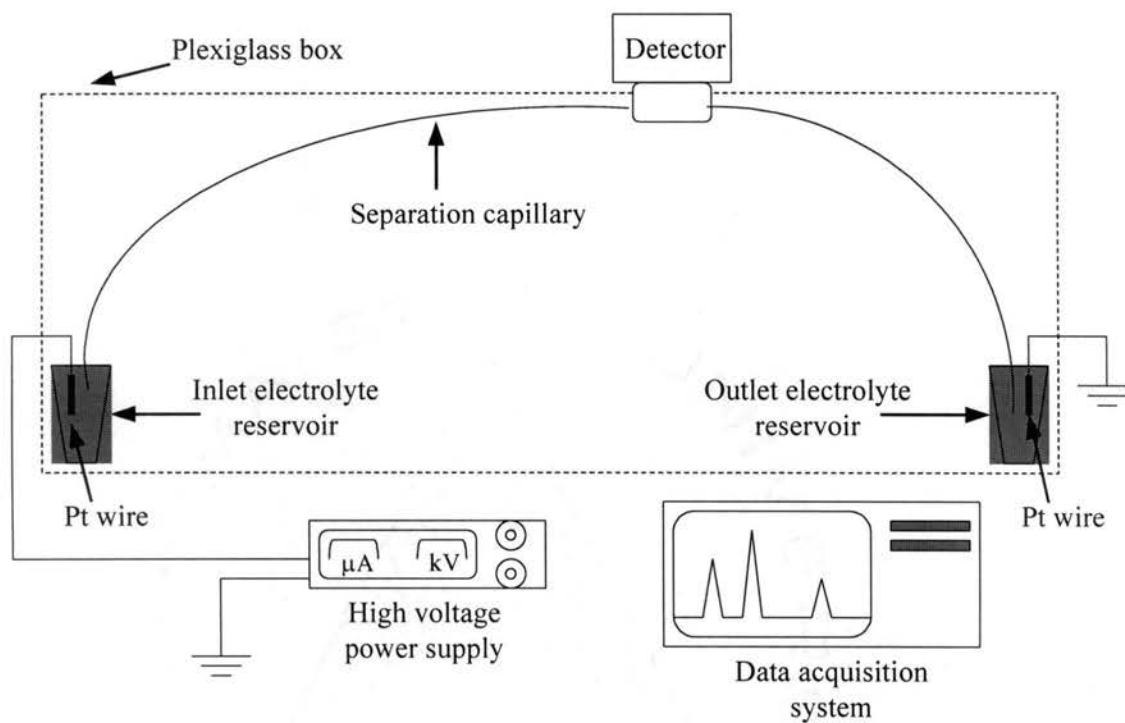
One of the most useful aspects of performing HPCE separations is the simplicity of the instrumental design. A schematic illustration of a basic HPCE instrument is shown in Figure 4. As can be seen from this illustration, all HPCE instruments have five basic parts in common. The first requirement is a high voltage power supply capable of

supplying of up to 30 kV. Secondly, most experiments are performed in a capillary composed of bare fused-silica. A detector is usually placed on-column for UV or fluorescence detection of the solutes, and some form of data acquisition device must also be connected for storing and processing the detected signal. Finally, the capillary and platinum electrodes are contained within a plexiglass box to protect the analyst from the applied high voltage. Upon opening, the lid of the plexiglass box is wired to a switch that will automatically switch off the high voltage. On commercially available instruments, other additional features are available such as temperature control systems, automated sample injection, autosampler, automated capillary flushing system to improve reproducibility, and sophisticated computerized data handling software.

Fused-silica is the main choice for the capillary because the chemistry of fused-silica is well understood and it is also UV transparent. The outside of the capillary is usually coated with a polyimide coating to improve flexibility and durability. A full and cross-sectional view of a fused-silica capillary is illustrated in Figure 5. This coating can be easily removed with heat from a butane lighter or from an electrical wire stripper to expose the fused-silica for an on-column detection window. However, any heat treatment of the capillary damages the capillary wall, so the outer coating of the capillary in this case is removed by using concentrated sulfuric acid at 100 °C. The internal diameter (i.d.) of the capillary ranges from 10-100  $\mu\text{m}$  depending on the precise application.

### Sample Injection

Sample injection in HPCE can be accomplished in one of two ways, (i) hydrodynamic or (ii) electrokinetic methods(36). The most widely used injection

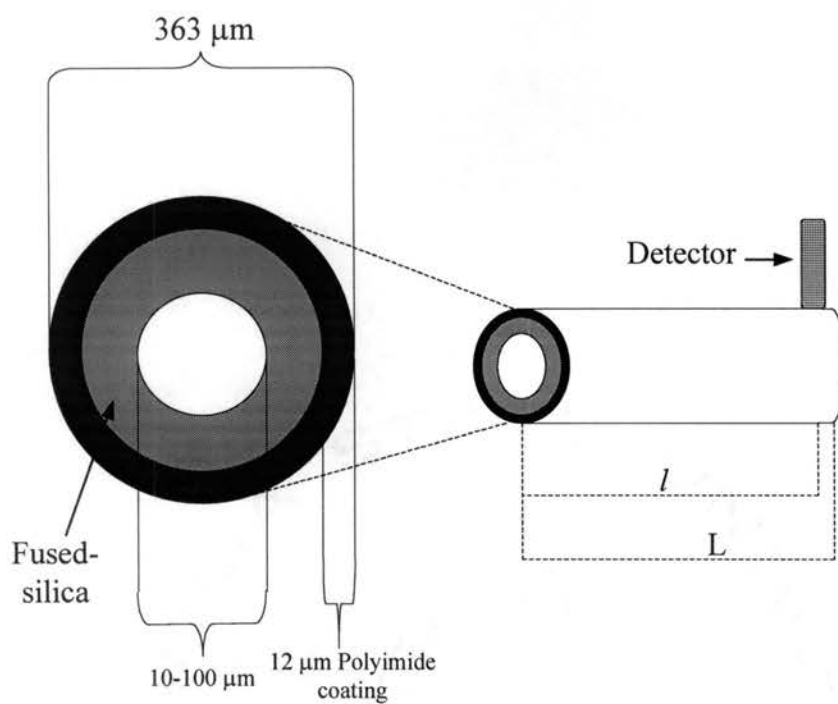


**Figure 4.** Instrumentation set-up of a typical manual electrophoresis instrument.

techniques of the two is hydrodynamic. Hydrodynamic injection can be accomplished by either head-space pressurization, vacuum injection, or gravimetric (siphoning). These three hydrodynamic injection techniques are shown in the cartoon in Figure 6. The gravimetric method is most commonly encountered with manual instruments. The inlet end of the capillary is raised a certain height above the outlet end of the capillary and dipped into the sample container, thus the sample is injected via siphoning. Commercially available instruments utilize both pressure and electrokinetic injection techniques. For electrokinetic injection, the quantity injected is dependent on the ionic strength of the sample matrix. Variation in conductivity, originating from the presence of ions of the electrolyte buffer will result in differences in voltage drop and quantity loaded. Despite these shortcomings, electrokinetic injection is extremely valuable when hydrodynamic techniques are not applicable (i.e., viscous media or gels). Another advantage of electrokinetic injection is the application in concentrating the sample on-column and is called "stacking". This concentration step is achieved with sample solutions having a lower conductivity than the separation buffer. The electric field in the sample zone is greater than that in the capillary which causes the solutes to move through the sample zone at an accelerated velocity until they enter the capillary where they slow down and stack into a narrow solute band. It should be noted that quantification with "sample stacking" can be difficult if the sample composition is not accurately known.

#### Detection in HPCE

Because of the small diameter of the capillary, solute detection in HPCE is a major concern. Though HPCE is considered a micro-separation technique, it is not a



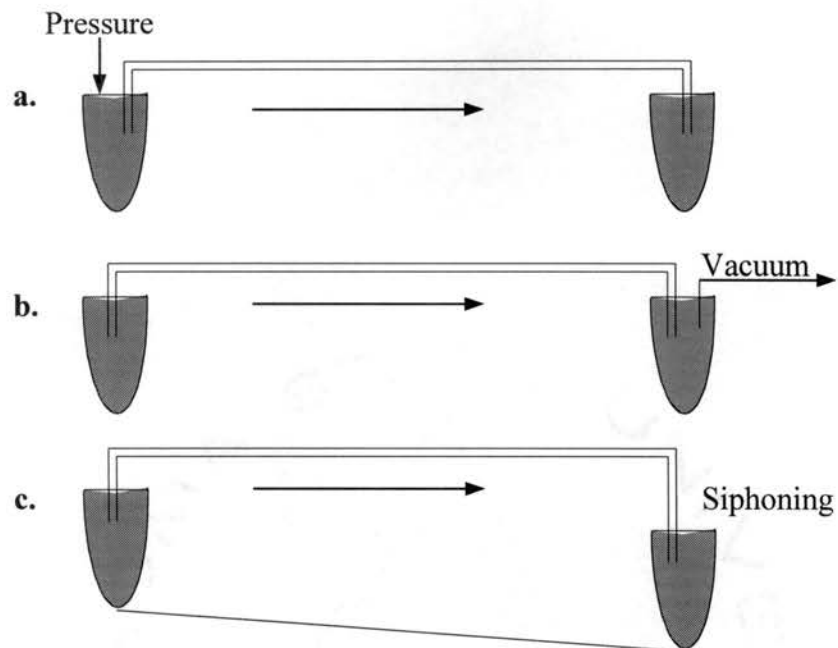
**Figure 5.** Full and cross-sectional view of a fused-silica capillary.  $L$  is the total length of the capillary and  $l$  is the length of the capillary to the detection point.

trace analysis technique. Many of the samples must be pre-concentrated prior to HPCE analysis. Still, the most common detection technique is UV. Gaining fast in popularity is fluorescence detection, in particular laser-induced fluorescence (LIF) detection. This detection scheme has allowed many HPCE methods the ability to analyze samples containing trace or minute amounts of analytes. Other detection techniques that have been performed with HPCE are amperometry, conductivity, mass spectrometry, nuclear magnetic resonance and indirect techniques (i.e., UV, fluorescence, and amperometry)(37-39).

### Conclusions

In summary, this chapter outlined the background, history, and development of modern HPCE. It has also discussed the instrumentation, various modes, basic concepts, as well as the most commonly employed detection systems in HPCE.

Thus, the aim of this dissertation is to exploit the many sound features of HPCE in developing micro-separation methods for the analysis of two important classes of compounds. These were the pesticides and metabolites and glucosinolates and their degradation products.



**Figure 6.** Different modes of hydrodynamic injection: pressure in (a), vacuum in (b), and gravimetric (siphoning) in (c).

## References

1. Smirnow, I. *Berl. Klin. Woch.* **1892**, 32, 645.
2. Field, C. W.; Teague, O. *J. Exp. Med.* **1907**, 9, 86.
3. Porath, J. *Biochem. Biophys. Acta* **1956**, 22, 151.
4. Coolidge, T. B. *J. Biol. Chem.* **1939**, 127, 551.
5. Tiselius, A.; Flodin, P. *Adv. Protein Chem.* **1953**, 8, 461.
6. Consden, R. A.; Gordon, A. H.; Martin, A. J. *Biochem. J.* **1946**, 40, 33.
7. Hjertèn, S. *Chromatogr. Rev.* **1967**, 9, 122.
8. Edstrom, J. E. *Nature* **1953**, 172, 908.
9. Virtanen, R. *Acta. Polytech. Scand.* **1974**, 123, 1.
10. Mikkers, F. E. P.; Everaerts, F. M.; Verheggen, T. P. E. M. *J. Chromatogr.* **1979**, 270, 11.
11. Jorgenson, J.; Lukacs, K. D. *Anal. Chem.* **1981**, 53, 1298.
12. Hjertèn, S. *J. Chromatogr.* **270**, 270, 1.
13. Hjertèn, S.; Zhu, M. D. *J. Chromatogr.* **1985**, 346, 265.
14. Cohen, A. S.; Karger, B. L. *J. Chromatogr.* **1987**, 397, 409.
15. Terabe, S.; Otsuka, K.; Ichikama, K.; Tsuchiya, A.; Ando, T. *Anal. Chem.* **1984**, 56, 111.
16. Gozel, P.; Gossman, E.; Michelsen, H.; Zare, R. N. *Anal. Chem.* **1987**, 59, 44.
17. Terabe, S.; Isemura, T. *Anal. Chem.* **1990**, 62, 650.
18. Terabe, S.; Ozaki, H.; Otsuka, K.; Ando, T. *J. Chromatogr.* **1985**, 332, 211.
19. Walbroehl, Y.; Jorgenson, J. W. *J. Chromatogr.* **1984**, 315, 135.
20. Gassman, E.; Kuo, J. E.; Zare, R. N. *Science* **1985**, 230, 813.



21. Smith, R. D.; Olivares, J. A.; Nguyen, N. T. *Anal. Chem.* **1988**, *60*, 436.
22. Wallingford, R. A.; Ewing, A. G. *Anal. Chem.* **1988**, *60*, 258.
23. Kuhr, W. G.; Young, E. S. *Anal. Chem.* **1988**, *60*, 1832.
24. Xue, Y.; Young, E. S. *Anal. Chem.* **1994**, *66*, 144.
25. Bruin, G. J. M.; Stegeman, G.; Asten, A. C. V.; Xu, X.; Kraak, J. C.; Poppe, H. *J. Chromatogr.* **1991**, *559*, 163.
26. Hjetèn, S. *J. Chromatogr.* **1985**, *347*, 191.
27. Lauer, H.; McManigill, D. *Anal. Chem.* **1986**, *58*, 166.
28. Mechref, Y.; El Rassi, Z. *Electrophoresis* **1995**, *16*, 617-624.
29. Nashabeh, W.; El Rassi, Z. *J. Chromatogr.* **1991**, *559*, 367-383.
30. Smith, J. T.; El Rassi, Z. *J. High Resol. Chromatogr.* **1992**, *15*, 573-580.
31. Smith, J. T.; El Rassi, Z. *Electrophoresis* **1993**, *14*, 396-406.
32. Hunter, R. J. *Zeta Potential in Colloid Science*; Academic Press: London, 1981.
33. Rice, C. L.; Whitehead, R. *J. Phys. Chem.* **1965**, *69*, 4017.
34. Adamson, A. In *Physical Chemistry of Surfaces*; Interscience: New York, **1967**.
35. Karger, B. L.; Snyder, L. R.; Horváth, C. *An Introduction to Separation Science*; John Wiley & Sons Inc.: New York, **1973**.
36. Grossman, P. D.; Colburn, J. C. ; *Capillary Electrophoresis*; Academic Press, **1992**.
37. Karcher, A.; El Rassi, Z. *Electrophoresis* **1999**, *20*, 3280-3296.
38. Karcher, A.; El Rassi, Z. *Electrophoresis* **1999**, *20*, 3181-3189.
39. Banks, J. F. *Electrophoresis* **1997**, *18*, 2255-2266.

## CHAPTER II

### SUMMARY OF HPCE OF GLUCOSINOLATES

#### AND PESTICIDES-RATIONALE

#### AND SIGNIFICANCE

##### Background and Rationale

In the ever changing fast paced agricultural industry, more and more technology has been designed for bigger and better production with an emphasis placed on lowering the overall financial cost. In this regard, one course of action is the application of a large number of economically inexpensive herbicides and insecticides to many plants, fruits, and vegetables as a way of controlling a large variety of pests. Unfortunately, many of these extremely toxic organic pesticides are applied to plants that already contain toxic and hazardous natural products, such as glucosinolates. Consequently, the toxicity of a given plant is the accumulation of several compounds. This is further complicated by the fact that the degradation products of many pesticides and natural products are also toxic. Therefore, accurate quantitation of all these compounds must be performed at extremely low levels to help proper food and feed safety. In this regard, CE which yields high separation efficiencies, is a technique that should be useful for this type of complicated analysis.

For example, toxic pyrethroid insecticides are widely used to control a large number of insects. They have been used not only in bulk applications, but they have also been formulated in commercially available aerosol sprays. Their toxicity towards insects and non-target organisms depends largely on their molecular shape and structure(1). Several major problems with trace level analysis of pyrethroids are attributed to their low water solubility, number of chiral centers, and their hydrolytic degradation to carboxylic acids(2,3). Thus, HPCE methods that analyze pyrethroid content via hydrolytic degradation products will yield a unique avenue for their trace level analysis from complex sample matrices, and this type of analysis avoids the pitfalls associated with the insolubility of the intact pyrethroids.

In the same sense, the trace level analysis of toxic natural products contained within plants and vegetables is also a high priority. One particular class of toxic natural products is glucosinolates. Glucosinolates are anionic thioglucosides contained throughout the *Cruciferae* family, and are commonly found in plants such as cabbage, turnips, mustards, horseradish, broccoli, Brussel sprouts, and rapeseed(4-7). Since there are currently over 100 known glucosinolates(5), these compounds are associated with various flavors, off-flavors, nutritive as well as toxic effects and are also involved in goitrogenic activity(6). The major problems associated with the trace level analysis of glucosinolates is the lack of authentic standards (currently only two are commercially available), and the enzymatic degradation products of glucosinolates via the hydrolytic enzyme, myrosinase. Upon crushing or masticating a given plant, myrosinase is released and hydrolyzes the glucosinolates. At pH 7.0, the glucosinolate is hydrolyzed into glucose,  $H^+$ , sulfate ion, and isothiocyanate ion(4, 5, 7). Consequently, HPCE methods

that analyze for intact glucosinolates are of little value. Like the pyrethroid insecticides, HPCE methods must be developed for the sensitive determination of glucosinolate degradation products from a given plant tissue (e.g., root, stems, or leaves).

### Recent Advancements in the CE of Pesticides and Glucosinolates

#### CE of Pesticides

In recent reports covering the analysis of all classes of pesticides by HPCE, several different modes of HPCE have been successfully applied, including achiral analysis via CZE(8-15), cyclodextrin-modified CZE(10), and MECC(10-12, 16-31). By far, the majority of the methods developed have utilized MECC. The large number of HPCE methods for the analysis of pesticides are, (i) reflective of the vast numbers of different pesticide classifications and (ii) representative of the broad scope of applications in HPCE. Pesticides such as quaternary ammonium herbicides, triazines, phenoxy acids, carbamates, sulfonylureas, imidazolinones, and pyrethroids are among a growing list of toxic analytes that have all been successfully separated with one of the previously mentioned HPCE modes.

Since many of these pesticides contain chiral centers (i.e., pyrethroid insecticides and phenoxy acid herbicides), much time has been devoted for their enantioresolution. Several researchers(26-29, 32-36) have also described methods for the chiral analysis of pesticides. Based on two very recent review articles(37, 38) on HPCE of pesticides and metabolites, only two reports(13, 20) have developed HPCE methods for the analysis of the pesticides via their degradation products. Therefore, there is not only an urgent need

for methodologies that detect the degradation products of pesticides, but as well as methods that can separate the enantiomers of these degradation products.

### CE of Glucosinolates

Only a limited number of research reports have been published describing the analysis of glucosinolates via HPCE(39-48), therefore, the state of the art in glucosinolate analysis is considered to be still in its infancy. A very recent review by Karcher and El Rassi(49), has already delineated this deficiency. Still, MECC profiling of eleven intact glucosinolates, that had been previously purified with other chromatographic techniques, has been demonstrated with a positively charged surfactant(44). A majority of the reports(39-44, 46) describe methods for the quantitation of glucosinolates through their degradation products, but these methods were developed using purified intact glucosinolates, and the researchers merely tested the linearity of the method. The methods were never applied to an actual sample extract. For example, a few research reports describe the separation of desulfoglucosinolates. Since the sulfonic acid group has been removed via the enzyme sulfatase, the desulfoglucosinolates are void of any charge and were separated with a charged micelle (MECC). This method proved promising, but no actual data was ever generated from actual samples. The problems associated with analyzing glucosinolates are related to, (i) lack of authentic standards, and (ii) inadequate chromophores. As previously mentioned, only two glucosinolate standards are available.

### Detection of Pesticides and Glucosinolates in CE

Another obstacle to overcome in the analysis of both glucosinolates and pesticides is the limitations imposed on detection in HPCE, see Chapter 1. In most of the publications that have appeared, the reported detection limits of these analytes are in the low ppb range (0.5-3.0), yet in order to obtain these limits excessive sample extraction and enrichment techniques were employed. In this endeavor, trace enrichment techniques such as solid phase extraction(13,20,21,25), field-amplified sample stacking(16,17,19,50), liquid-liquid extraction(22,33,51), and MECC zone narrowing(52) have been used to preconcentrate the sample before analysis. Consequently, the overall analysis time when employing precolumn concentration steps such as solid-phase extraction and liquid-liquid extraction greatly increased. Field-amplified sample stacking and MECC zone narrowing are sample concentration techniques requiring less time than the previously mentioned extraction techniques and are performed on-column. The problems that arise from these enrichment techniques are related to variations in consistency and reproducibility between runs. Therefore, as an alternative to the previous sample enrichment techniques, methods that describe selective pre-column fluorescent labeling of the pesticides, glucosinolates, or their degradation products are needed for their sensitive detection without the tedious and difficult to reproduce enrichment techniques. These needs are addressed in this dissertation.

Fluorescent labeling offers several merits not obtainable with the previous listed concentration techniques. First, fluorescent detection, in particular LIF detection, dramatically lowers the detection limit of a method. Secondly, fluorescent labeling is selective to molecules containing a particular functional group. The other concentration techniques are nonselective, so not only are the analytes of interest concentrated but all

the interferents as well. Furthermore, the difficulty in separating the solutes from other interferents is greatly reduced. Only those solutes that have been labeled and fluoresce at the proper detection wavelength are detected. Therefore, fluorescent labeling provides an excellent alternative to the preconcentration procedures for improving detection limits.

Therefore, methods are urgently needed that are rigorous enough to handle real sample matrices and at the same time provide the high sensitivity needed for trace level detection. This dissertation has investigated the separation and detection of fluorescently labeled degradation product of pyrethroids and glucosinolates. The analysis of the degradation products is advantageous since, (i) the degradation products contain active functional groups for easy fluorescent labeling, and (ii) they alleviate the need for authentic standards. For clarity, the rationale and significance for the study are discussed in the introduction of the Chapters in parts II and III.

### Conclusion

In essence, the development of methods for the analysis of pesticides and glucosinolates are interrelated. Both require HPCE methods that analyze the degradation products which are reflective of the intact parent compounds. Secondly, these two classes of compounds can coexist in many of the plants and vegetables consumed throughout the U.S. therefore, their degradation products also co-exist in these same samples. The chemical nature of these toxic compounds require methods that allow for their detection at low levels. Finally, both types of methods need the high separation efficiencies and low sample volume requirements of HPCE. These traits of HPCE make it an excellent tool for the analysis of solutes coming from complex plant extracts.

## References

1. Papadopoulou-Mourkidou, E. In *The Pyrethroid Insecticides*; Sherma, J., Ed.; Taylor & Francis: London, **1988**, pp 1-41.
2. Mao, J.; Erstfeld, K. M.; Fackler, P. H. *J. Agric. Food Chem.* **1993**, *41*, 596-601.
3. Muir, D. C.; Rown, G. P.; Girft, N. P. *J. Agric. Food Chem.* **1985**, *33*, 603-609.
4. Etten, C. H. V.; Tookey, H. L. In *Herbivores. Their Interaction with Secondary Plant Metabolites*; Rosenthal, G. A., Janzen, D. H., Eds.; Academic Press: New York, **1979**, pp 471-500.
5. Heaney, R. K.; Fenwick, G. R. In *Natural Toxicants in Food, Progress and Prospects*; Watson, D. H., Ed.; VCH: Weinheim, **1987**, pp 76-219.
6. Shibamoto, T.; Bjeldanes, L. F. In *Introduction to Food Toxicology*; Academic Press: San Diego, **1993**, pp 67-96.
7. Tookey, H. L.; Etten, C. H. V.; Daxenbichler, M. E. In *Toxic Constituents of Plant Foodstuffs*; Liener, I. V., Ed.; Academic Press: New York, **1980**, pp 103-142.
8. Lazar, I. M.; Lee, M. L. *J. Microcol. Sep.* **1999**, *11*, 117-123.
9. Galceran, M. T.; Carneiro, M. C.; Diez, M.; Puignou, L. *J. Chromatogr. A* **1997**, *782*, 289-295.
10. Farran, A.; Serra, C.; Sepaniak, M. J. *J. Chromatogr. A* **1999**, *835*, 209-215.
11. Tsai, C.-Y.; Chen, Y.-R.; Her, G.-R. *J. Chromatogr. A* **1998**, *813*, 379-386.
12. Carabias-Martínez, R.; Rodríguez-Gonzalo, E.; Domínguez-Alvarez, J.; Hernández-Méndez, J. *Anal. Chem.* **1997**, *69*, 4437-4444.



13. Frassanito, R.; Rossi, M.; Dragani, L. K.; Tallarico, C.; Longo, A.; Rotilio, D. *J. Chromatogr. A* **1998**, *795*, 53-60.
14. Cai, J.; El Rassi, Z. *J. Liq. Chromatogr* **1992**, *15*, 1179-1192.
15. Cai, J.; El Rassi, Z. *J. Liq. Chromatogr.* **1992**, *15*, 1193-2000.
16. Wu, Y. S.; Lee, H. K.; Li, S. F. Y. *J. Microcol. Sep.* **1998**, *10*, 239-247.
17. Tegeler, T.; El Rassi, Z. *J. AOAC* **1999**, *82*, 1542-1548.
18. Rossi, M.; Totilio, D. *J. High Resol. Chromatogr.* **1997**, *20*, 265-269.
19. He, Y.; Lee, H. K. *Electrophoresis* **1997**, *18*, 2036-2041.
20. Kubilius, D. T.; Bushway, R. J. *J. Chromatogr. A* **1998**, *793*, 349-355.
21. Kubilius, D. T.; Bushway, R. J. *J. Agric. Food Chem.* **1998**, *46*, 4224-4227.
22. Penmetsa, K. V.; Leidy, R. B.; Shea, D. *J. Chromatogr.* **1997**, *766*, 225-231.
23. Liu, C.-M.; Tzeng, Y.-M. *J. Chromatogr. A* **1998**, *809*, 258-263.
24. Lin, C.-E.; Hsueh, C.-C.; Wang, T.-Z.; Chiu, T.-C.; Chen, Y.-C. *J. Chromatogr. A* **1999**, *835*, 197-207.
25. Nejad, H.; Safarpour, M. M.; Cavalier, T.; Picard, G.; Souza, M.; Krynitsky, A. J.; Chiu, S.; Miller, P.; Stout, S. J. *J. Cap. Elec.* **1998**, *5*, 81-87.
26. Mechref, Y.; El Rassi, Z. *J. Chromatogr.* **1997**, *757*, 263-273.
27. Mechref, Y.; El Rassi, Z. *Electrophoresis* **1997**, *18*, 220-226.
28. Mechref, Y.; El Rassi, Z. *Chirality* **1996**, *8*, 515-524.
29. Mechref, Y.; El Rassi, Z. *Anal. Chem.* **1996**, *68*, 1771-1777.
30. Mechref, Y.; Smith, J. T.; El Rassi, Z. *J. Liq. Chromatogr.* **1995**, *18*, 3769-3786.
31. Smith, J. T.; El Rassi, Z. *J. Microcol. Sep.* **1994**, *6*, 127-138.

32. Fanali, S.; Aturki, Z.; Desiderio, C.; Bossi, A.; Righetti, P. G. *Electrophoresis* **1998**, *19*, 1742-1751.
33. Desiderio, C.; Polcaro, C. M.; Padiglioni, P.; Fanali, S. *J. Chromatogr. A* **1997**, *781*, 503-513.
34. O'Keeffe, F.; Shamsi, S. A.; Darcy, R.; Schwintè, P.; Warner, I. M. *Anal. Chem.* **1997**, *69*, 4773-4782.
35. Penmetsa, K. V.; Leidy, R. B.; Shea, D. *J. Chromatogr. A* **1997**, *790*, 225-234.
36. Otsuka, K.; Smith, C. J.; Grainger, J.; Barr, J. R.; Donald G. Patterson, J.; Tanaka, N.; Terabe, S. *J. Chromatogr. A* **1998**, *817*, 75-81.
37. Karcher, A.; El Rassi, Z. *Electrophoresis* **1999**, *20*, 3280-3296.
38. El Rassi, Z. *Electrophoresis* **1997**, *1997*, 2465-2481.
39. Karcher, A.; El Rassi, Z. *J. Agric. Food Chem.* **1999**, *47*, 4267-4274.
40. Karcher, A.; Melouk, H. A.; El Rassi, Z. *Anal. Biochem.* **1999**, *267*, 92-99.
41. Karcher, A.; El Rassi, Z. *J. Liq. Chrom. & Rel. Technol.* **1998**, *21*, 1411-1432.
42. Bjerregaard, C.; Michaelsen, S.; Møller, P.; Sørensen, H. *GCIRC 1991 Congress* **1991**, *8*, 822-827.
43. Bjerregaard, C.; Michaelsen, S.; Møller, P.; Sørensen, H. *J. Chromatogr. A* **1995**, *717*, 325-333.
44. Michaelsen, S.; Møller, P.; Sørensen, H. *J. Chromatogr.* **1992**, *608*, 363-374.
45. Morin, P.; Dreux, M. *J. Liq. Chromatogr.* **1993**, *16*, 3735-3755.
46. Morin, P.; Villard, F.; Qunisac, A.; Dreux, M. *J. High Resol. Chromatogr.* **1992**, *15*, 271-275.
47. Feldl, C.; Møller, P.; Otte, J.; Sørensen, H. *Anal. Biochem.* **1994**, *217*, 62-69.

48. Sørensen, H. In *Glucosinolates: Structure-Properties-Function*; Shahidi, F., Ed.; Van Nostrand Reinhold: New York, **1990**; Vol. 9, pp 149-172.
49. Karcher, A.; Rassi, Z. E. *Electrophoresis* **1999**, *20*, 3181-3189.
50. Wu, Y. S.; Lee, H. K.; Li, S. F. Y. *J. Microcol. Sep.* **1998**, *10*, 529-535.
51. Guardino, X.; Obiols, J.; Rosell, M. G.; Farran, A.; Serra, C. *J. Chromatogr. A* **1998**, *823*, 91-96.
52. Quirino, J. P.; Terabe, S. *Science* **1998**, *282*, 465-468.

## CHAPTER III

### ANALYSIS OF PYRETHROID INSECTICIDES VIA THEIR HYDROLYSIS PRODUCTS LABELED WITH A FLUORESCING AND UV ABSORBING TAG FOR LIF AND UV DETECTION\*

#### Introduction

Most pyrethroids may be recognized as having been derived from the constituent esters of pyrethrum, which are characterized by insecticidal activities(1). Synthetic insecticidal pyrethroids have shown increased usage in insecticide formulations for insect control in field crops as well as indoors such as households, stores and green-houses. Pyrethroids toxicity towards insects and non-target organisms depends largely on molecular shape and structure(2). Chemically, the pyrethroids are a relatively heterogeneous group of compounds whose molecules may possess geometric isomerism (*cis-trans*) and one to three chiral centers. Usually, pyrethroid insecticide formulations are mixtures of isomers. The toxicity of the various enantiomers of the pyrethroid insecticides is known to vary considerably(2). Thus, as there is an increasing need for rapid separation methods for the determination of individual pyrethroids, there is also a strong need for the separation and determination of the various enantiomeric

---

\* Published in Electrophoresis, 1997, 18, 1173-79.

species and geometric isomers of pyrethroids. This should enable the assessment and comparison of the overall toxicological properties of the mixtures of pyrethroid isomers present in formulated insecticides or in their residual deposit. Also, selective and sensitive detection methods for the determination of pyrethroid insecticides at low levels are urgently needed.

Pyrethroids have other characteristics that impose stringent requirements on the analytical methods used in their determination. Pyrethroids are known to have extremely low water solubilities, and to undergo degradation in the aquatic ecosystems, which may involve, among other things, hydrolysis with subsequent hydrolytic products(3,4). In addition, the pyrethroid esters do not possess a suitable functional group for tagging in the aim of facilitating their selective and sensitive detection.

Various chromatographic methods have been introduced for the separation of pyrethroids and their geometric and optical isomers. Gas-liquid chromatography (GC)(5-10) and high performance liquid chromatography (HPLC) in its various modes(4, 11-15) have been the traditional approaches for the analysis of pyrethroids. More recently, supercritical fluid chromatography (SFC) with packed and capillary column was applied to the determination of pyrethroids(16). Only a few attempts have been made so far for the determination of pyrethroids by capillary isotachopheresis (CITP)(17-19). While GC, HPLC and SFC provided some solutions to the analysis of pyrethroids, they required expensive columns and reagents and consumed large amounts of expensive mobile phases. CITP is a rather tedious approach whose successful application depends on the judicious control of separation conditions, especially the selection of the leading and

terminating electrolytes, and prior knowledge of the mobilities and ionization of all the sample components.

Thus far, besides CITP, there are virtually no reports on the use of other modes of high performance capillary electrophoresis (HPCE) in the determination of chiral pyrethroids. This despite the fact that HPCE offers many advantages including high separation efficiency, unique selectivity, shorter analysis time, small sample requirements, and more importantly, lower consumption of expensive reagents and solvents. Thus, the aim of the present chapter is to exploit the potentials of HPCE in the determination of pyrethroids.

In the present chapter, to render pyrethroids amenable to aqueous HPCE, and facilitate their determination at low levels by HPCE-laser induced fluorescence (LIF) detection, the analytes were first subjected to base hydrolysis which yielded the corresponding carboxylic acids. The active carboxylic acid groups in the well defined degradation products provided the sites for fluorescent tagging and subsequent determination by HPCE-LIF. One rationale for this approach was the fact that once applied in the environment, pyrethroids would eventually undergo hydrolytic degradation producing carboxylic acids reflective of the parent pyrethroids. Another benefit of this approach was simplifying the chiral separation problem by reducing the number of enantiomers in most cases from eight to four (e.g., cypermethrin, see Fig. 1), and from four to two optical isomers (e.g., sanmarton). This methodology does not conflict with the assessment of the toxicity of the original pyrethroid. The hydrolysis products are reflective of the toxicity of the parent pyrethroid even in the case of pyrethroids containing a chiral  $\alpha$ -cyanobenzyl alcohol portion where access to information on the

isomer composition of the alcohol portion is lost by base hydrolysis. In fact, it has been reported that the toxicity is dependent on the configuration of the chiral carbon adjacent to the carboxyl group(20). For instance, permethrin enantiomers having the *R* configuration at this carbon are about 25 times more toxic to houseflies than those with the *S* configuration. Also, the toxicity of the insecticides having a chiral cyano-group (e.g., sanmarton and cypermethrin, see Fig. 1) are also affected by the configuration of this chiral carbon, with the *S* configuration being more toxic to houseflies by a factor of 20-100(21).

The present chapter provides a continuation of our earlier efforts in designing rapid and sensitive HPCE methods for the separation and determination of pesticides(22-32). The various pyrethroids used in this study were analyzed by HPCE-LIF through their base hydrolytic products. In this regard, the carboxylated hydrolytic products were tagged with 7-aminonaphthalene-1,3-disulfonic acid (ANDSA) via a condensation reaction that was recently introduced by our laboratory for the selective tagging of various carboxylic compounds including some phenoxy acid herbicides(27, 33-36). In addition, two chiral alkylglycoside surfactants, namely octylglucoside (OG) and octylmaltoside (OM) which were recently introduced by our laboratory for the separation of chiral compounds including, phenoxy acid herbicides(25-27, 37) were further exploited here in the enantiomeric separation of the ANDSA-derivatives of the hydrolytic products of pyrethroids. Thus, our aim in this chapter was to tie together a novel precolumn derivatization to a newly introduced chiral selector for the labeling and chiral separation of the hydrolytic products of pyrethroids by HPCE-LIF.

## Materials and Methods

### Reagents and materials

The pyrethroid insecticides including permethrin, phenothrin, fenpropathrin, sanmarton and cypermethrin were purchased from Chem Service (West Chester, PA, USA). The structures and solubility of these model solutes are shown in Fig. 1. While cypermethrin has three stereogenic centers, permethrin, sanmarton and phenothrin have two stereogenic centers each, and fenpropathrin have one stereogenic center. Chrysanthemic acid (CA) which was purchased from Sigma (St. Louis, MO, USA) has two stereogenic centers. The achiral solutes 3-phenoxybenzoic acid (3-PBA) and 2,2,3,3-tetramethylcyclopropanecarboxylic acid (TCCA) were obtained from Aldrich (Milwaukee, WI, USA). Octyl- $\beta$ -glucopyranoside (OG) was purchased from Anatrace (Mumee, OH, USA), and octyl- $\beta$ -D-maltopyranoside (OM) and octanoylsucrose (OS) were purchased from Calbiochem (San Diego, CA, USA). A 1.0 M solution of 1,3-dicyclohexylcarbodiimide (DCC) dissolved in dichloromethane, 1,1'-binaphthyl-2,2'-diyl hydrogenphosphate and 3-phenoxybenzyl alcohol (3-PBAL) were purchased from Aldrich. The precolumn labeling agents 7-aminonaphthalene-1,3-disulfonic acid (ANDSA) was purchased from TCI America Inc. (Portland, OR, USA).

### Capillary electrophoresis instruments

Two Beckman P/ACE instruments (Fullerton, CA, USA) were used. They consisted of Models 5510 and 5010 equipped with a diode array detector and an Omnichrome (Chino, CA, USA) Model 3056-8M He-Cd laser multimode, 8 mW at 325



nm, respectively. The data was handled with an IBM personal computer and System Gold software. The detection of the underivatized pyrethroid hydrolysis products was performed at 200 nm. The UV detection of the ANDSA derivatives was performed at 255 nm. For the LIF detection the pyrethroid degradation products tagged with ANDSA, a fluorescence emission band-pass filter of  $380 \pm 2$  nm was purchased from Corion (Holliston, MA, USA). A 360 nm cut-on filter purchased from Corion was used to reject the laser beam. The experiments were performed in fused-silica capillaries obtained from Polymicro Technology (Phoenix, AZ, USA). The dimensions of the capillaries were 50 cm to the detection window and 57 cm total length with 50  $\mu\text{m}$  internal diameter and 365  $\mu\text{m}$  outer diameter. In all experiments, the temperature was held constant at 20 °C by the instrument thermostating system. Samples were pressure injected at 0.034 bar (i.e., 3.5 kPa) for various lengths of time. In between runs, the capillary was rinsed with 0.1 M NaOH, distilled water, and running electrolyte for two, three and one minute, respectively.

## Procedures

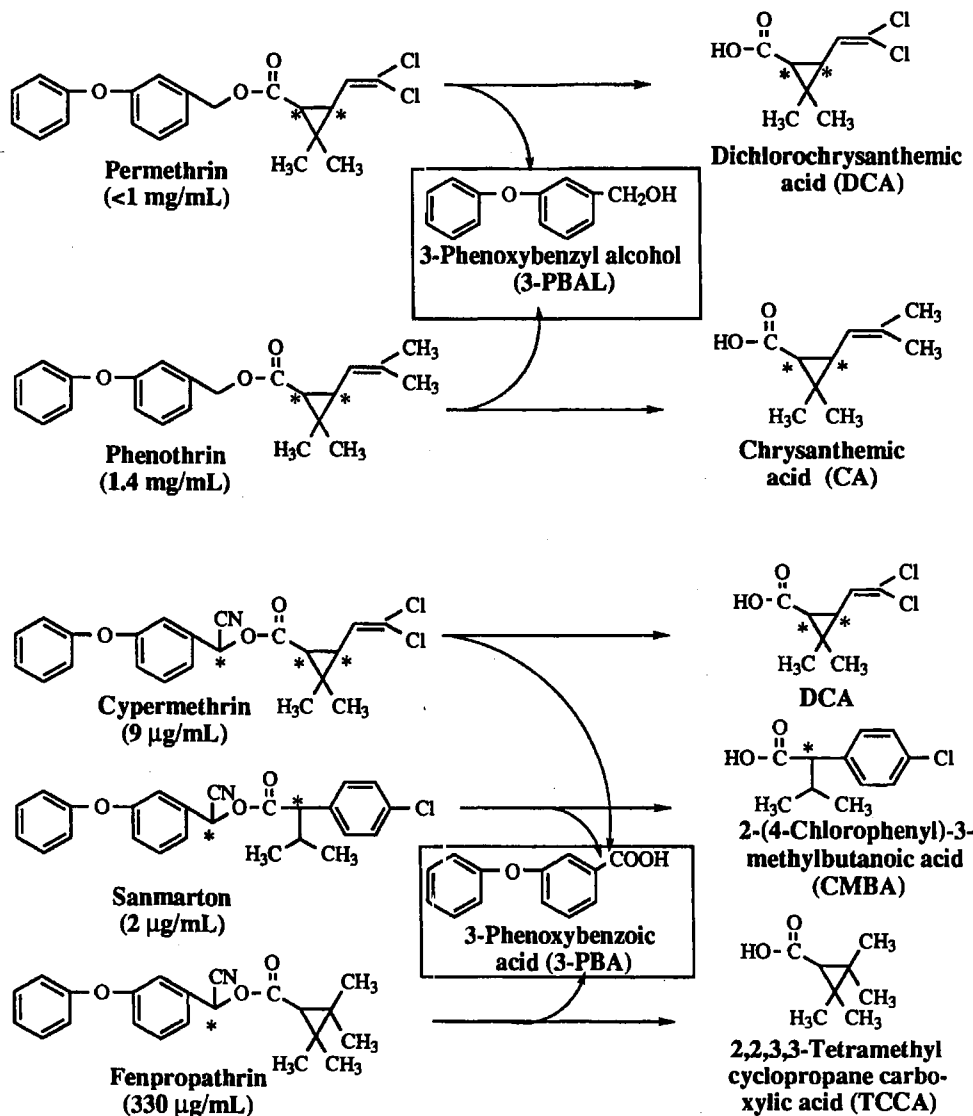
### Pyrethroid hydrolysis

The base hydrolysis reaction for the pyrethroids was performed according to the procedure given by Dombek and Dombek and Stránsky(17-19) with slight modifications. Briefly, a solution with buffer:ethanol ratio of 1.25:1.00 was used in the hydrolysis of permethrin while solutions with buffer:tert.-butyl alcohol of 1.50:1.00 were used for the hydrolysis of phenothrin, cypermethrin and fenpropathrin. The buffer was 50 mM sodium phosphate, pH 12.0. The solution containing the pyrethroid was hydrolyzed in tightly

closed reaction vials heated at 105 °C. Figure 1 shows the base catalyzed hydrolysis reaction schemes for each insecticide. The hydrolysates were analyzed by CE using 50 mM sodium phosphate, pH 7.0, as the running electrolyte, 15 kV as the applied voltage and 200 nm as the detection wavelength. For analyzing the extent of hydrolysis via 3-PBAL, 60 mM OM and 40 mM OS mixed micellar system in 200 mM sodium borate, pH 10, was used as the running electrolyte instead of 50 mM sodium phosphate while keeping other conditions the same. In all cases, 1,1'-binaphthyl-2,2'-diyl hydrogenphosphate was used as the internal standard.

#### Precolumn derivatization

The standard degradation products as well as the five carboxylated degradation products of the pyrethroid insecticides produced by hydrolysis were tagged by first mixing 2.0 mL of a  $2.0 \times 10^{-3}$  M solution of the analyte dissolved in pyridine with an equivalent concentration of DCC, and then adding the correct mass needed to produce a  $2.0 \times 10^{-2}$  M solution of the ANDSA tag. After reacting overnight, the solvent was removed by a speed vacuum concentrator. The derivatized solution was prepared for analysis by redissolving the tagged analyte in 2 mL of a 50% aqueous-acetonitrile solution. The extent of precolumn derivatization was assessed by CE using 50 mM sodium phosphate, pH 6.5, as the running electrolyte, 19 kV as the applied voltage and 200 nm as the detection wavelength. The internal standard was 1,1'-binaphthyl-2,2'-diyl hydrogenphosphate.



**Figure 1.** Structures of the pyrethroids used in this study, and their hydrolytic reactions under basic conditions. Numbers in parentheses represent solubility in water (solubility values are from Ref. (38)).

## Results and discussion

### Hydrolysis

The extent of hydrolysis of pyrethroids (see Fig. 1) was determined with phenothrin, permethrin, cypermethrin and fenpropathrin simply because the degradation products of these pyrethroids are available as pure standards. The percent pyrethroid hydrolyzed under the conditions outlined in the experimental section was 42, 43, 54 and 62% for phenothrin, permethrin, fenpropathrin and cypermethrin, respectively. These percents were determined by subjecting the hydrolysate of each insecticide to CE analysis. The percent of phenothrin, cypermethrin and permethrin hydrolyzed was determined through the amount of CA, 3-PBA and 3-PBAL produced, respectively, while the percent of fenpropathrin hydrolyzed was deduced from the amount of 3-PBA and TCCA produced. The percents pyrethroid degraded corroborate those reported by Dombek and Stránský (17,18) for similar pyrethroids using the degradation product CA. Dombek reported under the best conditions and 48 hrs digestion time, a yield of 55.9% by estimating it using the hydrolytic product CA(18). However, Dombek and Stránský(17) reported not greater than 19.3% yield using the degradation product 3-PBA. The limited percent yield for hydrolysis may be associated in part with the limited solubility of the pyrethroids and their degradation products. This can be substantiated by the fact that the percent hydrolysis was reported to be largely influenced by the alcohol:buffer ratio in the hydrolysis solution(18). In fact, performing the hydrolysis in aqueous NaOH at pH 13.0 did not degrade more than 28% of the pyrethroids under investigation and precipitation was observed.

### Precolumn derivatization

The extent of derivatization with ANDSA was determined on three of the pyrethroid hydrolysis products, namely 3-PBA, CA, and TCCA, since these three compounds were the only commercially available standards. The amounts of unreacted 3-PBA, CA and TCCA in the derivatization reactions were determined by CE at 200 nm, a wavelength that corresponds to the maximum characteristic absorption band of the underivatized analytes. The CE analysis of the ANDSA-labeled samples revealed that the reaction was free from side products, and the precolumn derivatization proceeded to near completion (>98%). Also, the UV spectra generated by the P/ACE diode array detector showed that the ANDSA derivatives had maximum absorption bands at 255 nm.

Another appreciable aspect of this precolumn derivatization technique, was that the carboxylic acid group on each of the pyrethroid hydrolysis products was replaced with two strong sulfonic acid groups. The solubility of the pyrethroid insecticides was extremely low in aqueous solutions as indicated in Fig. 1. Phenothrin had the highest solubility of any pyrethroid used in this study of 1.4 mg/L. The products of base hydrolysis were insoluble to sparingly soluble in aqueous solutions at low pH, and higher amounts of the hydrolysates were dissolved at higher pH values. Upon reaction with the derivatizing agent, ANDSA, the labeled analytes exhibited good solubility over a wide range of pH due to the complete ionization of the sulfonic acid groups. The increased solubility upon tagging with ANDSA rendered the solutes more amenable to analysis by aqueous CE.

### Limit of detection

Table 1 lists some typical limits of detection (LOD) that were obtained using UV and LIF with the underivatized degradation products as well as their ANDSA derivatives. The UV limit of detection (LOD) for the analytes was increased by almost one order of magnitude from  $1.4 \times 10^{-4}$  M for TCCA to  $3.2 \times 10^{-5}$  M for the TCCA-ANDSA derivatized analyte. Using the LIF detection, the LOD achieved ( $9.3 \times 10^{-8}$  M) for the TCCA-ANDSA derivative was improved by almost four orders of magnitude with respect to underivatized TCCA, see Table 1. For underivatized CA and 3-PBA, the UV LOD was  $4.5 \times 10^{-5}$  M and  $2.5 \times 10^{-5}$  M, respectively. These LOD were almost the same as those obtained upon derivatization with ANDSA, see Table 1. This is due to the fact that both underivatized CA and 3-PBA possess a strong chromophoric group in their structure, see Fig. 1. However, LIF improved the LOD of CA-ANDSA by almost two orders of magnitude with respect to the underivatized CA.

The fluorescence properties for the ANDSA derivatives of the pyrethroid hydrolytic fragments for which standards are commercially available (i.e., 3-PBA, CA and TCCA) were studied. The tagging agent, ANDSA, showed two excitation maxima, one intense at 315 nm and the other less intense at 350 nm while its maximum emission was at 450 nm. The derivatives exhibited either shifted excitation and emission maxima or no significant fluorescence. The excitation maxima of CA-ANDSA and TCCA-ANDSA were observed at 325 nm, which is the spectral line of the He/Cd laser used in the LIF detector. The emission maxima of CA-ANDSA and TCCA-ANDSA were observed at 388 nm, and the only difference is that TCCA-ANDSA emitted about 7 times

TABLE I

LIMITS OF DETECTION OF THE ANDSA DERIVATIVES OF THE  
HYDROLYTIC PRODUCTS OF THE PYRETHROIDS

Analytes	UV LOD at 200 nm of underivatized analytes (M)	UV LOD at 255 nm of ANDSA derivatives (M)	LIF LOD of ANDSA derivatives (M)
3-PBA	$2.5 \times 10^{-5}$	$2.0 \times 10^{-5}$	NF
CA	$4.5 \times 10^{-5}$	$4.8 \times 10^{-5}$	$1.4 \times 10^{-7}$
TCCA	$1.4 \times 10^{-4}$	$3.2 \times 10^{-5}$	$9.8 \times 10^{-8}$

NF: no fluorescence

more than the CA-ANDSA. This may explain the lower LOD attained with TCCA-ANDSA than with CA-ANDSA in LIF. The 3-PBA-ANDSA derivative did not exhibit any significant fluorescence. This may be explained by the fact that 3-PBA lacks structural rigidity a phenomenon that causes an enhanced internal conversion rate in the 3-PBA-ANDSA, and a consequent increase in the probability for radiationless deactivation.

#### Capillary electrophoresis with neutral surfactant systems

Optimum conditions for the separation of the pyrethroid hydrolytic degradation products labeled with ANDSA were determined through a systematic study which

involved changing the nature and amount of the alkylglycoside surfactant (i.e., OG and OM) at a constant sodium phosphate concentration in the running electrolyte and vice versa. The electropherograms produced with OG and OM under optimum conditions for the separation of the ANDSA labeled analytes are shown in Fig. 2a and 2b, respectively.

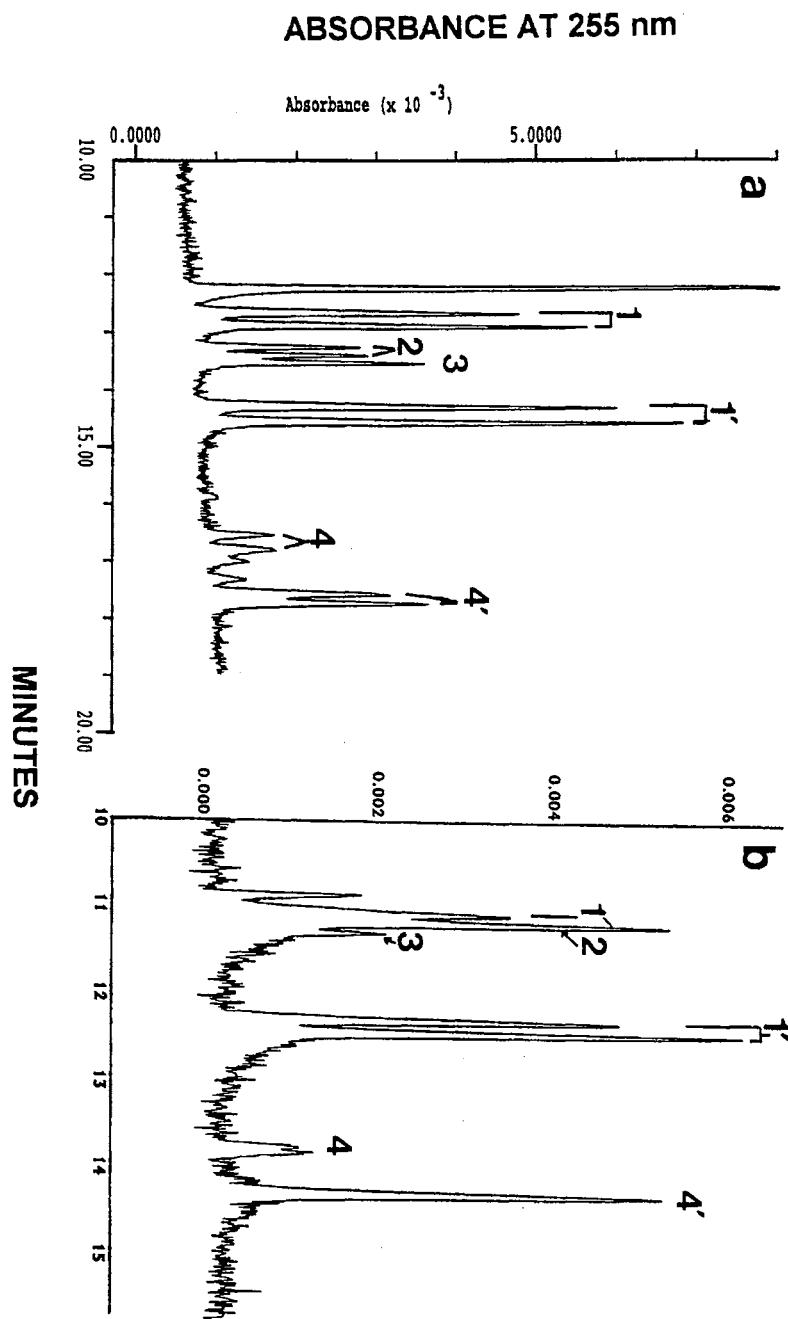
With OM, the optimum surfactant concentration for the achiral and chiral separation of the three optically active degradation products (i.e., CA, CMBA and DCA) was 25 mM of this surfactant in 100 mM sodium phosphate, pH 6.5. As can be seen in Fig. 2b, only the DCA-ANDSA derivatives are chirally separated, while the CA-ANDSA are only partially chirally separated and CMBA-ANDSA co-eluted with the DCA-ANDSA peaks. This partial chiral separation only occurs at an OM concentration that is very close to the CMC of the OM surfactant. Increasing the OM concentration decreased both the enantioresolution (for  $[OM] > 25$  mM) and the average electrophoretic mobility for the ANDSA labeled derivatives. Varying the ionic strength of the running electrolyte yielded little or no improvement in the chiral and achiral resolution of the various analytes. The net effect of increasing the ionic strength at pH 6.5 was increasing the analysis time as a result of decreasing both the effective electrophoretic mobility of the analytes and decreasing the EOF (results not shown). At high ionic strength the analytes are believed to solubilize deeper in the palisade layer (see below for more details), a fact that may have contributed to loss in enantioresolution at higher phosphate concentration. In summary, the OM micellar system never produced complete chiral separation for the ANDSA derivatized analytes.

With OG, optimum separation conditions for maximum resolution are shown in Fig. 2a. As established earlier with other kinds of chiral solutes using OG, higher ionic



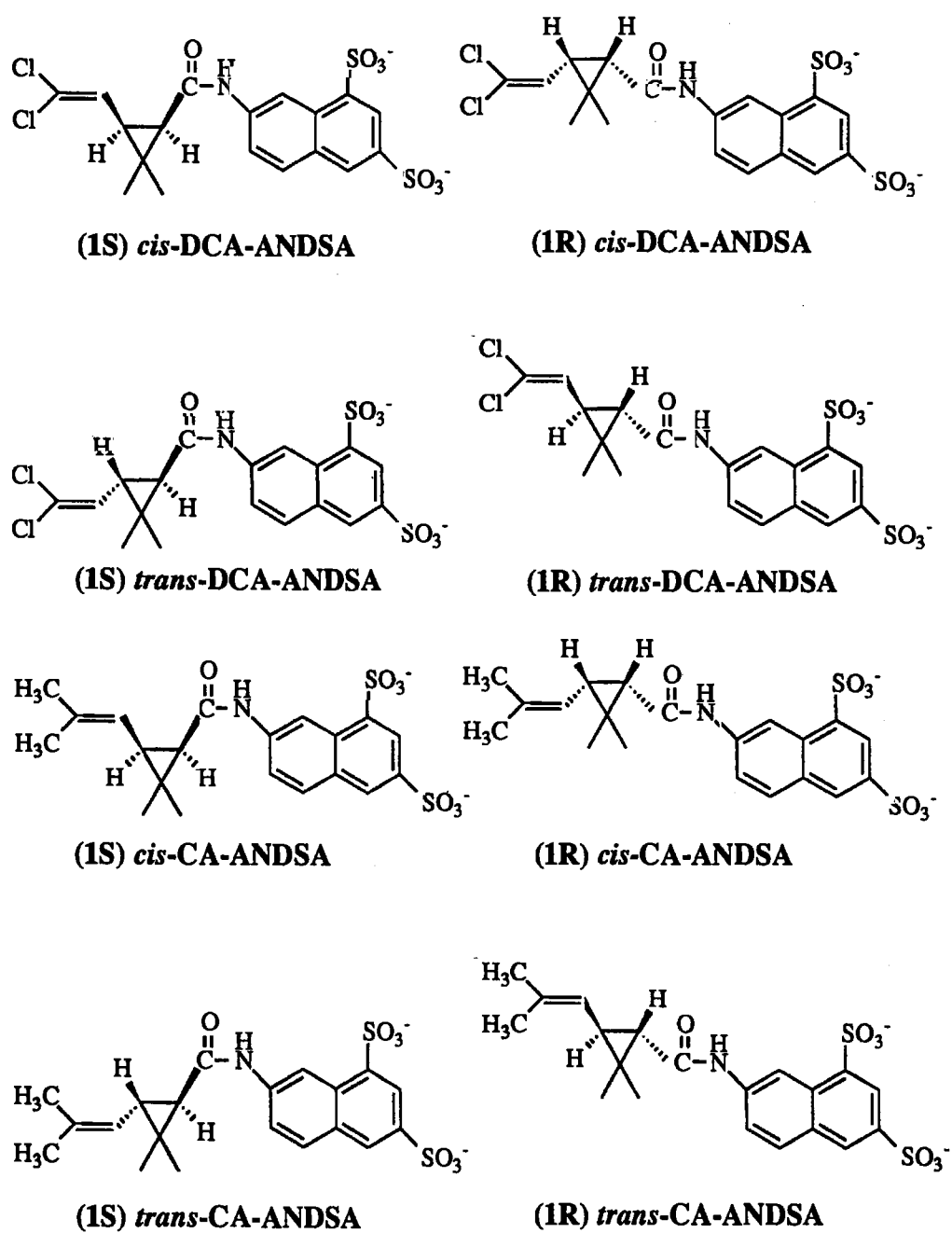
strength (i.e., 100 mM sodium phosphate) enhanced enantioresolution (26, 37). Also, the addition of a small amount of acetonitrile (i.e., 10% v/v) improved further the overall enantioresolution. This is in agreement with our previous findings with other chiral solutes using alkylglycoside surfactants as chiral selectors (27). As can be seen in Fig. 2a, and as expected, two of the three optically active pyrethroid hydrolysis products (CA and DCA) exhibited four enantiomers. Figure 3 shows the four possible enantiomeric forms for the DCA-ANDSA and CA-ANDSA derivatives. These sets of optical isomers are also resolved along with the isomers from the CMBA-ANDSA derivative.

Since the alkylglycoside surfactants used in this study are of the neutral type, their micelles will migrate through the capillary at the speed of the electroosmotic flow which is toward the cathode and opposite in direction with respect to the sulfonated analytes (for details of the separation principles, see Ref. (26)). Thus, the stronger the solute-micelle association is, the faster the migration of the negatively charged solutes toward the cathode will be, i.e., the shorter their migration time. This will correspond to a decrease in the effective electrophoretic mobility of the solutes. 3-PBA-ANDSA, CMBA-ANDSA and DCA-ANDSA have about the same charge-to-mass ratio of  $-4.02 \times 10^{-3}$ ,  $-4.03 \times 10^{-3}$  and  $-4.06 \times 10^{-3}$ , respectively. These solutes (i.e., 3-PBA-ANDSA, CMBA-ANDSA and DCA-ANDSA) associated relatively strongly with OG and migrated rapidly past the detection point. ANDSA-DCA and ANDSA-TCCA with a higher charge-to-mass ratio of  $-4.40 \times 10^{-3}$  and  $-4.70 \times 10^{-3}$ , respectively, eluted last. The order of hydrophobicity seems to be decreasing in the order *cis*-DCA > 3-PBA > *trans*-DCA > CA > TCCA. The neutral alcohol 3-PBAL eluted with the electroosmotic flow at 8.60 min. Increasing the surfactant concentration in the running electrolyte should increase the time the solute will



**Figure 2.** Electropherogram of the hydrolytic products of pyrethroids derivatized with ANDSA. Electrolytes: 100 mM sodium phosphate, pH 6.5, containing in (a) 10% (v/v) acetonitrile and 40 mM octylglucoside and in (b) 25 mM OM; 19 kV; 20 °C; capillary, fused-silica,  $l = 50$  cm,  $L = 57$  cm,  $50 \mu\text{m}$  i.d.. Solutes: 1, *cis*-DCA-ANDSA; 1', *trans*-DCA-ANDSA; 2, CMBA-ANDSA; 3, 3-PBA-ANDSA; 4, *cis*-DCA-ANDSA; 4' *trans*-DCA-ANDSA.

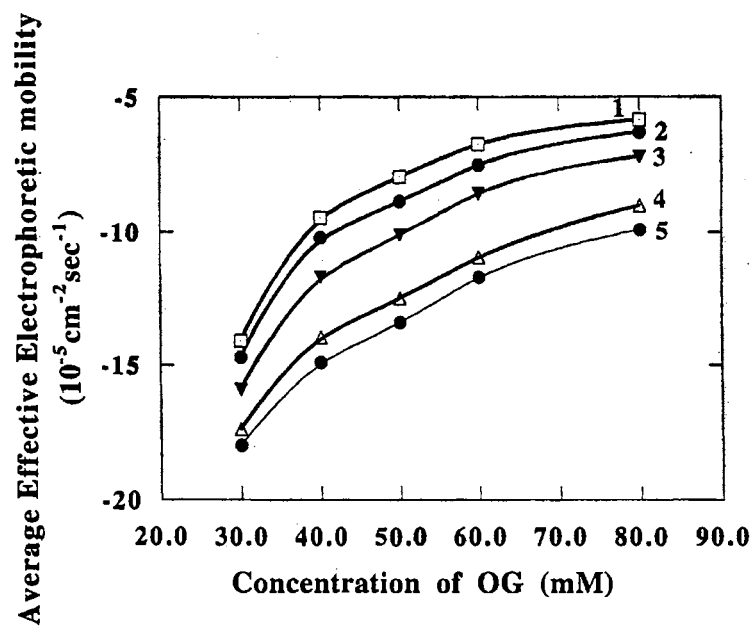
spend in the micellar phase, and as a result the effective electrophoretic mobility of the solutes will decrease, i.e., faster analysis time. Figure 4 shows the average effective electrophoretic mobility for the ANDSA labeled analytes as a function of OG concentration. As can be seen the effective electrophoretic mobility decreases with increased surfactant concentration. At a surfactant concentration above the optimal one for maximum enantioresolution, adding a small amount of acetonitrile seems to restore enantioresolution to its maximum probably by a competing effect (see Fig 5a, b and c). The addition of small amount of acetonitrile is thought to adjust the depth of solute penetration into the palisade layer of the micelle(25, 26). The palisade layer is the layer between the hydrophilic groups and the first few carbon atoms of the hydrophobic tails that comprise the outer core of the micellar interior (see Ref. (26) for details of the loci of solute solubilization into micelles). This would favor better interaction between the solute chiral center and the chiral head group of the surfactant, thus leading to improved enantioresolution. In other words, the addition of an organic modifier to a surfactant concentration higher than the optimum can have a positive effect on enantioresolution. The electropherogram shown in Fig. 5a contains no organic modifier. Consequently, the CMBA-ANDSA and DCA-ANDSA analytes co-eluted. Upon the addition of ten percent acetonitrile (Fig. 5c), all three labeled analytes are resolved into their enantiomeric components. Figure 5 shows also the useful property of the ANDSA labeling agent, which is the LIF detection capability. One noticeable difference between this electropherogram and the UV detected electropherogram (Fig. 2), is the absence of the 3-PBA-ANDSA peak in the LIF detection. As discussed above the 3-PBA-ANDSA derivative did not fluoresce when excited at 325 nm.



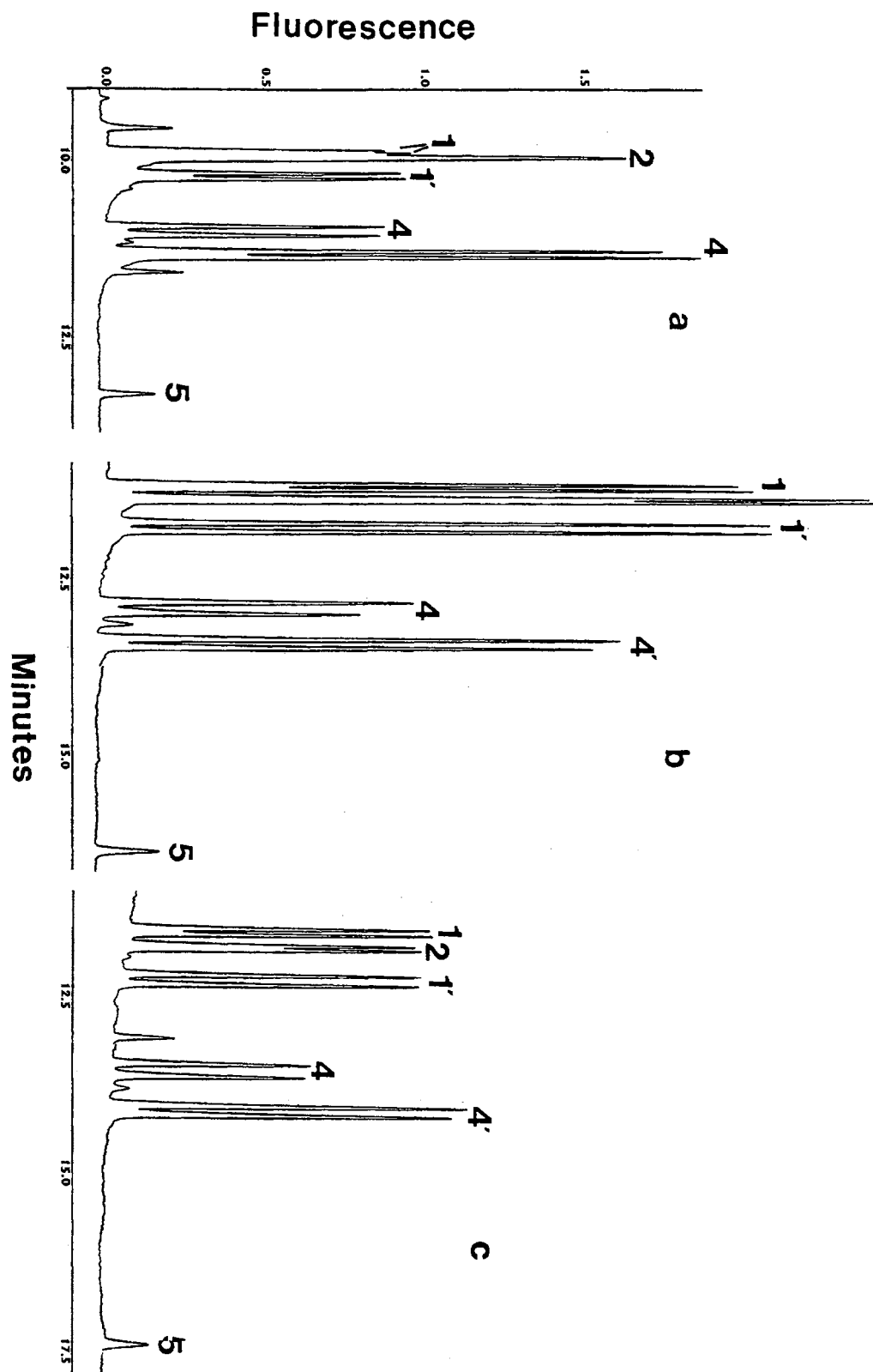
**Figure 3.** Structures of the enantiomers of DCA-ANDSA and CA-ANDSA.

## CONCLUSION

The determination of pyrethroid insecticides by capillary electrophoresis *via* their base hydrolytic products that are reflective of the individual insecticides proved to be a useful approach. In fact, the base fragmentation led to the formation of products with carboxylic acid active sites which were selectively and quantitatively tagged with fluorescing ANDSA, thus permitting the detection of the pyrethroids at the  $10^{-7}$  to  $10^{-8}$  M levels by HPCE-LIF. The base hydrolysis of the pyrethroids followed by the tagging with ANDSA allowed the determination of the pyrethroids by aqueous CE. Under these circumstances, the various ANDSA derivatives of the pyrethroid hydrolytic products were separated into their optical and geometric isomers in the presence of chiral alkylglycoside surfactants, namely OG and OM.



**Figure 4.** Plots of the effective electrophoretic mobility of the ANDSA derivatives of the hydrolytic products of the pyrethroids as a function of the OG concentration in the running electrolyte. Lines 1 and 3, *cis*- and *trans*-DCA-ANDSA, respectively; 2, CMBA-ANDSA; 4 and 5, *cis*- and *trans*-CA-ANDSA, respectively. Conditions as in Fig. 2.



**Figure 5.** Electropherograms of the ANDSA derivatives of the hydrolytic products of pyrethroids obtained by LIF detection. Electrolytes; 100 mM sodium phosphate, pH 6.5, containing 70 mM OG at 0% in (a), 5% in (b), and 10% v/v acetonitrile in (c). Solutes as in Fig. 2 and in addition 5, TCCA-ANDSA. Other conditions as in Fig. 2.

## References

1. Davies, J.H., in: J. P. Leahey (Ed.), *The Pyrethroid Insecticides*, Taylor & Francis, London, **1985**, pp 1-41.
2. Papadopoulou-Mourkidou, E., in: J. Sherma (Ed.), *Analytical Methods for Pesticides and Plants Regulators*, Academic Press, San Diego, **1988**, pp 179-206.
3. Muir, D.C.G., Rown, G.P., Grift, N.P., *J. Agric. Food Chem.*, **1985**, *33*, 603-609.
4. Mao, J., Erstfeld, K.M.; Fackler, P.H., *J. Agric. Food Chem.*, **1993**, *41*, 596-601.
5. Kutter, J.P., Class, T.J., *Chromatographia*, **1992**, *33*, 103-112.
6. Doi, T., Sakaue, S., Horiba, M., *J. Assoc. Off. Anal. Chem.*, **1985**, *68*, 911-916.
7. Chapman, R.A., Harris, C.R., *J. Chromatogr.*, **1979**, *174*, 369-377.
8. Murano, A., *Agri. Biol. Chem.*, **1972**, *36*, 2203-2211.
9. Bolygó, E., Zakar, F., *J. Assoc. Off. Anal. Chem.*, **1983**, *66*, 1013-1017.
10. Ling, Y.-C., Huang, I.-P., *J. Chromatogr. A*, **1995**, *695*, 75-82.
11. Chapman, R.A., *J. Chromatogr.*, **1983**, *258*, 175-182.
12. Oi, N., Kitahara, H., Kira, R., *J. Chromatogr.*, **1990**, *515*, 441-450.
13. Køppen, B., *J. AOAC Int.*, **1994**, *77*, 810-814.
14. Martínez Galera, M., Martínez Vidal, J.L., Garrido Frenich, A., Gil García, M.D., *J. Chromatogr. A*, **1996**, *727*, 39-46.
15. García Sánchez, F., Navas Díaz, A., García Pareja, A., *J. Chromatogr. A*, **1996**, *754*, 97-102.
16. Nishikawa, Y., *Anal. Sci.*, **1992**, *8*, 817-822.
17. Dombek, V., Stránsky, Z., *J. Chromatogr.*, **1989**, *470*, 235-240.
18. Dombek, V., *J. Chromatogr.*, **1991**, *545*, 427-435.



19. Dombek, V., Stránský, Z., *Anal. Chim. Acta*, **1992**, *256*, 69-73.
20. Burt, P.E., Elliott, M., Farnham, A.W., Janes, N.F., Needham, P.H., Pulman, D.A., *Pestic. Sci.*, **1974**, *5*, 791.
21. Elliott, M., Farnham, A.W., Janes, N.F., Soderlund, D.M., *Pestic. Sci.*, **1978**, *9*, 112-116.
22. Cai, J., El Rassi, Z., *J. Chromatogr.*, **1992**, *608*, 31-45.
23. Mechref, Y., El Rassi, Z., *J. Chromatogr. A*, **1996**, *724*, 285-296.
24. Mechref, Y., El Rassi, Z., *Anal. Chem.*, **1996**, *68*, 1771-1777.
25. Mechref, Y., El Rassi, Z., *Chirality*, **1996**, *6*, 515-524.
26. Mechref, Y., El Rassi, Z., *J. Chromatogr. A*, **1997**, *757*, 263-273.
27. Mechref, Y., El Rassi, Z., *Electrophoresis*, **1997**, *18*, 220-226.
28. Smith, J.T., El Rassi, Z., *Electrophoresis*, **1994**, *15*, 1248-1259.
29. Smith, J.T., El Rassi, Z., *J. Chromatogr. A*, **1994**, *685*, 131-143.
30. Smith, J.T., El Rassi, Z., *J. Microcol. Sep.*, **1994**, *6*, 127-138.
31. Smith, J.T., Nashabeh, W., El Rassi, Z., *Anal. Chem.*, **1994**, *66*, 1119-1133.
32. Smith, J.T., El Rassi, Z., *J. Cap. Elec.*, **1994**, *2*, 136-143.
33. Mechref, Y., Ostrander, G.K., El Rassi, Z., *Electrophoresis*, **1995**, *16*, 1499-1504.
34. Mechref, Y., Ostrander, G.K., El Rassi, Z., *J. Chromatogr. A*, **1995**, *695*, 83-95.
35. Mechref, Y., El Rassi, Z., *Electrophoresis*, **1994**, *15*, 627-634.
36. El Rassi, Z., Postlewait, J., Mechref, Y., Ostrander, G.K., *Anal. Biochem.*, **1997**, *244*, 283-290.
37. Mechref, Y., El Rassi, Z., *Electrophoresis*, **1997**, *18*, 1148-56.
38. Ray, D.E., in; Hayes, W. J., Laws, E. R. (Eds.), *Handbook of Pesticide Toxicology*,

Academic Press, San Diego 1991, pp 585-631.

## CHAPTER IV

# EFFECTS OF THE NATURE OF FLUORESCENT LABELS ON THE ENANTIOSEPARATION OF PESTICIDES AND THEIR DEGRADATION PRODUCTS BY CAPILLARY ZONE ELECTROPHORESIS WITH UV AND LASER INDUCED FLUORESCENCE DETECTION\*

### Introduction

The application of a wide variety of herbicides and insecticides in agriculture and other areas of commerce is growing at a highly accelerated rate. Most of these pesticides and their degradation products are classified as harmful toxicants, therefore, this continued application of toxic pesticides adversely effects the quality of the environment (e.g., ground water, soils, food sources). Furthermore, some pesticides are applied as racemic mixtures. This is an alarming concern, since most of the activity of a particular pesticide can be attributed to a single enantiomer. Through an increased awareness of ecological hazards associated with applying racemic mixtures, there is an urgent need for analytical methodologies that are efficient in the chiral separations needed to monitor the enantiomeric content of pesticide formulations.

In recent reports from our laboratory (1, 2), methodologies have been introduced

---

\* *Electrophoresis*, 2000, in press.

for the chiral separation of underivatized phenoxy acid herbicides with chiral alkylglycoside surfactants. These same surfactants have also been successfully used in the chiral separation of derivatized phenoxy acid herbicides(3), as well as for the chiral separation of derivatized degradation products of pyrethroid insecticides(4). In all cases, the precolumn derivatization was based on the tagging of the analytes with 7-aminonaphthalene-1,3-disulfonic acid (ANDSA). This derivatization not only imparts the solutes with two strong sulfonic acid groups that are ionized over a wide range of pH, but it also introduces new physical and chemical properties. The derivatives are (i) easily detected at low levels through laser-induced fluorescence (LIF), (ii) show a change in overall hydrophobicity, and (iii) exhibit different chiral properties when compared to the parent molecules. Therefore, this study was intended to extend the scope of the previous reports by evaluating the magnitude of chiral resolution as a function of the number of sulfonic acid groups in the fluorescent tag (1, 2, or 3 sulfonic acid groups), with two alkylglycoside chiral surfactants, namely, octyl- $\beta$ -D-glucoside (OG) and octyl- $\beta$ -D-maltoside (OM). The fluorescent tags are 5-aminonaphthalene-1-sulfonic acid (ANSA), 7-aminonaphthalene-1,3-disulfonic acid (ANDSA), and 8-aminonaphthalene-1,3,6-trisulfonic acid (ANTS).

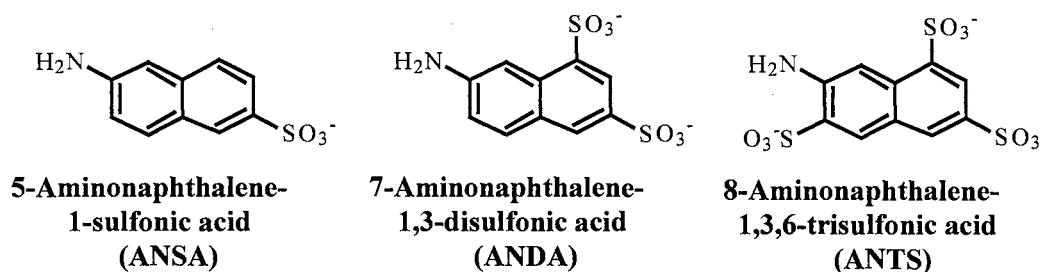
## Materials and methods

### Reagents and materials

All the pyrethroid insecticides used in this study, namely phenothrin, cypermethrin and sanmarton were purchased from Chem Service (West Chester, PA). The pyrethroid hydrolysis standard, chrysanthemic acid (CA) was obtained from Sigma

(St. Louis, MO). The phenoxy acid herbicides including 2-(2,4-dichlorophenoxy) propionic acid (Dichlor), 2-(4-chlorophenoxy) propionic acid (2,4-CPPA) and 2-phenoxypropionic acid (2-PPA) were purchased from Aldrich (Milwaukee, WI). The structures of the analytes are listed on page 50, see chapter III.

The three fluorescent tags, including 5-amino-1-naphthalenesulfonic acid (ANSA), 7-aminonaphthalene-1,3-disulfonic acid (ANDSA) was purchased from TCI America (Portland, OR) and 8-aminonaphthalene-1,3,6-trisulfonic acid (ANTS) was obtained from Molecular Probes (Eugene, OR) and are shown below. The two surfactants n-octyl- $\beta$ -D-glucoside (OG) and n-octyl- $\beta$ -D-maltopyranoside (OM) were purchased from Anatrace (Mumee, OH).



### Capillary electrophoresis instruments

A Beckman P/ACE System 5510 (Fullerton, CA) was used for all experiments. It was equipped with an Omnichrome (Chino, CA) Model 3056-8M He-Cd laser multimode, 8 mW at 325 nm. For data handling purposes, P/ACE station software was utilized. Emission band-pass filters of  $380 \pm 2$  nm and  $420 \pm 2$  nm were purchased from Corion (Holliston, MA) for the LIF detection of the ANSA and ANDSA derivatives and

the ANTS derivatives, respectively. A 360 nm cut-on filter purchased from Corion was used to reject the laser beam. The experiments were performed in fused-silica capillaries obtained from Polymicro Technology (Phoenix, AZ). The dimensions of the capillaries were 50 cm to the detection window and 57 cm total length, with 50  $\mu\text{m}$  internal diameter and 365  $\mu\text{m}$  outer diameter. In all experiments, the temperature was held constant at 18  $^{\circ}\text{C}$  by the instruments thermostating system. Samples were pressure injected at 0.034 bar (*i.e.*, 3.5 kPa) for various lengths of time. Between runs, the capillary was rinsed with 0.1 M NaOH, distilled water and running electrolyte for 2, 3 and 1 min, respectively.

## Procedures

### Pyrethroid hydrolysis

The base hydrolysis of the pyrethroids used in this report followed our previously modified procedure that was described by Dombek and co-workers (5-8). Briefly, a solution of a buffer:tert-butanol of 1.50:1.00 was used for the hydrolysis of phenothrin, sanmarton and cypermethrin. The buffer consisted of 50 mM sodium phosphate, pH 12.0. The reaction was carried out at 105  $^{\circ}\text{C}$  overnight. The hydrolysis reaction is illustrated in chapter IV on page 50.

### Precolumn derivatization

The phenoxy acid herbicides were tagged using the previously published procedure by Mechref and El Rassi(3). One hundred microliters of a  $1.0 \times 10^{-3}$  M

solution of analyte was mixed for five minutes with 100  $\mu\text{L}$  of  $1.0 \times 10^{-3}$  M derivatizing agent (i.e., ANSA, ANDSA or ANTS). Next, 100  $\mu\text{L}$  of  $1.0 \times 10^{-3}$  M EDAC was added, and this solution was allowed to react overnight. These solutions were subsequently diluted and used for all sample injections in this study. The carboxylated degradation products of the pyrethroid insecticides were tagged by following the procedure outlined in chapter III, page 52(4). For further details concerning the yields of this derivatization and limits of detection, see Mechref and El Rassi(3) and chapter III(4). For the structures of typical derivatives see Fig. 3, chapter III. The derivatives are formed via a condensation reaction between the carboxylic acid group of the solute and the amino group of the tag in the presence of a suitable carbodiimide.

## Results and discussion

The effects of the derivatizing agent on the chiral separation by CE in the presence of two alkylglycoside chiral micellar systems were determined under different ionic strength and surfactant concentration conditions. The two alkylglycoside surfactants systems used were OG and OM.

### OG micellar system

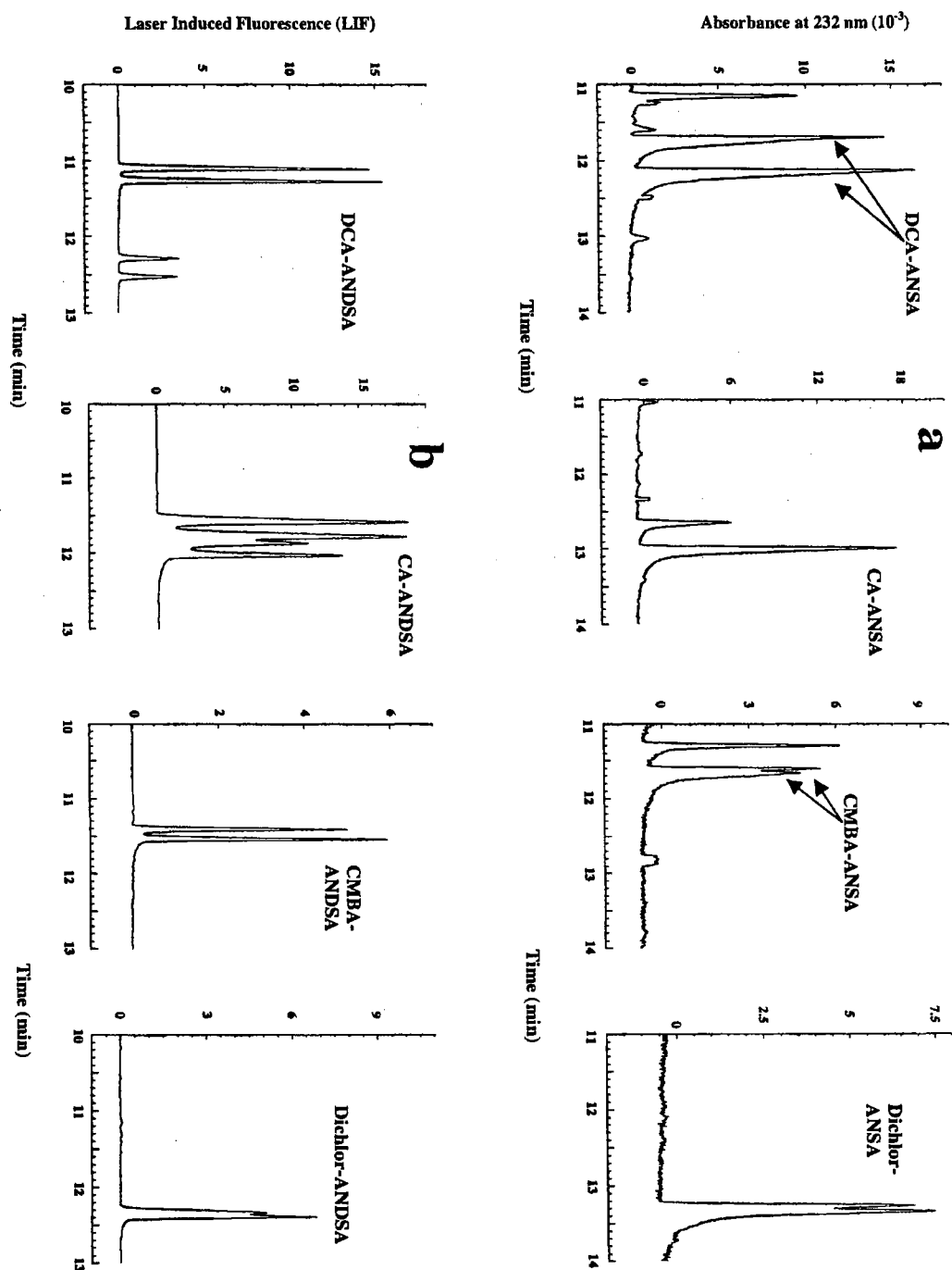
Nature of the fluorescent tag. A systematic study was undertaken to determine the extent of enantioresolution with electrophoresis buffers containing 30 mM OG when the analytes were derivatized with fluorescent tags containing one, two or three sulfonic acid groups, i.e., ANSA, ANDSA or ANTS, respectively. With the ANSA derivatives at 150 mM sodium phosphate, we have found that only CMBA and Dichlor were resolved

into their enantiomeric forms, while DCA and CA were only split into their *cis* and *trans* isomers, see Table 1, and Fig. 1.

When the ANDSA derivatives were studied, CMBA, DCA, CA, and Dichlor were resolved into their enantiomeric forms. When compared to the ANSA derivatives, the enantioresolution of ANDSA-Dichlor remained similar, while the enantioresolution of CMBA-ANDSA increased by more than a factor of three, see Table 1. Some typical electropherograms are shown in Fig. 1. The ANDSA derivatives showed an overall improvement in the chiral recognition when compared to the chiral recognition for the ANSA derivatives. However, the analytes 2,4-CPPA and 2-PPA, were still not resolved with either tag (ANSA or ANDSA) using an OG micelle.

Finally, the analytes were labeled with the trisulfonic acid tag, ANTS, and subsequently electrophoresed with a running electrolyte containing 30 mM OG. None of the ANTS derivatives were resolved into their enantiomeric forms. The lack of enantioselectivity exhibited by the ANTS derivatives may be the result of the stronger hydrophilic nature of the ANTS tag arising from the presence of three sulfonic acid groups. This lowers the hydrophobic interactions of the solute with the neutral micelle. The weak solute-micelle interactions were manifested by the significantly longer migration times of the ANTS derivatives when compared to the migration times of ANSA and ANDSA derivatives. The ANTS derivatives were about 3 times more retarded than those of ANSA and ANDSA, under otherwise similar conditions. Evidently, the polarity of the three tags increases in the order ANTS < ANDSA < ANSA. The effectiveness of the ANDSA tag in yielding a higher enantioresolution





**Figure 1.** Electropherograms of the chiral separation of the (a) ANSA and (b) ANDSA derivatives. Conditions: running electrolyte, 150 mM sodium phosphate, pH 6.5, containing 30 mM OG.; voltage 18 kV; capillary, bare fused silica capillary 50 cm (to detection point)/57 cm (total length) x 50  $\mu$ m I.D.; temperature, 18°C.

Table I

ENANTIORESOLUTION VALUES OF THE ANSA AND ANDSA DERIVATIVES  
 AT 150 mM PHOSPHATE, CONTAINING 30 mM OG, pH 6.5; VOLTAGE 18kV;  
 CAPILLARY, BARE FUSED-SILICA, 50 CM (TO DETECTION  
 POINT)/57 CM (TOTAL LENGTH) x 50  $\mu$ m  
 i.d.; TEMPERATURE, 18 °C.

Solute	Enantioresolution			
	ANSA		ANDSA	
	OG	OM	OG	OM
DCA	0	0	2.05/3.065*	0.426/1.372*
CA	0	0	1.356/1.724*	1.093/0.859*
CMBA	0.424	0.964	1.856	1.347
Dichlor	0.549	0.8	0.345	1.041
2,4-CPPA	0	0	0	0.724
2-PPA	0	0	0	0.749

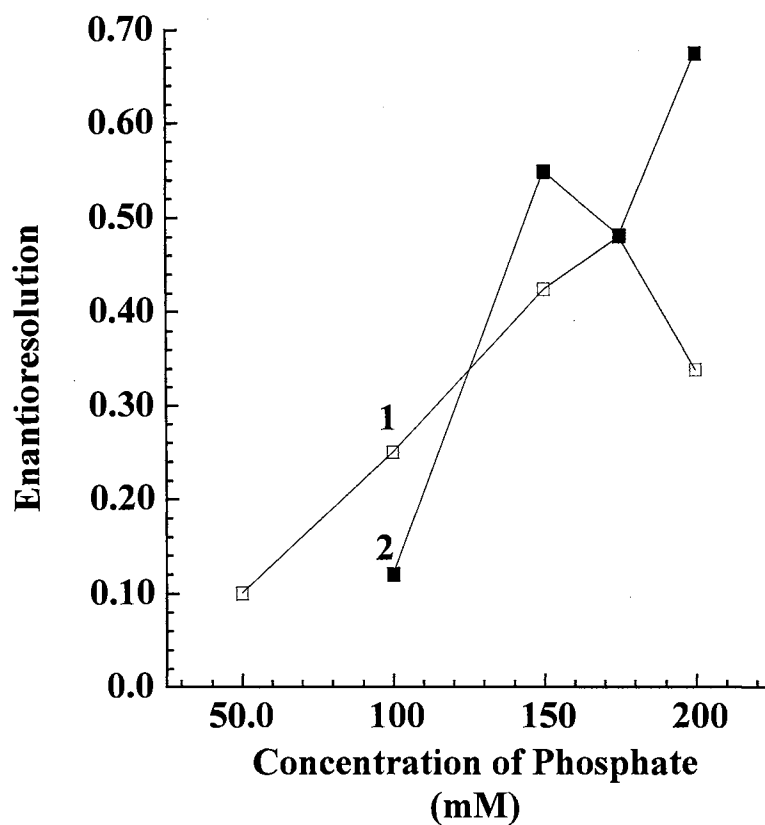
\* DCA and CA have two chiral centers yielding 2 pairs of enantiomers (i.e., 4 optical isomers)

among the analytes investigated indicates that the medium polarity of the ANDSA, which may have afforded more equitable hydrophilic and lipophilic interactions between solutes and micelles, is an essential component for the chiral recognition.

Ionic strength. It is known that increasing the ionic strength decreases the critical micellar concentration (CMC) and increases the aggregation number of a micelle(9, 10). In effect, this would increase the micellized surfactant concentration,  $[S]-CMC$ , where  $[S]$  is the surfactant concentration. This translates into increasing the concentration of micellized chiral centers. Furthermore, an increase in ionic strength has a salting out effect, which will increase nonpolar interactions with the chiral OG micelles.

Initially, the ANSA derivatives were electrophoresed with running electrolytes at constant OG concentration of 30 mM while varying the amount of sodium phosphate from 30-200 mM. At 200 mM, the amount of current was relatively high ( $\sim 100 \mu A$ ), therefore, the amount of phosphate was kept below 200 mM to reduce the amount of Joule heat and other adverse effects of such a high current. Upon inspection of Fig. 2, it can be seen that the enantioresolution of CMBA-ANSA and Dichlor-ANSA increased with increasing phosphate concentration to a maximum at 175 mM for CMBA-ANSA and at 150 mM phosphate for Dichlor-ANSA before it increased again for Dichlor-ANSA between 175 and 200 mM phosphate.

When electrophoresing the ANDSA derivatives, an increase in phosphate concentration yielded no substantial change in the enantioresolution for CA-ANDSA but led to a significant increase in the resolution for the enantiomers of DCA-ANDSA, see Fig. 3. For CMBA-ANDSA and Dichlor-ANDSA, the concentrations of phosphate that yielded maxima in enantioresolution were at 150 mM and 175 mM, respectively.



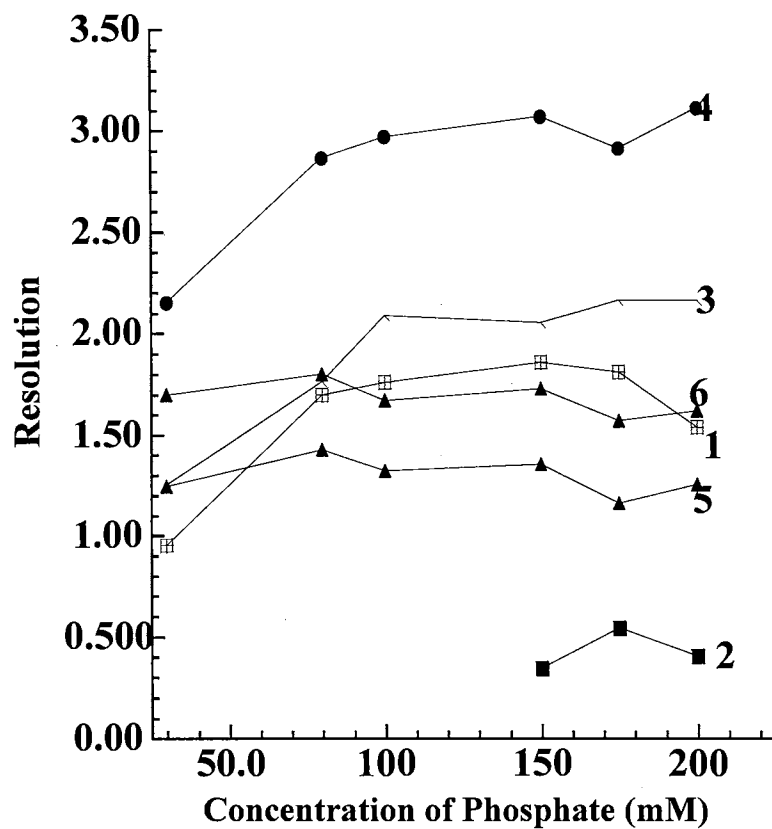
**Figure 2.** Plots of enantioresolution of ANSA derivatized analytes versus sodium phosphate concentrations. Conditions: running electrolyte, various concentrations of sodium phosphate, pH 6.5, containing 30 mM OG. Curves: 1, CMBA-ANSA; 2, Dichlor-ANSA. Other conditions are the same as in Fig. 1.

When the ANTS derivatives were tested, no resolution was achieved for any of the analytes with the OG micellar system. The concentration of phosphate tested was limited to 80 mM, because the migration times of the trisulfonated ANTS derivatives were extremely long. Some chiral resolution may have been achieved at higher concentrations of phosphate, but as just mentioned these conditions were not tested.

OG concentration. The OG concentration in the running electrolyte was also varied from 30-80 mM, while holding the phosphate concentration at 150 mM for all three sets of derivatives. It was found that, in all cases enantioresolution decreased with an increase in concentration of OG. For example, the resolution of CMBA labeled with ANSA decreased from 0.42 at 30 mM OG to no resolution at 80 mM OG. The ANDSA derivative of CMBA had a resolution of 1.6 at 30 mM OG and decreased to 0.32 at 80 mM OG. The increase of surfactant concentration increased the concentration of micellized surfactant, and consequently the concentration of solute partitioned into the micellar phase. This decreased the charge-to-mass ratios of the analytes and in turn the migration times. At elevated surfactant concentrations, the effective electrophoretic mobility of the solutes approaches that of the neutral micelle, and as a result the difference between the effective electrophoretic mobilities of the two enantiomers becomes very small (approaches zero), a fact that explains the decrease in resolution.

#### OM micellar system

Nature of the fluorescent tag. As in the case of the OG micellar system, only CMBA-ANSA and Dichlor-ANSA showed chiral recognition with the OM micelle, see Table 1. When compared to the OG micelle, CMBA-ANSA and Dichlor-ANSA showed

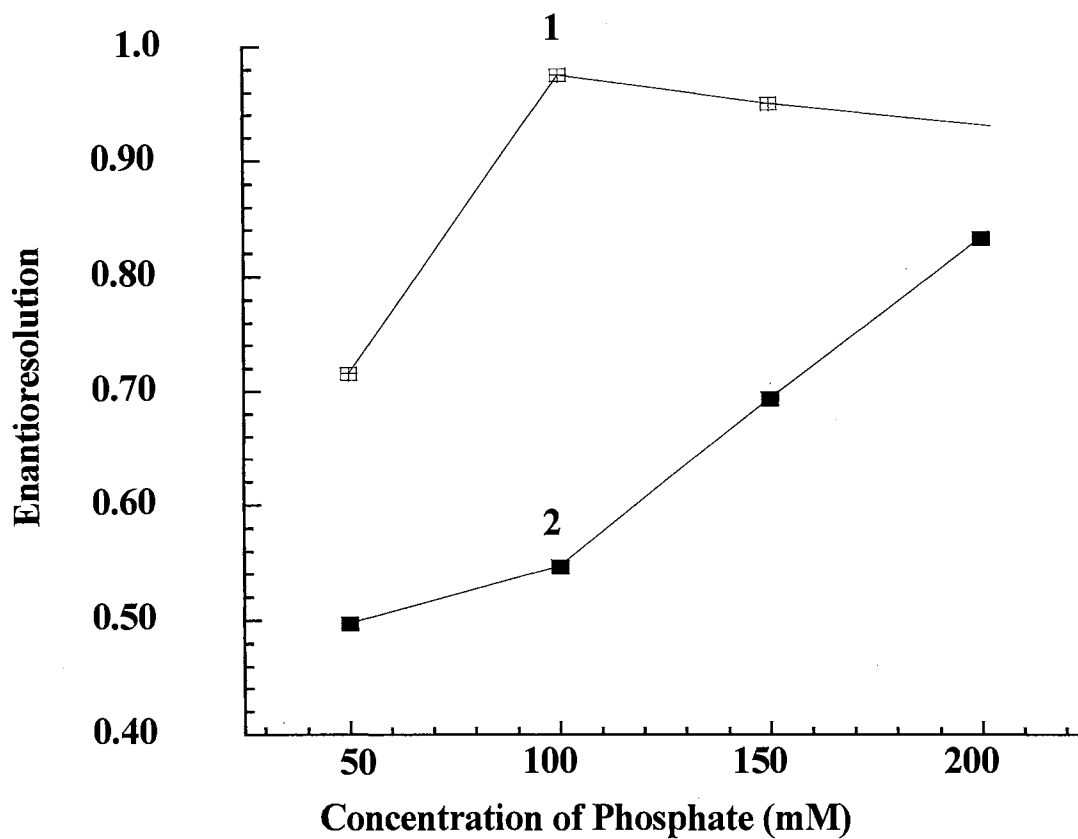


**Figure 3.** Plots of enantioresolution of ANDSA derivatized analytes versus sodium phosphate concentrations. Curves: 1, CMBA-ANDSA; 2, Dichlor-ANDSA; 3 and 4, DCA-ANDSA; 5 and 6, CA-ANDSA. Other conditions are the same as in Fig. 1.

an overall increase in enantioresolution with the OM micelle. Again, the enantiomers of ANSA labeled 2,4-CPPA and 2-PPA were not resolved.

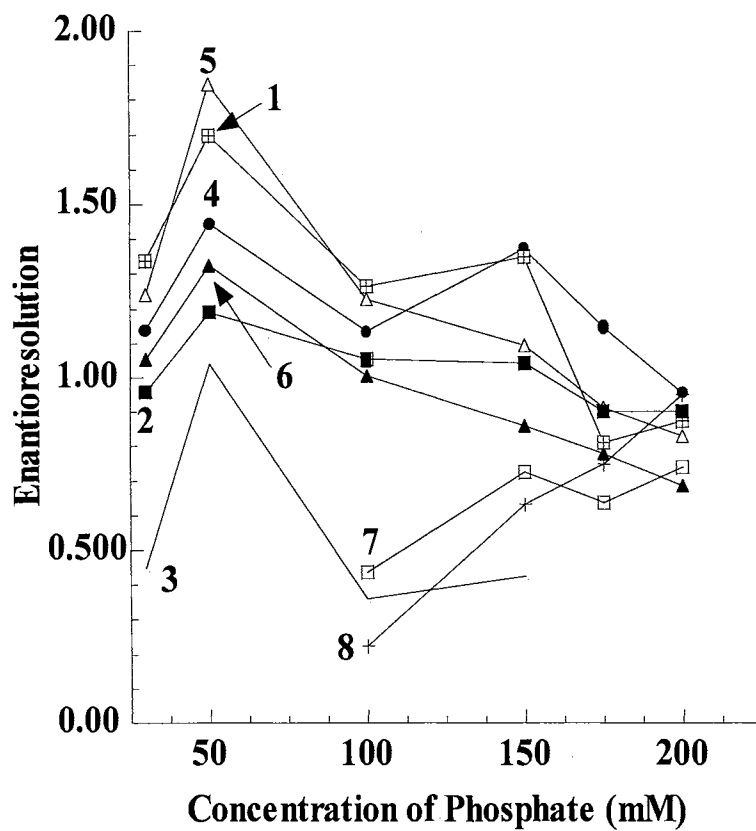
With the OM micellar system, it was found that all the ANDSA derivatized solutes were resolved, see Table 1. On the other hand, when the ANTS labeled analytes were electrophoresed in the presence of the OM micelle, only one of the analytes, 2-PPA-ANTS, was enantioresolved when at least 100 mM OM was added to 80 mM phosphate, see later for more detailed discussion.

Ionic strength. The dependence of enantioresolution on phosphate concentration in the case of the OM micelle was for the most part similar to what was observed with the OG micellar system. From inspection of Fig. 4, it is noticed that an increase in phosphate concentration had increased the resolution of the enantiomers of ANSA derivatives of CMBA and Dichlor. For the ANDSA derivatives, dramatic changes in resolution were observed with an increase in ionic strength, see Fig. 5. The most hydrophobic analytes, namely DCA-ANDSA, CMBA-ANDSA, CA-ANDSA, and Dichlor-ANDSA, all reached maxima in enantioresolution at 50 mM phosphate. At a higher ionic strength, a decrease in resolution was observed. On the other hand, 2,4-CPPA-ANDSA and 2-PPA-ANDSA, which are the least hydrophobic solutes, were not resolved until at least 100 mM phosphate was added, see Figs 5 and 6, and the resolution increased with increasing phosphate concentrations. The enantioresolution of 2,4-CPPA-ANDSA and 2-PPA-ANDSA was not possible with the OG micelle. The OM micelle with its disaccharide head group seemed to be more effective in the chiral separation of the derivatized analytes.



**Figure 4.** Plots of enantioresolution of ANSA derivatized analytes versus sodium phosphate concentrations. Conditions: running electrolyte, various concentrations of sodium phosphate, pH 6.5, containing 30 mM OM. Curves: 1, CMBA-ANSA; 2, Dichlor-ANSA. Other conditions are the same as in Fig. 1.





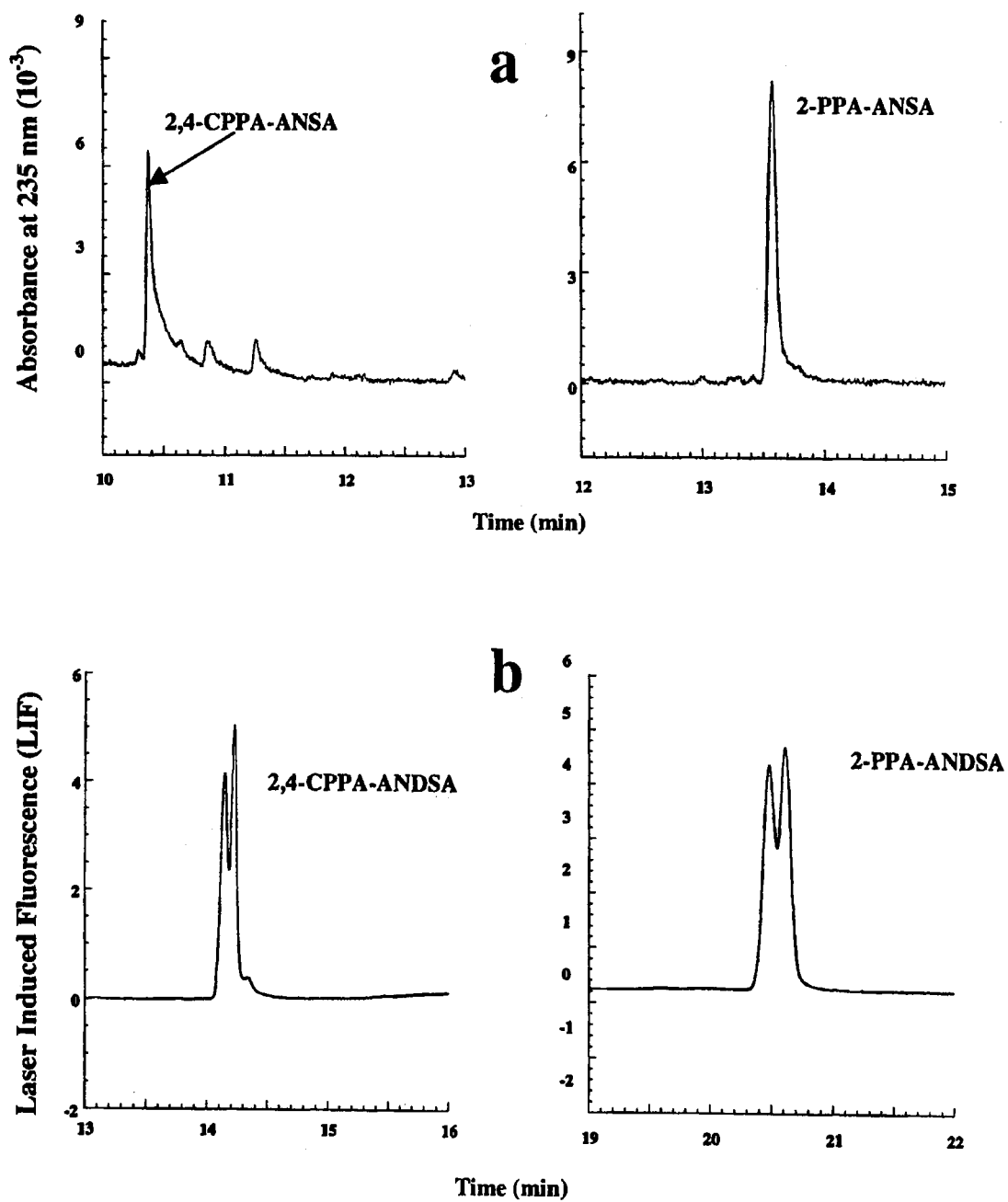
**Figure 5.** Plots of enantioresolution of ANDSA derivatized analytes versus sodium phosphate concentrations. Conditions: running electrolyte, various concentrations of sodium phosphate, pH 6.5, containing 30 mM OM. Curves: 1, CMBA-ANDSA; 2, Dichlor-ANDSA; 3 and 4, DCA-ANDSA; 5 and 6, CA-ANDSA. Other conditions are the same as in Fig. 1.

OM concentration. When the concentration of OM was increased, the enantioresolution decreased for all of the ANSA and ANDSA derivatives except for 2-PPA labeled with ANDSA. This derivative showed an increase in resolution with increasing surfactant concentration up to 80 mM OM, which correlates with the study by Mechref and El Rassi(3).

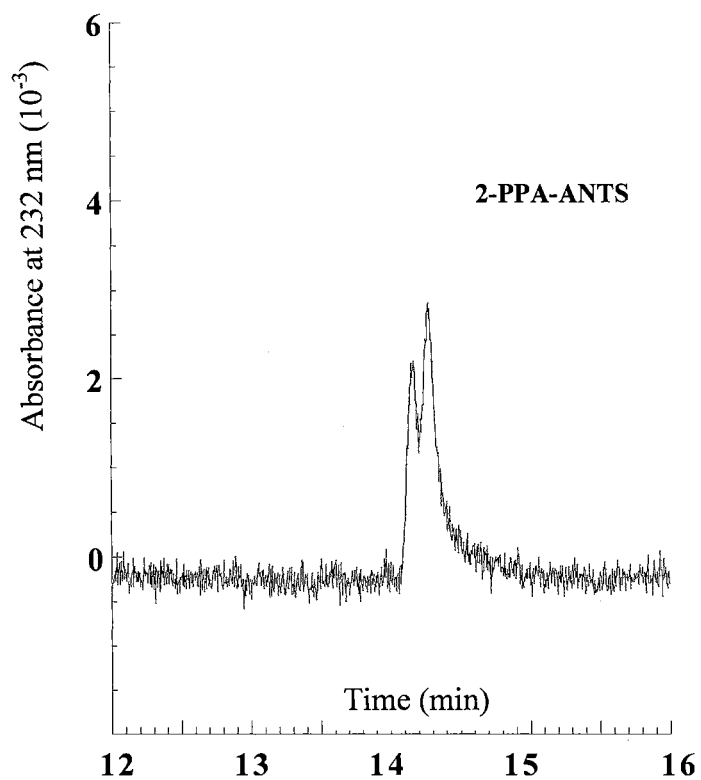
In the case of the ANTS derivatives, only 2-PPA-ANTS showed a limited amount of enantioresolution. It required at least 100 mM OM in 80 mM phosphate before 2-PPA-ANTS was partially enantioresolved, see Fig. 7. That 2-PPA-ANTS was enantioseparated at such high micelle concentration may be because of the strong hydrophilic character of the ANTS tag.

### Conclusions

The enantioseparation of derivatized phenoxy acid herbicides and degradation products of pyrethroid insecticides with various labeling agents (i.e., ANSA, ANDSA, and ANTS) was investigated by capillary electrophoresis. The magnitude of enantioseparation was shown to vary greatly among the fluorescent labels, with ANDSA providing the best overall enantioresolution. Furthermore, a change in enantioresolution was observed when changing the ionic strength as well as the nature and concentration of the alkylglycoside surfactant, i.e., OG and OM.



**Figure 6.** Electropherograms of (a) ANSA and (b) ANDSA derivatives. Conditions: running electrolyte, 175 mM phosphate, pH 6.5, containing 30 mM OM. Other conditions as in Figure 1.



**Figure 7.** Electropherogram of 2-PPA labeled with ANTS. Conditions: running electrolyte, 80 mM sodium phosphate, pH 6.5, containing 100 mM OM; voltage, 25 kV. Other conditions are the same as in Fig. 1.

## References

1. Mechref, Y. El Rassi, Z., *Chirality*, **1996**, *6*, 515-524.
2. Mechref, Y. El Rassi, Z., *J. Chromatogr. A*, **1997**, *757*, 263-273.
3. Mechref, Y. El Rassi, Z., *Electrophoresis*, **1997**, *18*, 220-226.
4. Karcher, A. El Rassi, Z., *Electrophoresis*, **1997**, *18*, 1173-1179.
5. Cavies, J.H., in: Leahey, J.P. (Ed.) *The Pyrethroid Insecticides*. Taylor & Francis, London, **1985**, 1-41.
6. Dombek, V. Stránsky, Z., *J. Chromatogr.*, **1989**, *470*, 235-240.
7. Dombek, V., *J. Chromatogr.*, **1991**, *545*, 427-435.
8. Dombek, V. Stránsky, Z., *Anal. Chim. Acta*, **1992**, *256*, 69-73.
9. Brito, R.M.M. Vaz, W.L.C., *Anal. Biochem.*, **1986**, *152*, 250-255.
10. Chattopadhyay, A. London, E., *Anal. Biochem.*, **1984**, *139*, 408-412.

## CHAPTER V

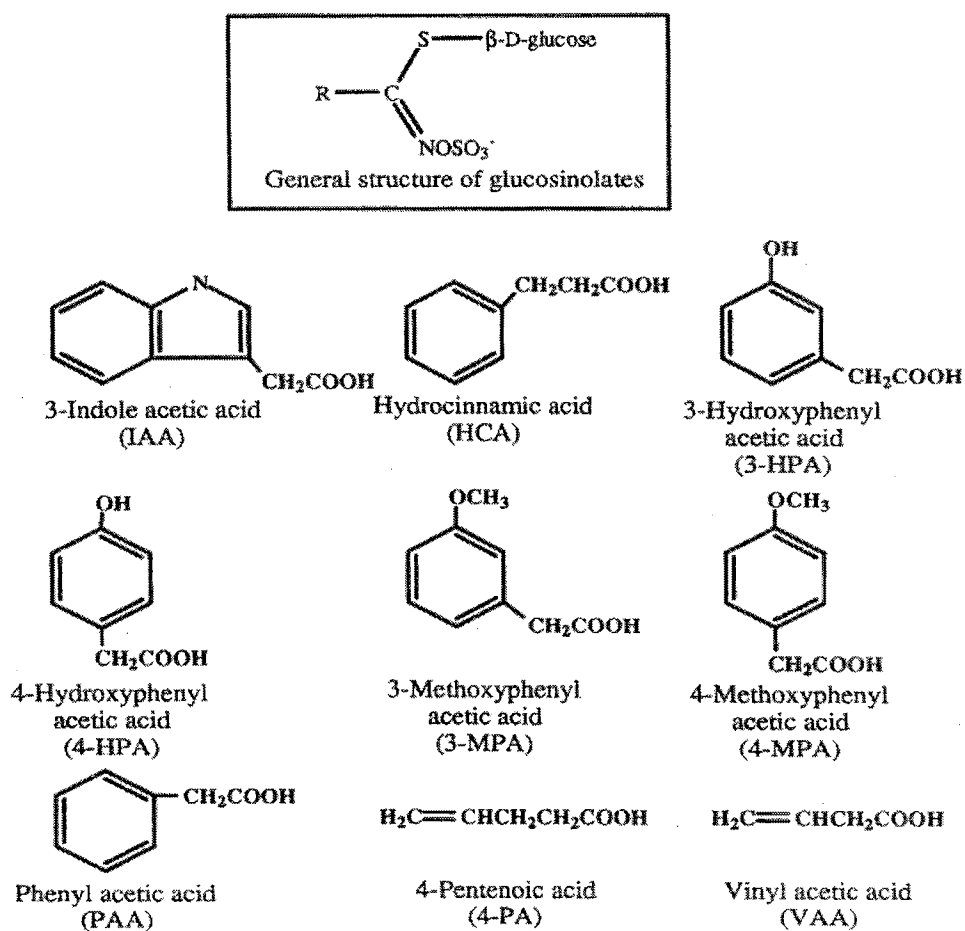
### CAPILLARY ELECTROPHORESIS OF THE FLUORESCENTLY LABELED ACID HYDROLYSIS PRODUCTS OF GLUCOSINOLATES—PROFILING OF GLUCOSINOLATES IN WHITE AND RED CABBAGES\*

#### Introduction

Glucosinolates are anionic thioglucosides whose structures vary mainly by the nature of the side chain (R-group) which can be aliphatic or aromatic, see Fig. 1. There are currently more than 100 known glucosinolates(1). All species of the Cruciferae family including forages, rapeseed, cole crops, mustards and horseradish contain one or more glucosinolates, occurring throughout the plant, in root, stem, leaf and seed(1-4). Several of these glucosinolate-containing taxa, possess vast economic importance. The major horticultural crop containing glucosinolates is cabbage, and it is consumed throughout the world including the USA by millions of tons. Glucosinolates are classified among the most important naturally occurring toxins in plant foodstuffs(5). Glucosinolates are associated with various flavor, off-flavor, and antinutritive effects and are involved in goitrogenic activity(5).

---

\* Published in *J. Liq. Chrom. & Rel. Technol.*, **1998**, *21*, 1411-32



**Figure 1.** General structure of glucosinolates and structures of the standard acid hydrolysis products used in this study. Characters in parenthesis represent the compounds abbreviation in this report.

The determination of glucosinolates has been performed by various analytical separation methods including gas chromatography (GC), GC-mass spectrometry (GC-MS)(6,7), high performance liquid chromatography (HPLC)(8,9) and HPLC-MS(10). Due to their ionic nature, glucosinolates are not directly amenable to GC and require a precolumn derivatization. High performance liquid phase separation methods such as HPLC and HPCE are therefore more readily applicable to the analysis of glucosinolates. In fact, HPLC using reversed-phase chromatography has been shown an efficient method for the isolation of intact glucosinolates(11,12). Very recently, high performance capillary electrophoresis (HPCE) has become an important tool in the analysis of glucosinolates. Using micellar electrokinetic chromatography (MECC), Sørensen et al. effectively separated eleven intact glucosinolates from double-low rapeseed(13). In another report from the same research group, HPCE proved useful in the determination of indolyl glucosinolates and their transformation products(14).

One existing major difficulty in the analysis of glucosinolates is the lack of authentic standards. In fact, among the 100 known glucosinolates, only one of them, namely sinigrin (i.e. allylglucosinolate) is available from commercial sources as a relatively pure standard. This makes routine analysis of glucosinolates in food and feed very difficult to achieve. To overcome this difficulty, glucosinolates can be readily broken down by chemical and enzymatic means into fragments reflective of the individual glucosinolates. Several of these degradation products are available as relatively pure standards or can be synthesized readily and more easily than the parent glucosinolates. Usually, glucosinolates occur in food and feed together with a hydrolyzing enzyme called myrosinase. When a part of a given plant is masticated or



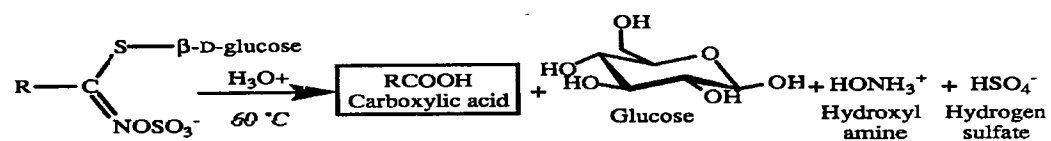
crushed, the myrosinase comes into contact with the glucosinolates and hydrolyzes them into fragments that are reflective of the parent glucosinolates(1,2). There are also chemical means that can be used to degrade glucosinolates(15). For instance, acid hydrolysis of glucosinolates yields carboxylated degradation products as seen in Fig. 2. Although these carboxylated degradation products can be used for the determination of individual glucosinolates, some of them lack strong chromophores needed for adequate UV detection (see Fig. 1). Thus, there is a need to develop a method for the rapid and sensitive analysis of glucosinolates through their degradation products. Usually, the degradation products offer reactive sites for the attachment of fluorescent tags.

The aim of this chapter, which is a continuation to our laboratories previous investigation(16), is to introduce a selective precolumn derivatization for the sensitive determination of glucosinolates via their acid hydrolysis degradation products. This involves the targeting of the degradation products in real world samples with a specific reagent, which converts the degradation products to fluorescently labeled derivatives independently of the origin of the glucosinolate sample. This should enable the rapid HPCE-laser induced fluorescence (LIF) detection of the parent glucosinolates.

## Materials and Methods

### Reagents and Materials

The acid hydrolysis standards of the glucosinolates including 4-methoxyphenylacetic acid (4-MPA), 3-methoxyphenylacetic acid (3-MPA), 4-hydroxyphenylacetic acid (4-HPA), phenylacetic acid (PAA), 3-hydroxyphenylacetic acid (3-HPA), hydrocinnamic acid (HCA), 4-pentenoic acid (4-PA) and vinylacetic acid



**Figure 2.** Reaction scheme depicting the products produced from the acid hydrolysis of a glucosinolate.

(VAA) were purchased from Aldrich (Milwaukee, WI, USA), while indole-3-acetic acid (IAA) was purchased from Sigma (St. Louis, MO, USA). Structures for the acid hydrolysis product standards are given in Fig. 1. Red and white cabbages were purchased from a local grocery outlet. Octyl- $\beta$ -D-glucopyranoside (OG) was purchased from Anatrace (Mumee, OH, USA). A 1.0 M solution of 1,3-dicyclohexylcarbodiimide (DCC) dissolved in dichloromethane and 1,1'-binaphthyl-2,2'-diyl hydrogenphosphate were purchased from Aldrich. The precolumn labeling agent 7-aminonaphthalene-1,3-disulfonic acid (ANDSA) was purchased from TCI America Inc. (Portland, OR, USA). Myrosinase (thioglucosidase, EC 3.2.3.1) used in the enzymatic hydrolysis of glucosinolates was purchased from Sigma. One unit of myrosinase produces 1.0  $\mu$ mole glucose per min from sinigrin (a glucosinolate) at pH 6.0 and at 25 °C.

#### Capillary Electrophoresis Instruments

Two Beckman P/ACE instruments (Fullerton, CA, USA) were used. They consisted of Models 5510 and 5010 equipped with a diode array detector and an Ominichrome (Chino, CA, USA) Model 3056-8M He-Cd laser multimode, 8 mW at 325 nm, respectively. By use of the instruments thermostating capabilities, the temperature of the capillary was held constant at 25 °C. A personal computer and P/ACE Station software were utilized for data handling purposes. The UV detection of the underivatized acid hydrolysis standards was performed at 200 nm. The UV detection of the ANDSA labeled derivatives was performed at 255 nm. A wavelength of 225 nm was selected for the detection of intact glucosinolates. For the LIF detection of the ANDSA derivatives, a fluorescence emission band-pass filter of  $380 \pm 2$  nm and  $420 \pm 2$  nm were purchased

from Corion (Holliston, MA, USA). A 360 nm cut-on filter purchased from Corion was used to reject the laser beam. All experiments were performed in fused-silica capillaries obtained from Polymicro Technology (Phoenix, AZ, USA). The dimensions of the capillaries were 50 cm to the detection window and 57 cm total length with 50  $\mu\text{m}$  internal diameter and 365  $\mu\text{m}$  outer diameter. Samples were pressure injected at 0.034 bar (i.e., 3.5 kPa) for various lengths of time. Between runs, the capillary was rinsed with 0.1 M NaOH, distilled water, and running electrolyte for two, three and one minute, respectively.

### Procedures

#### Extraction and acid hydrolysis of glucosinolates from red and white cabbages.

The extraction of the glucosinolates from both the white and red cabbages was performed by the following procedures(15). One leaf of cabbage was carefully removed, weighed and frozen with liquid nitrogen. The frozen leaf was then placed in a freeze drying apparatus and dried for twenty-four hours. A mortar and pestle that had been previously cooled to -5 °C was used to grind the dried cabbage leaf. Immediately following grinding, approximately 25 mL of boiling methanol was pipetted over the ground leaf. The resulting mixture was filtered through a Whatman # 1 filter to remove the solid particulates, with the filtrate containing the intact glucosinolates. In another extraction procedure cabbage leaves (60 g) were placed in a dewar containing liquid nitrogen until frozen. The frozen leaves were then ground to a fine solid in a Regal Coffee Grinder (Kewaskum, WI). The ground cabbage was then placed in a beaker containing 70 mL of boiling methanol. The methanol-ground cabbage mixture was heated at 65 °C for 10 min.

After cooling, the resulting mixture was filtered as above to yield the methanol which contained the glucosinolates.

The filtrate (obtained from both types of extraction) was equally split into vials amenable for evaporation via a speed vacuum concentrator and the methanol was removed. A portion of the extract was acid hydrolyzed with 6 M HCl(17). The resulting solution was evaporated by speed vacuum and reconstituted with 2 mL of dry pyridine. A representative reaction scheme for the acid hydrolysis of glucosinolates is illustrated in Fig. 2.

Precolumn derivatization of the acid hydrolysis products of glucosinolates. The standard acid hydrolysis products were tagged according to our published procedure(18-20) by first mixing 2.0 mL of a  $2.0 \times 10^{-3}$  M solution of the analyte dissolved in dry pyridine. The appropriate amount of DCC was added to these solutions, followed by the appropriate mass of ANDSA to yield a  $20 \times 10^{-3}$  M solution. This was allowed to react overnight, and the pyridine was removed via speed vacuum. The solution was prepared for analysis by redissolving the derivatized analyte with a 50% aqueous-acetonitrile solution.

To derivatize the acid hydrolysis products obtained from the red and white cabbage samples, a slightly different precolumn derivatization procedure was used. Enough DCC was added to the final pyridine solution obtained from the acid hydrolysis procedure to produce a concentration of  $20 \times 10^{-3}$  M. To this, the correct mass of ANDSA was added to yield a 0.10 M solution. Upon reaction, the pyridine was evaporated, and the tagged analyte was redissolved with the previously stated acetonitrile solution. This solution was analyzed by CE to profile some of the glucosinolates present

in the red and white cabbage leaves.

## Results and Discussion

### Precolumn Derivatization, Fluorescence Properties and Limits of Detection

Figure 3 shows two typical derivatives of the acid hydrolysis products with ANDSA. In this derivatization reaction, a stable amide bond is formed by condensation between the amino group of ANDSA and the carboxylic group of the analyte(21,22). The extent of the precolumn derivatization with ANDSA was assessed by CE using 1,1'-binaphthyl-2,2'-diyl hydrogenphosphate as the internal standard under the running conditions of Fig. 4. Table 1 lists the yields of this derivatization procedure for some of the acid hydrolysis standards. The derivatization is highly quantitative as indicated by the percent derivatized which ranged from 88% for 4-MPA to a high of 94% for IAA. Figure 4 shows typical electropherograms obtained before and after derivatization for IAA where it can be seen that the amount of remaining underivatized IAA can be hardly seen.

Figure 5 shows the fluorescence spectra obtained for four of the acid hydrolysis product standards labeled with ANDSA. Each of the spectra was obtained with the concentration of each individual derivative constant. This spectral information provided the insight for optimum working conditions for detection with the LIF system. Utilizing this information, the 380 nm band pass filter was chosen. Figure 5 shows that the 325 nm laser excitation source provides an excellent source for the fluorescence of these derivatized analytes. Both the emission and excitation spectra support the data for the LOD studies, see next page.

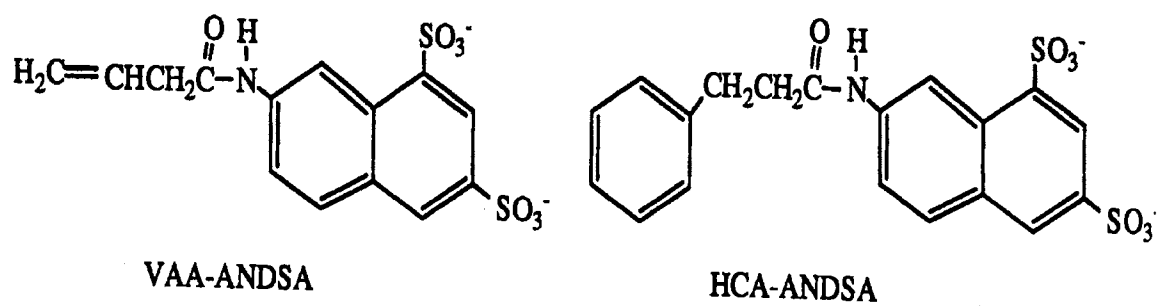
Table I

PERCENT DERIVATIZED AND LIMITS OF DETECTION OF THE ACID  
HYDROLYSIS PRODUCT STANDARDS OF THE GLUCOSINOLATES.  
FOR FLUORESCENCE DETECTION  $\lambda_{\text{ex}} = 325 \text{ nm}$   
(the He/Cd 325 nm laser line)  
and  $\lambda_{\text{em}} = 380 \text{ nm}$ .

Analyte	Percent derivatized	UV LOD at 200 nm of underivatized	UV LOD at 255 nm of ANDSA derivaitves (M)	LIF LOD of ANDSA derivatives (M)
IAA	94	$2.9 \times 10^{-5}$	$2.0 \times 10^{-5}$	$9.4 \times 10^{-6}$ $2.4 \times 10^{-5}$
4-HPA	93	$2.0 \times 10^{-5}$	$1.0 \times 10^{-5}$	$1.9 \times 10^{-6}$
4-MPA	88	$2.0 \times 10^{-5}$	$1.0 \times 10^{-5}$	$4.4 \times 10^{-7}$
4-PA	91	$4.0 \times 10^{-4}$	$1.0 \times 10^{-5}$	$8.5 \times 10^{-7}$
PAA	88	$8.5 \times 10^{-5}$	$1.8 \times 10^{-5}$	$2.0 \times 10^{-7}$
HCA	93	$2.0 \times 10^{-5}$	$1.0 \times 10^{-5}$	$2.5 \times 10^{-8}$
VAA	-	$1.0 \times 10^{-3}$	$1.0 \times 10^{-5}$	$4.0 \times 10^{-7}$

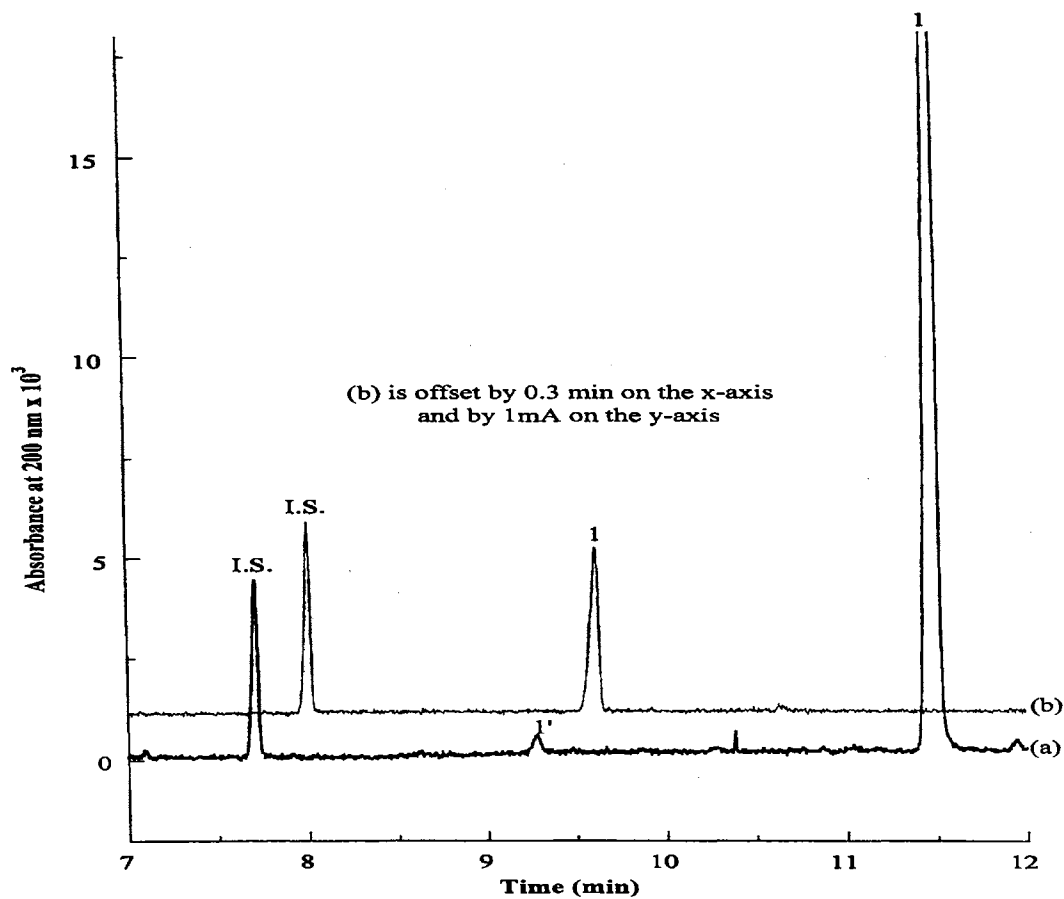
The two strongest fluorescing species, namely HCA-ANDSA and VAA-ANDSA, show the most intense emission and excitation spectra.

Table 1 lists the limits of detection that were determined using UV and LIF detection schemes. The LOD for the underivatized analytes closely parallels that for the derivatized analytes. All those containing aromatic groups (e.g., 4-HPA, 4-MPA, PAA and HCA) allowed adequate UV detection ranging from  $8.5 \times 10^{-5} \text{ M}$  to  $2.0 \times 10^{-5} \text{ M}$ . Some of the other hydrolytic products (e.g., 4-PA and VAA) listed in Fig. 1, lack strong chromophoric centers needed for sensitive UV detection. The LIF detection scheme decreased the overall LOD for 4-MPA by almost two orders of magnitude from  $2.0 \times 10^{-5}$

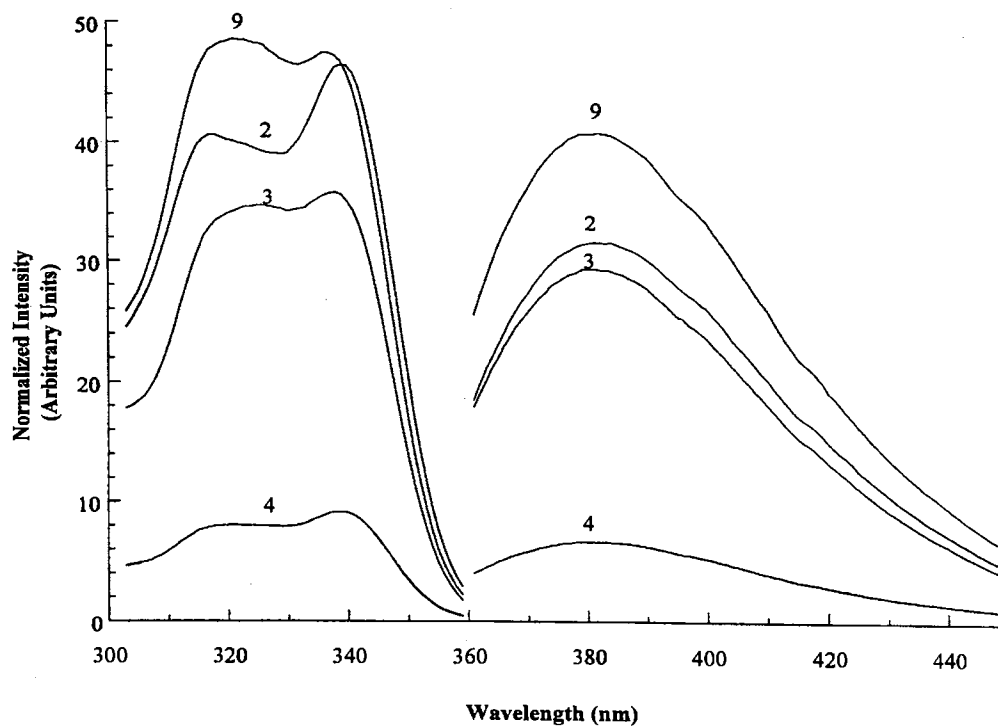


**Figure 3.** Two representative ANDSA derivatives of the acid hydrolysis products of glucosinolates.





**Figure 4.** Electropherograms of IAA (a) before and (b) after derivatization with ANDSA. Electrolyte: 50 mM sodium phosphate, pH 6.5; 15 kV; 25 °C; capillary, fused-silica,  $l = 50$  cm,  $L = 57$  cm,  $50 \mu\text{m}$  i.d.. Solutes: I.S., internal standard; 1', underivatized IAA; 1, IAA-ANDSA derivative.

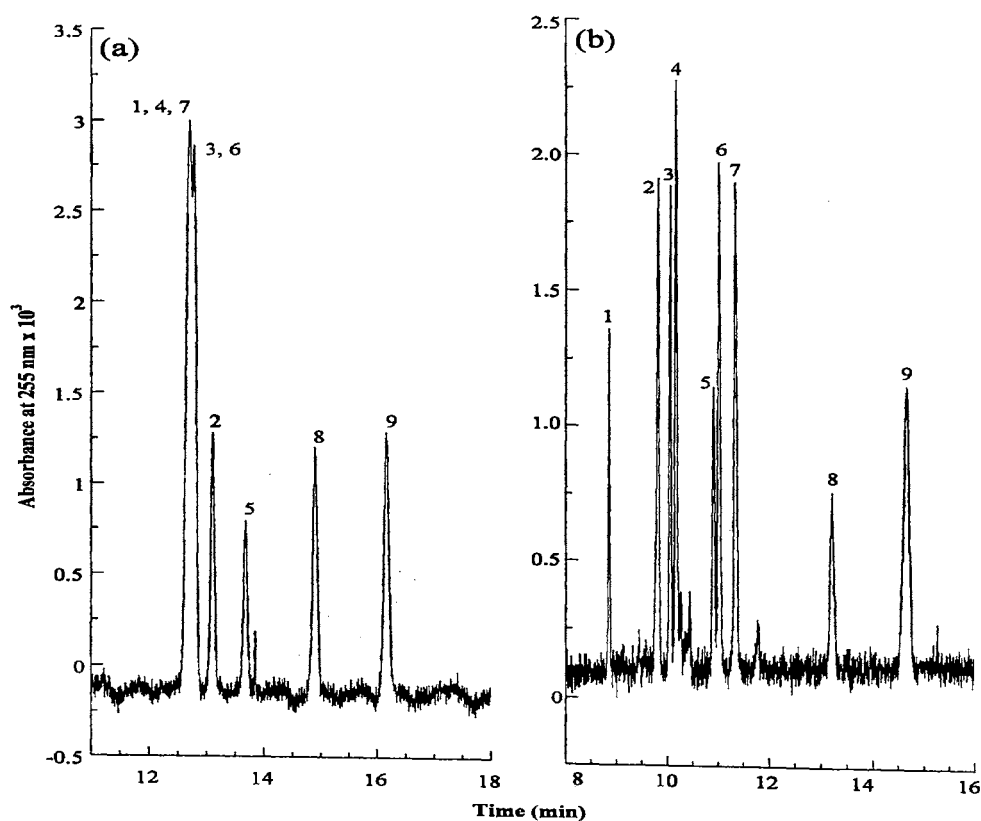


**Figure 5.** Excitation and emission spectra for four of the ANDSA derivatized acid hydrolysis products. (2), HCA-ANDSA; (3), 4-MPA-ANDSA; (4), 4-HPA-ANDSA; (9), VAA-ANDSA.

M with UV to  $4.4 \times 10^{-7}$  M with LIF. The lowest LOD for LIF detection was  $2.5 \times 10^{-8}$  M for the HCA derivative. For VAA labeled with ANDSA the LIF LOD was  $4 \times 10^{-7}$  M compared to that of 1 mM for UV detection. IAA exhibited a high LIF LOD. This can be explained by the fluorescence quenching of the indole ring(23). The LIF LOD for IAA can be slightly lowered by using a 420 nm band pass filter at the expense of higher LOD's for the remaining analytes.

#### Capillary Electrophoresis with a Neutral Surfactant System

Using 50 mM sodium phosphate, pH 6.5, as the running electrolyte, a 20 kV applied voltage and a separation distance of 50 cm, the underivatized standard analytes shown in Fig. 1 migrated over a narrow range of time from 9.44 to 10.65 min. IAA migrated first (at 9.44 min) separated from HCA (at 9.66 min), while 3-MPA and 4-MPA co-migrated at 9.729 min and also PAA, 3-HPA and 4-HPA co-migrated at 10.65 min. The separation was improved by incorporating 200 mM OG in 100 mM sodium phosphate while keeping other conditions the same. However, PAA and 4-PA co-migrated at 17.86 min (results not shown). Upon tagging the standard carboxylic acids with ANDSA, the derivatives migrated slower toward the detection end than the underivatized analytes due to the increased charge-to-mass ratios. A typical electropherogram of the ANDSA labeled analytes run with 50 mM sodium phosphate, pH 6.5 as the running electrolyte is shown Fig. 6a. Although a slight change in the migration order occurred as compared to the underivatized analytes, the complete separation of all ANDSA derivatives solely on the basis of small differences in the charge-to-mass ratio is still not achievable under the specified conditions. This is



**Figure 6.** Electropherogram of the ANDSA derivatives of the acid hydrolysis product standards. Electrolytes: (a) 50 mM sodium phosphate, pH 6.5; (b), same as in (a) containing 50 mM OG. Solutes: (1), IAA; (2), HCA; (3), 3-MPA; (4), 4-MPA; (5), PAA; (6), 3-HPA; (7), 4-HPA; (8), 4-PA; (9), VAA. Other conditions as in Fig. 4.

particularly true for two pairs of positional isomers, namely 4-MPA/3-MPA and 4-HPA/3-HPA. Table 2 lists the charge-to-mass ratio for the nine ANDSA derivatized

Table II

CHARGE-TO-MASS RATIOS FOR THE ANDSA DERIVATIVES OF THE ACID  
HYDROLYSIS PRODUCT STANDARDS.

Analyte	(Charge-to-mass ratio) x 10 <sup>5</sup>
IAA	-3.85
3-MPA, 4-MPA	-3.94
3-HPA, 4-HPA	-4.05
HCA	-4.07
PAA	-4.19
4-PA	-4.53
VAA	-4.68

analytes. Overall, the charge-to-mass ratio for many of the analytes are similar making the separation on this basis alone difficult. As shown in Fig. 6b, the complete separation of the ANDSA derivatives has required the incorporation of OG in the running electrolyte while keeping other conditions the same. The optimum separation conditions for the ANDSA labeled acid hydrolysis product standards was determined via changing the amount of alkylglucoside surfactant (i.e., OG) at a constant sodium phosphate concentration in the running electrolyte or vice versa. For this system the optimum concentration of OG surfactant was 50 mM, and the corresponding optimum sodium phosphate concentration was 50 mM at a pH of 6.5.

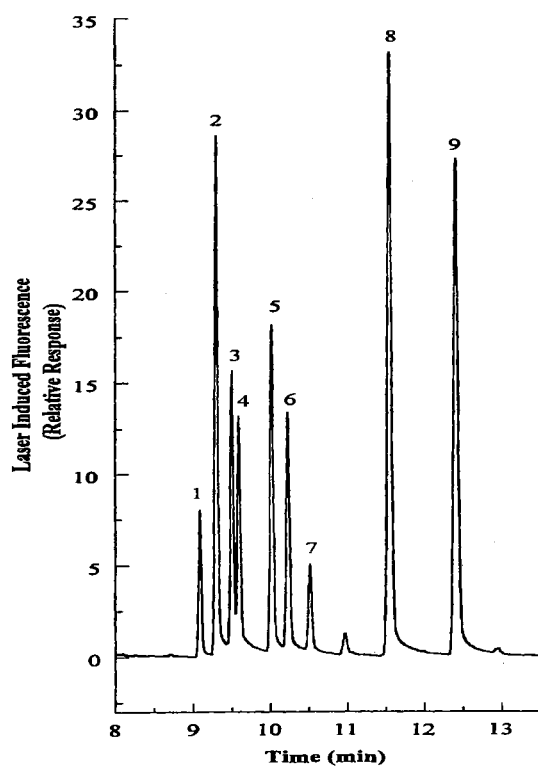
In the CZE system just described, the OG surfactant which is functioning as a hydrophobic selector(18,24), effectively separated all of the nine ANDSA labeled acid hydrolysis product standards. The neutral micelle migrates with the EOF and the most

hydrophobic species elute first and the least hydrophobic species elute last(18,24). Of course, in the presence of the OG neutral micellar phase, the charge-to-mass ratios also influenced the migration of the analytes. For the positional isomers, the separation rested primarily on the hydrophobic character of the solute. Different positioning of the same functional group on a molecule allows positional isomers to exhibit different hydrophobicities. From Fig. 6b, with the OG micelle functioning as a hydrophobic selector, the positional isomers with the methoxy and hydroxyl groups (3-MPA and 3-HPA) in the meta position elute first, therefore indicating that they are more hydrophobic than the isomers with the ortho substituents.

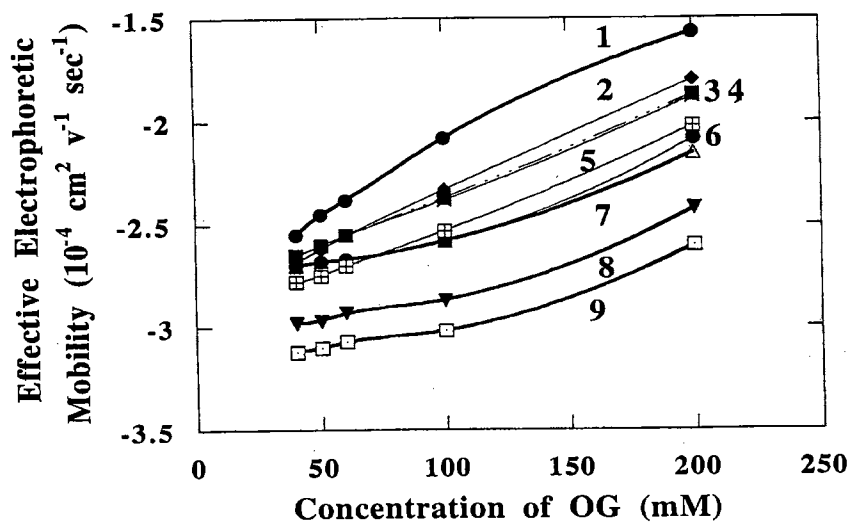
#### Capillary Electrophoresis with In-Situ Charged Surfactant System

Electrolyte systems containing in situ charged surfactants are generated by complexing alkylglycoside surfactants via their sugar head groups with borate(25-31). On this basis, OG can be converted readily to an anionic species in the presence of borate, and at a surfactant concentration above the CMC, an in situ charged micellar system is obtained. Figure 7 shows the separation of the ANDSA labeled acid degradation products using LIF detection and the OG-borate complex as the running electrolyte. Because of the charge introduced dynamically to the OG, the selectivity of the OG-borate electrolyte can be varied over a wide range by varying the charge on the micelle. One way to vary the surface charge density of the OG-borate micelle is through varying the OG concentration(25-31).

Figure 8 shows the effective electrophoretic mobilities for the derivatized analytes as a function of OG concentration at fixed borate concentration and pH. At low



**Figure 7.** Electropherogram of the ANDSA derivatives of the acid hydrolysis product standards obtained by LIF detection. Electrolytes: 200 mM borate, pH 8.0, containing 200 mM OG. Solutes as in Fig. 6. Other conditions as in Fig. 4.



**Figure 8.** Plots of the effective electrophoretic mobility of the ANDSA derivatives of the acid hydrolysis product standards as a function of the OG concentration in the running electrolyte containing 200 mM borate, pH 8.0. Lines: (1), IAA; (2), HCA; (3), 3-MPA; (4), 4-MPA; (5), PAA; (6), 3-HPA; (7), 4-HPA; (8), 4-PA; (9), VAA. Other conditions as in Fig. 4.



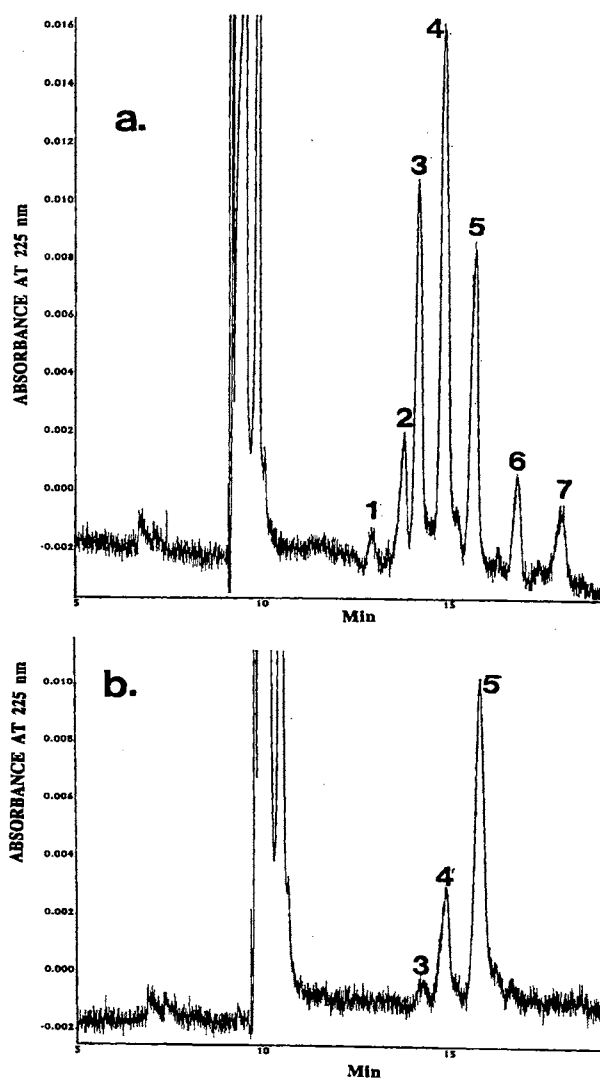
concentrations of OG, many of the analytes exhibit similar effective mobilities which is expected because there are positional isomers. It takes addition of about 200 mM OG to the running electrolyte (i.e., 200 mM borate, pH 8.0) for all of the analytes to exhibit different mobility values. As the amount of OG was increased from 40 mM to 200 mM, the negative surface charge density of the micelle decreased, a fact that decreased the extent of repulsion between the micelle and analytes thus leading to a stronger association between the negatively charged solutes and micelles.

As can be seen in Fig. 8, with the charged micelle system the optimum concentration of OG was 200 mM in 200 mM borate, pH 8.0. The efficiency for this surfactant system was 298000 compared to 250000 for the efficiency for the CE with the neutral micellar system. Thus, inducing repulsion between the solute and micelle could alter the selectivity of the micelle and provide different separation conditions. At 200 mM OG and 200 mM borate, the migration order for the analytes resembles that for the neutral micellar system. By increasing the amount of surfactant, the amount of complexation with borate is reduced, making the MECC system behave similar to the CZE system.

#### Profiling of Glucosinolates in Cabbages

To assess the utility of the method described here, which consists of detecting glucosinolates via their acid degradation products, it was important first to determine the number of detectable intact glucosinolates in the cabbage. From this piece of information, and using a given detection system, one would expect to find at least a similar number of the side chain degradation products. A white cabbage sample extracted according to the

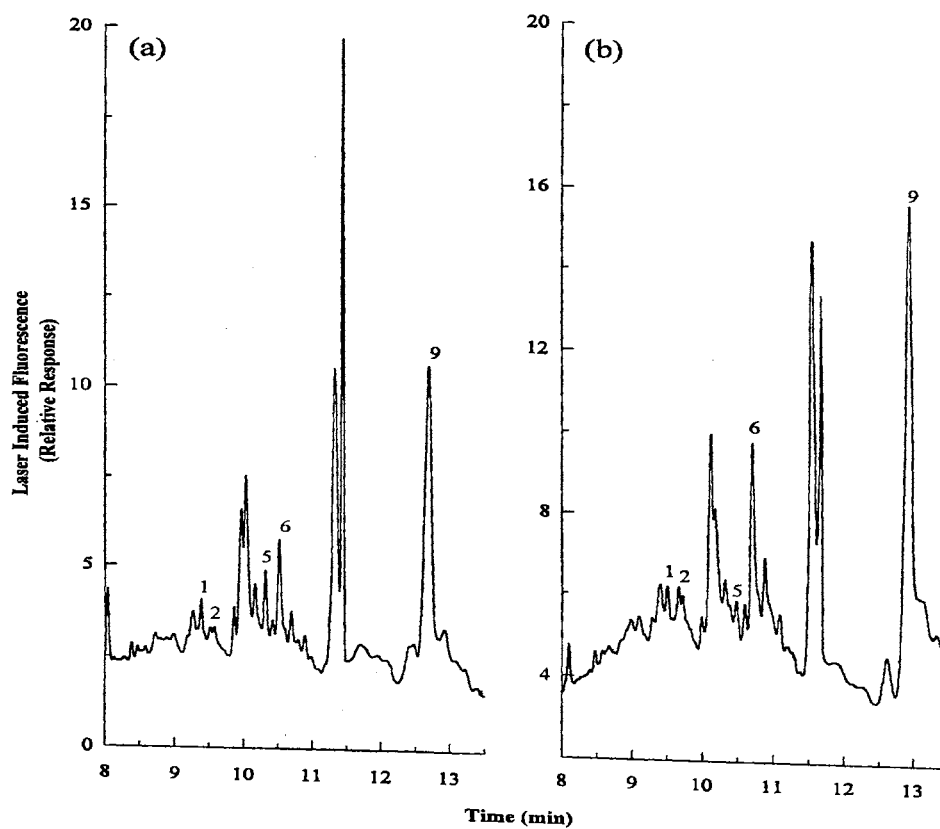
second procedure described in the experimental section was analyzed by CE. Fig. 9 shows the electropherograms before and after treatment of the extract with myrosinase. As can be seen in Fig. 9a, the peak numbered 5 seems to be an acidic solute of nonglucosinolate nature, while the others are glucosinolates because they disappeared from the electropherogram after treatment with myrosinase, compare Fig. 9a and 9b. However, peaks numbered 3 and 4 contain small amounts of negatively charged nonglucosinolate compounds. Peak number 6 is sinigrin as confirmed by spiking the sample with this glucosinolate standard. Upon myrosinase digestion of the glucosinolates in the white cabbage sample, the peak corresponding to the EOF has increased in size due to the generation of neutral compounds. The neutral products are most likely to be isothiocyanates ( $R-N=C=S$ ), thiocyanate ( $R-S-C\equiv N$ ) and nitriles ( $R-C\equiv N$ )(2,3). This indicates that in the white cabbage sample there are at least 6 glucosinolates. According to recent reports on glucosinolate content of cabbages, white cabbage contains large amounts of glucosinolates with three-carbon chains (e.g., allylglucosinolate or sinigrin and 3-methylsulfinylpropylglucosinolate), while red cabbage contains more of the four-carbon glucosinolates (e.g., 4-methylsulfinylbutylglucosinolate). Both cabbages contain 3-indolylmethylglucosinolates (including both 3-indolylmethylglucosinolate and 3-(*N*-methoxy)indolylmethylglucosinolate)(2), see Table 3. Minor glucosinolates are 3-butenylglucosinolates and 2(*R*)-hydroxy-3-butenylglucosinolate, 2-phenylethylglucosinolate(2), while 3-methylthiopropylglucosinolate, butenylglucosinolate, 4-methylsulfonylbutylglucosinolate and benzylglucosinolates(2) are present in lesser amounts. Other references have listed the presence of propylglucosinolate, butylglucosinolate, and methylthiomethylglucosinolate(32). This



**Figure 9.** Analysis of white cabbage extract by HPCE-UV (a) before and (b) after myrosinase treatment. Electrolyte: 150 mM phosphate, pH 6.5, containing 100 mM OG; running voltage, 17 kV. Other conditions as in Fig. 4.

brings the number of possible glucosinolates that may occur in cabbages to around 14. However, considerable variation was reported to occur in both individual and total glucosinolate content due to genetic origin and nature of the growing plant as well as the age, the cultural and environmental factors associated with the growth of a particular plant(32). Returning to Fig. 9 which shows the intact glucosinolates, it is not surprising to see that most of the glucosinolates are hardly detected due to the fact that most of the glucosinolates reported to occur in cabbage have R side chains that lack strong chromophores. The only glucosinolates that may absorb well in the UV are 3-indolylmethylglucosinolates, 2-phenylethylglucosinolate and benzylglucosinolate. But only 3-indolylmethylglucosinolates are abundant enough to be detected.

Following the extraction, acid hydrolysis and derivatization procedures for the glucosinolates from both the red and white cabbages, the samples were analyzed under the optimum conditions for separation by MECC. LIF detection was used to sensitively and selectively detect the acid hydrolysis products that are reflective of the glucosinolates and for which standards were available. Figs. 10a and 10b are typical electropherograms for the labeled acid hydrolysis products of the glucosinolates from red and white cabbages, respectively. As can be seen in this figure, several major and minor peaks can be detected indicating that cabbages may contain a larger number of glucosinolates than previously reported. LIF detection is more sensitive than any other detection approach used previously. By spiking the derivatized hydrolyzates from both red and white cabbages with the standard derivatized acids, one can detect the presence of glucosinolates whose degradation products are IAA, HCA, PAA, 3-HPA and VAA. Although the IAA is suppose to be the most abundant glucosinolate, its peak is not



**Figure 10.** Electropherograms of the ANDSA derivatives of the acid hydrolysis products from the cabbage samples. Samples: red cabbage in (a), white cabbage in (b). Solutes and electrolyte as in Fig. 7. Other conditions as in Fig. 4.

intense for both red and white cabbages. This is because the LIF limit of detection of the IAA is the highest, see Table 1.

## References

1. Heaney, R.K., Fenwick, G.R., "Identifying toxins and their effects: glucosinolates," in: *Natural Toxicants in Food, Progress and Prospects*, Watson, D.H. (Ed.), VCH, Weinheim, **1987**, pp. 76-109.
2. Van Etten, C.H., Tookey, H.L., "Chemistry and biological effects of glucosinolates," in: *Herbivores, Their Interaction with Secondary Plant Metabolites*, Rosenthal, G.A. Janzen, D.H. (Ed.), Academic Press, New York, **1979**, pp. 471-500.
3. Tookey, H.L., VanEtten, C.H., Daxenbichler, M.E., "Glucosinolates," in: *Toxic Constituents of Plant Foodstuffs*, Liener, I.E. (Ed.), Academic Press, New York, **1980**, pp. 103-142.
4. Heaney, R.K., Fenwick, G.R., "Glucosinolates," in: *Methods of Enzymatic Analysis*, Bergmeyer, H.U. (Ed.), VCH, Weinheim, **1984**, pp. 208-219.
5. Shibamoto, T., Bjeldanes, L.F., "Natural toxins in plant foodstuffs," in: *Introduction to Food Toxicology*, (Ed.), Academic Press, San Diego, **1993**.
6. MacLeod, A.J., MacLeod G., Reader, G., *Phytochemistry*, **1989**, 28, 1405-1407.
7. Chistensen, B.W., Ogaard Madison, J., *Tetrahedron*, **1982**, 38, 353-359.
8. Björkvist, B., Hase, A., *J. Chromatogr.*, **1988**, 435, 501-507.
9. Helboe, P., Olsen, O., Sorensen, H., *J. Chromatogr.*, **1980**, 197, 199-205.
10. Wolfender, J.-L., Maillard, M., Hostettmann, K., *Phytochem. Anal.*, **1994**, 5, 153-

182.

11. Prestera, T., Fahey, J.W., Holtzclaw, W.D., Abeygunawardana, C., Kachinski, J.L., Talalay, P., *Anal. Biochem.*, **1996**, *239*, 168-179.
12. Sang, J.P., Minchinton, I.R., Johnstone, P.K.T., *Can. J. Plant Sci.*, **1984**, *64*, 77-93.
13. Michaelsen, S., Møller, Sørensen, P., *J. Chromatogr.*, **1992**, *608*, 363-374.
14. Feldl, C., Møller, P., Otte, J., Sørensen, H., *Anal. Biochem.*, **1994**, *217*, 62-69.
15. McGregor, D.L., Mullin, W.J., Fenwick, G.R., *J. Assoc. Off. Anal. Chem.*, **1983**, *66*, 825-849.
16. Wasserkrug, K., El Rassi, Z., *J. Liq. Chromatogr.*, **1997**, *20*, 335-349.
17. Olsen, O., Sorensen, H., *Phytochemistry*, **1979**, *18*, 1547-1552.
18. Karcher, A., El Rassi, Z., *Electrophoresis*, **1997**, *18*, 1173-1179.
19. Mechref, Y., El Rassi, Z., *Anal. Chem.*, **1997**, *69*, 114-23.
20. Mechref, Y., Ostrander, G.K., El Rassi, Z., *Electrophoresis*, **1995**, *16*, 1499-1504.
21. Mechref, Y., El Rassi, Z., *Electrophoresis*, **1994**, *15*, 627-634.
22. Mechref, Y., Ostrander, G.K., El Rassi, Z., *J. Chromatogr. A*, **1995**, *695*, 83-95.
23. Berlman, I.B., Academic Press, New York, **1971**.
24. Mechref, Y., El Rassi, Z., *J. Chromatogr. A*, **1997**, *757*, 263-273.



25. Smith, J.T., Nashabeh, W., El Rassi, Z., *Anal. Chem.*, **1994**, *66*, 1119-1133.
26. Smith, J.T., El Rassi, Z., *J. Microcol. Sep.*, **1994**, *6*, 127-138.
27. Smith, J.T., El Rassi, Z., *J. Chromatogr. A*, **1994**, *685*, 131-143.
28. Smith, J.T., El Rassi, Z., *Electrophoresis*, **1994**, *15*, 1248-1259.
29. Mechref, Y., El Rassi, Z., *J. Chromatogr. A*, **1996**, *724*, 285-296.
30. Mechref, Y., Smith, J.T., El Rassi, Z., *J. Liq. Chromatogr.*, **1995**, *18*, 3769-3786.
31. Cai, J., El Rassi, Z., *J. Chromatogr.*, **1992**, *608*, 31-45.
32. Fenwick, G.R., Heaney, R.K., Mullin, W.J., *CRC Crit. Rev. Food Sci. Nutrition*, **1983**, *18*, 123-201.

## CHAPTER VI

# DETERMINATION OF INDIVIDUAL GLUCOSINOLATES IN CABBAGE AND RAPESEED BY LASER INDUCED FLUORESCENCE-CAPILLARY ELECTROPHORESIS VIA THE ENZYMATICALLY RELEASED ISOTHIOCYANATE AGLYCONES\*

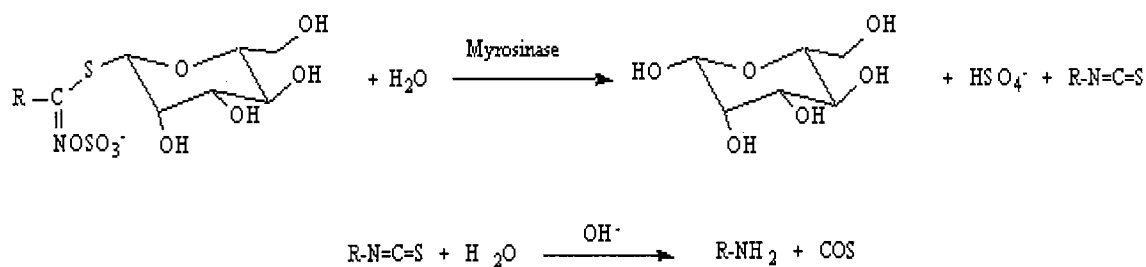
### Introduction

Glucosinolates (GS's) are important natural products (Figure 1) occurring mainly in plants of the Cruciferae family, e.g., broccoli, cabbage, radish, Brussels sprouts, etc.. GS's are found in all parts of the plant, i.e., in roots, stems, leaves, and seeds (5,6,13,15,17). GS's differ among themselves by the nature of the R group (Figure 1). This leads to a wide range of flavors, off-flavors and nutritive as well as toxic effects upon consumption of the crucifers (16).

As a continuation to our recent contribution to the determination of individual glucosinolates via the carboxylated and degradation products ( see chapter V) in a given plant tissue by capillary electrophoresis (CE) via the glucose released upon myrosinase digestion (Figure 1) (8), we are reporting here a CE method for the determination of individual GS's via the isothiocyanate degradation products that are obtained by the

---

\* Published in *J. Food Agric. Chem.*, **1999**, *47*, 4267-4274



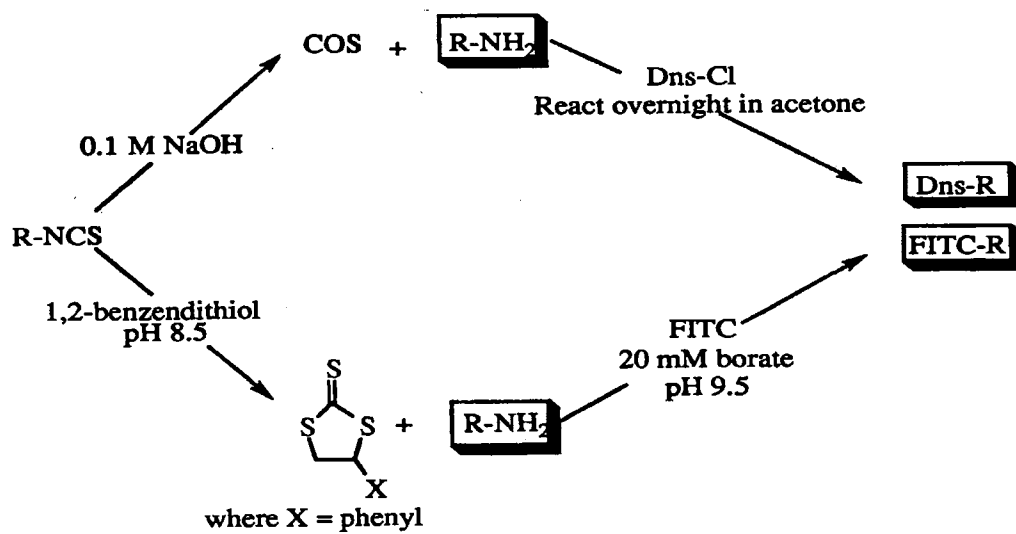
Where R =	Parent glucosinolate	Corresponding isothiocyanate	Corresponding FITC or Dns-Cl labeled amine
	Glucoberin	3-(methylsulfanyl)-propylisothiocyanate (Iberin) (1)	3-(methylsulfanyl)-propylamine (1)
	Glucoraphanin	4-(methylsulfinyl)-butylisothiocyanate (Sulphoraphane) (2)	4-(methylsulfinyl)-butylamine (2)
	Sinigrin	Allyl-NCS (3)	Allylamine (3)
	Glucotropaeolin	Benzyl-NCS (4)	Benzylamine (4)
	Gluconarsturtiin	Phenethyl-NCS (5)	Phenethylamine (5)
	Glucobrictin	4-Methoxyphenyl-NCS (6)	4-Methoxyphenylamine (6)

**Figure 1.** Degradation of GS's to isothiocyanates by the enzyme myrosinase, and the subsequent transformation of the isothiocyanates to amines upon base hydrolysis. Also, shown in this figure are the structures of the GS's for which standard isothiocyanates and amines were commercially available for our study.

myrosinase digestion of GS's. The structures of the isothiocyanate degradation products are reflective of their parent GS's. Myrosinase is an enzyme that accompanies the GS's in the same plant tissue. When the plant tissue is crushed or masticated, the enzyme myrosinase enters into an intimate contact with the GS's, and consequently hydrolyzes the GS's into glucose and their corresponding isothiocyanates (Figure 1). This natural enzymatic process was exploited in this chapter for the determination of the individual GS's. This was accomplished by first denaturing the endogenous myrosinase, followed by extracting the GS's from the plant of interest, and finally adding to the GS extract the exogenous myrosinase to produce the corresponding isothiocyanates. To enhance the detectability of the individual GS's via their corresponding isothiocyanates, the isothiocyanates were first converted to amine compounds and then the resulting amines were labeled with a fluorescent tag (Figure 2) for sensitive detection by laser-induced fluorescence (LIF).

The CE method described in this chapter for the determination of individual GS's via their isothiocyanate degradation products was based on micellar electrokinetic capillary chromatography (MECC) with in situ charged micelles. In situ charged micelles, which were introduced from our laboratory (2,11,14), consisted of glycosidic surfactants complexed with borate. The surface charge density of the resulting in situ charged glycosidic micelle can be conveniently varied by changing the pH and the borate concentration, thus allowing the adjustment of the migration time window to best suit a given separation problem (2,11,14).

The rationale behind the MECC-LIF method described here for the determination of GS's via their isothiocyanate degradation products is the lack of authentic GS



**Figure 2.** Reaction schemes for the conversion of isothiocyanates to amines via base hydrolysis or 1,2-benzenedithiol reaction, and the fluorescent labeling of the resulting amines with either Dns-Cl or FITC.

standards. In fact, only two GS standards are currently available from commercial sources. These are sinigrin (i.e., allyl glucosinolate) and gluconasturtiin. On the other hand, some of the isothiocyanate degradation products, whose structures are reflective of the parent GS's, are available as pure standards or can be readily synthesized. The applicability of the MECC-LIF method to the determination of individual GS's in real samples was demonstrated with extracts from rapeseed leaves, rapeseed roots and white cabbage.

## Materials and Methods

### Reagents and Materials

The isothiocyanates (R-NCS) including benzyl-NCS, allyl-NCS, phenethyl-NCS and 4-methoxyphenyl-NCS were purchased from Aldrich (Milwaukee, WI, USA). 3-(Methylsulfinyl)propyl-NCS (iberin) and 4-(methylsulfinyl)butyl-NCS (sulphoraphane) were purchased from LKT Labs (St. Paul, MN, USA). Structures for these aglycones produced from myrosinase hydrolysis of glucosinolates are shown in Figure 1. The myrosinase (thioglucosidase, EC 3.2.3.1) was purchased from Sigma (St. Louis, MO, USA). 1,2-Benzenedithiol that was used to convert the isothiocyanates to amines was also obtained from Aldrich. All the amines (R-NH<sub>2</sub>) including benzylamine, allylamine, phenethylamine, 4-methoxyphenylamine and the internal standard *N,N*-dimethylaniline, as well as the derivatizing agent, 5-dimethylamino-1-naphthalenesulfonyl chloride (Dns-Cl) and fluorescein isothiocyanate (FITC) were supplied by Aldrich. The two surfactants, n-octyl- $\beta$ -D-glucoside (OG) and n-nonyl- $\beta$ -D-glucoside (NG) were obtained from Anatrace (Mumee, OH, USA).

## Capillary Electrophoresis Instrument and Capillary Column

The instrument for CE was a Beckman P/ACE instrument (Fullerton, CA, USA). It consisted of a Model 5510 equipped with a diode array detector and an Omnichrome (Chino, CA, USA) Model 3056-8M He-Cd laser multimode, 8 mW at 325 nm. For the detection of the FITC derivatives, a Beckman Laser Pace System Model 488 was used as the excitation source. It consisted of a 3 mW 488 nm (air cooled) argon ion laser. Unless otherwise stated, in all experiments, the temperature of the capillary was held constant at 25 °C. A personal computer and P/ACE station software were utilized for data handling purposes. The UV detection of the isothiocyanates and their corresponding amines was performed at 200 nm. For the LIF detection of the fluorescent derivatives, a fluorescence emission band-pass filter of  $520 \pm 20$  nm was purchased from Corion (Holliston, MA, USA). A 360 nm cut-on filter obtained from Corion was used to reject the laser beam of the He-Cd and a 488 nm notch filter for rejection of the laser beam of the Ar ion laser. All experiments were performed in fused-silica capillaries obtained from Polymicro Technology (Phoenix, AZ, USA). The dimensions of the capillaries were 50 cm to the detection window and 57 cm total length with 50  $\mu$ m internal diameter and 365  $\mu$ m outer diameter. Samples were pressure injected at 0.034 bar (i.e., 3.5 kPa) for various lengths of time. Between runs, the capillary was rinsed with 0.1 M NaOH, distilled water, and running electrolyte for two, three and one minute, respectively.

### Sources of GS's

The GS standard was sinigrin, which was purchased from Sigma. The white cabbage was bought at a local grocery outlet. Dr. H.A. Melouk, USDA-ARS,

Department of Entomology and Plant Pathology, Oklahoma State University, grew the rapeseed plants in the USDA-ARS greenhouse in Stillwater, OK. At the time of the harvesting, the rapeseed plants (Dwarf Essex) were approximately ten inches tall and had been growing for 102 days.

#### Extraction of the Intact GS's and Their Isothiocyanate Degradation Products After Treatment with Myrosinase

The GS's from the cabbage and the rapeseed leaves and roots were extracted following the previously developed procedures (7,8), but with the following modifications. After isolating the intact GS's in methanol, four vials were dried via speed vac and then reconstituted with 250  $\mu$ L of a 50 mM sodium phosphate buffer pH 6.2. These solutions were combined and filtered through a 0.2  $\mu$ m Titan syringe filter from Scientific Resources Inc. (Eatontown, NJ, USA). To this solution, approximately 1.0 mg of solid myrosinase was added and stirred for one hour. After which 500  $\mu$ L of methylene chloride was pipetted into the solution and stirred. The organic layer, which contained the isothiocyanates, was removed and the aqueous solution was washed twice more with 500  $\mu$ L portions of methylene chloride. The combined washings were dried via speed vac, then reconstituted with acetonitrile and analyzed for isothiocyanate content.

#### Conversion of the Isothiocyanates to Amines by Reaction with 1,2-Benzenedithiol

The schematic of the reaction of 1,2-benzenedithiol with R-NCS is shown in Figure 2. This well established conversion has been previously performed by numerous



other research groups (1,21,22). Briefly, 25 mM of 1,2-benzenedithiol dissolved in methanol was mixed with 5.0 mM standard isothiocyanates in methanol and finally an equal volume of 100 mM potassium phosphate, pH 8.5, were added. This solution was stirred at room temperature for at least four hrs. Thereafter, the hydro-organic solution (i.e., water-organic mixture) was dried via speed vac and reconstituted in 600  $\mu$ L of methylene chloride ( $\text{CH}_2\text{Cl}_2$ ) and stored at 0  $^\circ\text{C}$ .

#### Conversion of the Isothiocyanates to Amines by Base Hydrolysis

For this reaction, 100  $\mu$ L of the R-NCS was pipetted into 300  $\mu$ L of 0.1 M NaOH and stirred magnetically. This chemical conversion of the R-NCS to amine is shown in Figure 2. Following this, the solution was dried under reduced pressure and reconstituted with  $\text{CH}_2\text{Cl}_2$  and stored at 0  $^\circ\text{C}$ .

#### Labeling of Amines with Dansyl Chloride

The reaction of dansyl chloride (Dns-Cl) with primary amines (Figure 2) has been studied in detail in numerous research reports, see (4) as a typical reference. Briefly, 300  $\mu$ L of the amine dissolved in methylene chloride was pipetted into an amber vial and roughly 30 mg of solid sodium carbonate was added. Following this, 320  $\mu$ L of an equal molar solution of Dns-Cl in acetone was added and heated at 45  $^\circ\text{C}$  for 45 min. Next, the volume of the solution was reduced to approximately 100  $\mu$ L via a gentle stream of nitrogen and allowed to react overnight at 45  $^\circ\text{C}$ . The solution was then dried via stream of nitrogen and reconstituted with acetonitrile and filtered through a 0.45  $\mu\text{m}$  syringe filter.

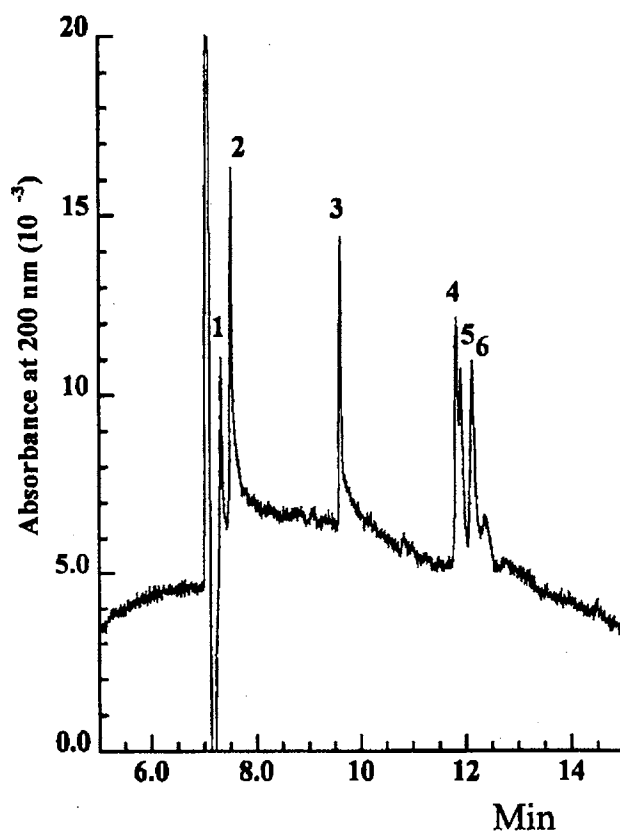
### Labeling of Amines with Fluorescein Isothiocyanate (FITC)

The labeling of the amine compounds with FITC was adapted from the procedure described by Li et al. (12). Briefly, 1.0 mL of  $1.0 \times 10^{-4}$  M analyte dissolved in 20 mM borate, pH 9.5, was reacted overnight with constant stirring with 40  $\mu$ L of  $2.5 \times 10^{-3}$  M FITC dissolved in acetone. To minimize degradation of the derivatives and initial reactants, all reactions and solutions were stored in amber vials. The schematic of this reaction is shown in Figure 2.

## Results and Discussion

### CE of Isothiocyanates

The CE profiling of GS's in a given plant tissue via their isothiocyanate degradation products (Figure 1) must be preceded by a CE method for the separation of standard isothiocyanates. In this regard, we first performed a systematic study on the optimum conditions for the micellar electrokinetic capillary chromatography (MECC) of some standard isothiocyanates of interest. It is well established that MECC is the most suitable CE approach for the separation of neutral solutes such as isothiocyanates. Figure 3 shows the optimum results, which were determined through a systematic study of pH, NG concentration and borate concentration. As can be seen in Figure 3, satisfactory separation of all the analytes was achieved for the sole purpose of qualitative analysis involving (i) the profiling of GS's via their isothiocyanate degradation products and (ii)



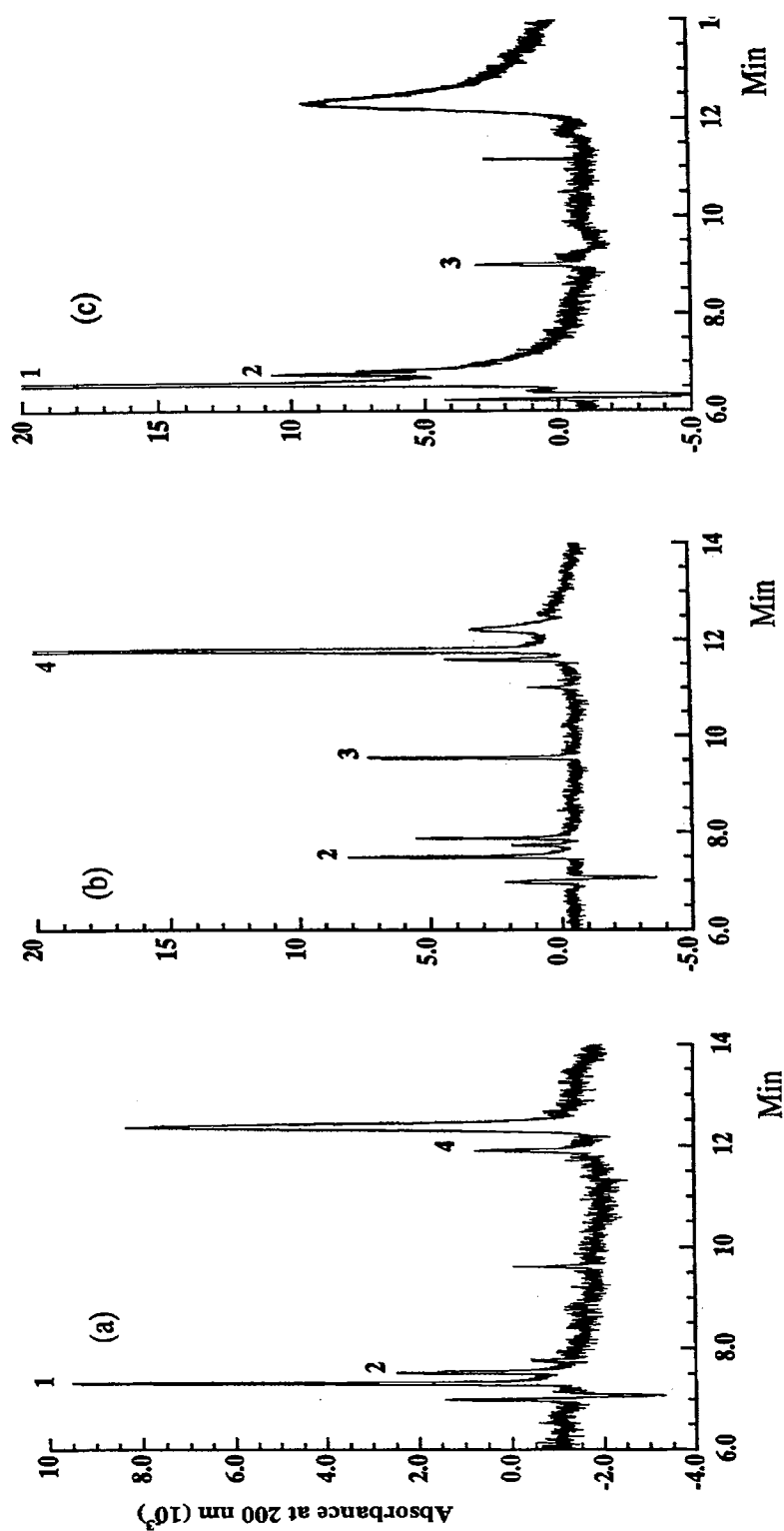
**Figure 3.** Separation of the standard isothiocyanates. Electrolyte: 200 mM borate, pH 9.5, containing 100 mM NG; voltage, 18 kV; thermostating the capillary, 25 °C; capillary, fused-silica,  $l = 50$  cm,  $L = 57$  cm, 50 mm i.d.. Solutes: (1), 3-(methylsulfinyl)propyl-NCS; (2), 4-(methylsulfinyl)butyl-NCS; (3), allyl-NCS; (4), benzyl-NCS; (5), phenethyl-NCS; (6), 4-methoxyphenyl-NCS.

the monitoring of the extent of the degradation of GS's to isothiocyanates by myrosinase(Figure 1). In general, isothiocyanates are reactive and degrade slowly to amines in aqueous media. Thus, the isothiocyanates liberated from the glucosinolates by the myrosinase action can only be qualitatively determined. From Figure 3, the isothiocyanates containing sulfinyl groups, e.g., iberin and sulphoraphane, yielded short migration times and eluted right after  $t_0$ , which is the time of an unretained species in MECC. This can be explained by the presence of the polar sulfinyl functional groups at the end of the molecules of both isothiocyanates, Figure 1. The other four analytes were much more retarded by the micellar system due to their greater hydrophobicity. Allyl-NCS eluted before the aromatic-NCS standards, which eluted in the order benzyl-NCS, phenethyl-NCS and 4-methoxyphenyl-NCS, respectively.

In summary, with the control over the amount of charge on the NG micelle via borate complexation, the migration time window was successfully adjusted to allow for the separation of both hydrophilic and hydrophobic isothiocyanate analytes. These optimum conditions were used for the analysis and profiling of the isothiocyanates from the rapeseed and cabbage samples, see the following section.

#### Profiling of Isothiocyanates in Fresh Rapeseed Leaves and Roots, and in Fresh White Cabbage

Figure 4a, 4b and 4c show the electropherograms of the methanol extracts of the rapeseed leaves and roots, and cabbage, respectively. From Figure 4a, it can be seen that there are at least three identifiable isothiocyanates in the rapeseed leaves. Through successive spiking of the rapeseed leaf extract with standard isothiocyanates, the three



**Figure 4.** Profiling of the isothiocyanates in rapeseed leaves (a) in rapeseed roots (b) and in white cabbage (c) by HPCE-UV. Other conditions as described in the legend to Figure 3.

isothiocyanates were determined to be iberin, sulphoraphane, and benzyl-NCS. Likewise, there are at least three identifiable isothiocyanates contained in the extract of the rapeseed roots (Figure 4b). These were determined to be sulphoraphane, allyl-NCS and benzyl-NCS. The three identifiable isothiocyanates present in the cabbage extract were determined to be iberin, sulphoraphane and allyl-NCS (Figure 4c).

In a previous article from our laboratory (8), we reported at least nine minor intact glucosinolates and two major glucosinolates in the rapeseed leaves totaling eleven intact glucosinolates. In that same report, we also observed that there are five minor intact glucosinolates in the rapeseed roots, and one major and six minor intact glucosinolates in the white cabbage. By inspecting Figure 4a, it can be seen that in the extract of the rapeseed leaves there are two major peaks with one of them corresponding to iberin and four other possible minor isothiocyanates. The examination of Figure 4b shows that the rapeseed roots contain one major isothiocyanate corresponding to benzyl-NCS and possibly six other minor isothiocyanates. Furthermore, there is one major isothiocyanate corresponding to iberin and three minor possible isothiocyanates in the cabbage (Figure 4c). In all cases (i.e., Figure 4a, 4b and 4c), the few other peaks that may correspond to other isothiocyanates could not be identified due to the limited number of isothiocyanate standards that are commercially available at this point in time.

The observed, reduced number of isothiocyanates with respect to the number of intact GS's previously reported in the extracts from rapeseed roots and leaves and from white cabbage (8) may be explained as follows. Most of the isothiocyanates lack strong chromophores needed for adequate UV detection, a fact that renders their detection at low levels extremely difficult. In fact, from the UV spectra of sinigrin, allyl-NCS and

allylamine, the molar absorptivities were calculated to be 8244, 3890 and 351  $M^{-1}cm^{-1}$  at 228 nm, respectively, and 4531, 3890 and 1519  $M^{-1}cm^{-1}$  at 204 nm, respectively. While 228 nm is the best wavelength for maximum absorbance by GS's, 204 nm is the wavelength where isothiocyanates and amines exhibit the maximum absorbance. These results demonstrate that intact GS's show greater detectability than their corresponding isothiocyanate and amine aglycones. Furthermore, since the molar absorptivities of the isothiocyanates are quite low, an extensive preconcentration step (i.e., solvent evaporation) is required to acquire sufficiently concentrated samples of isothiocyanates. This preconcentration step renders the sample very viscous and difficult to inject from. Therefore, there is a limit on the amount of preconcentration before analysis. On the other hand, many of the isothiocyanates are reactive in an aqueous environment degrading slowly to amines (10) during the myrosinase hydrolysis of the glucosinolate extract. The amine degradation products possess the lowest molar absorptivities with respect to glucosinolates and isothiocyanates. This may explain why no peaks corresponding to amine degradation products were detected.

#### Comparison of the Two Conversion Schemes of Isothiocyanates to Amines

Since the isothiocyanates degrade slowly to amines in aqueous solutions, it was imperative to convert the isothiocyanates to their corresponding amines in order to provide a more accurate and quantitative determination of GS's through their isothiocyanate degradation products. Although they are reactive species, the amine compounds derived from isothiocyanates are quite stable and do not degrade in aqueous solutions. In this regard, two different schemes were examined for the conversion of

isothiocyanates to amines followed by the labeling of the resulting amine instead of labeling the isothiocyanates (Figure 2).

Two different procedures based on either a 1,2-benzendithiol reaction or a base hydrolysis reaction for converting isothiocyanates to amines were studied (Figure 2). By inspecting the data listed in Table 1, it is easily noticed that the base hydrolysis yields a higher percent conversion than the conversion via 1,2-benzenedithiol. Not only does the base hydrolysis show a higher percent conversion, but it is also much simpler experimentally.

Table I

PERCENT CONVERSION OF ISOTHIOCYANATES TO AMINES VIA BASE  
HYDROLYSIS AND 1,2-BENZENEDITHIOL

Analyte	Percent conversion via base hydrolysis	Percent conversion via 1,2-benzenedithiol
Phenethyl-NCS	80	64
Benzyl-NCS	85	58
4-Methoxyphenyl- NCS	84	68



### Comparison of Two Labeling Procedures

As stated above, neither the isothiocyanates nor their corresponding amines are good candidates for relatively sensitive UV detection of their parent GS's in plant extracts. Therefore, it was necessary to derivatize the amine compounds derived from the isothiocyanates degradation products of GS's before analysis by CE. In this regard, two different derivatization procedures based on either Dns-Cl (9) or FITC (12) for labeling amines were examined in order to find the most suitable derivatives for separation and detection by MECC. Both procedures offer simple and easy experimental steps, but the FITC reaction was chosen for the quantitative analysis of the rapeseed and cabbage samples because it offers several merits not obtainable with the Dns-Cl derivatization.

Table 2 shows that the FITC labeling of amines is more quantitative than the Dns-Cl labeling. The percent yield with the FITC derivatization reaction ranged between 84 and 94% as opposed to ranging between 71 and 80% for the Dns-Cl derivatization reaction. Figure 5a shows the electropherogram of the standard amines labeled with Dns-Cl. From this electropherogram, it can be seen that the migration order of Dns-amines is different than that of their corresponding isothiocyanates. The Dns-amine derivatives are neutral (as the isothiocyanates) at the pH of the experiment (i.e., pH 9.5). This is because the Dns-amine derivatives are only charged positively at very acidic pH ( $pK_a$  of the dimethylamino group of dansyl moiety is between 3.0 and 4.0) or negatively at very alkaline pH (the amino group adjacent to the sulfonyl group of the dansyl moiety has a  $pK_a$  of 11.7) (20). The derivatization with Dns-Cl increases the nonpolar character of each solute to the same extent. However, when compared to isothiocyanates, the elution order, as far as peaks # 4, 5 and 6 are concerned, was different indicating that in MECC

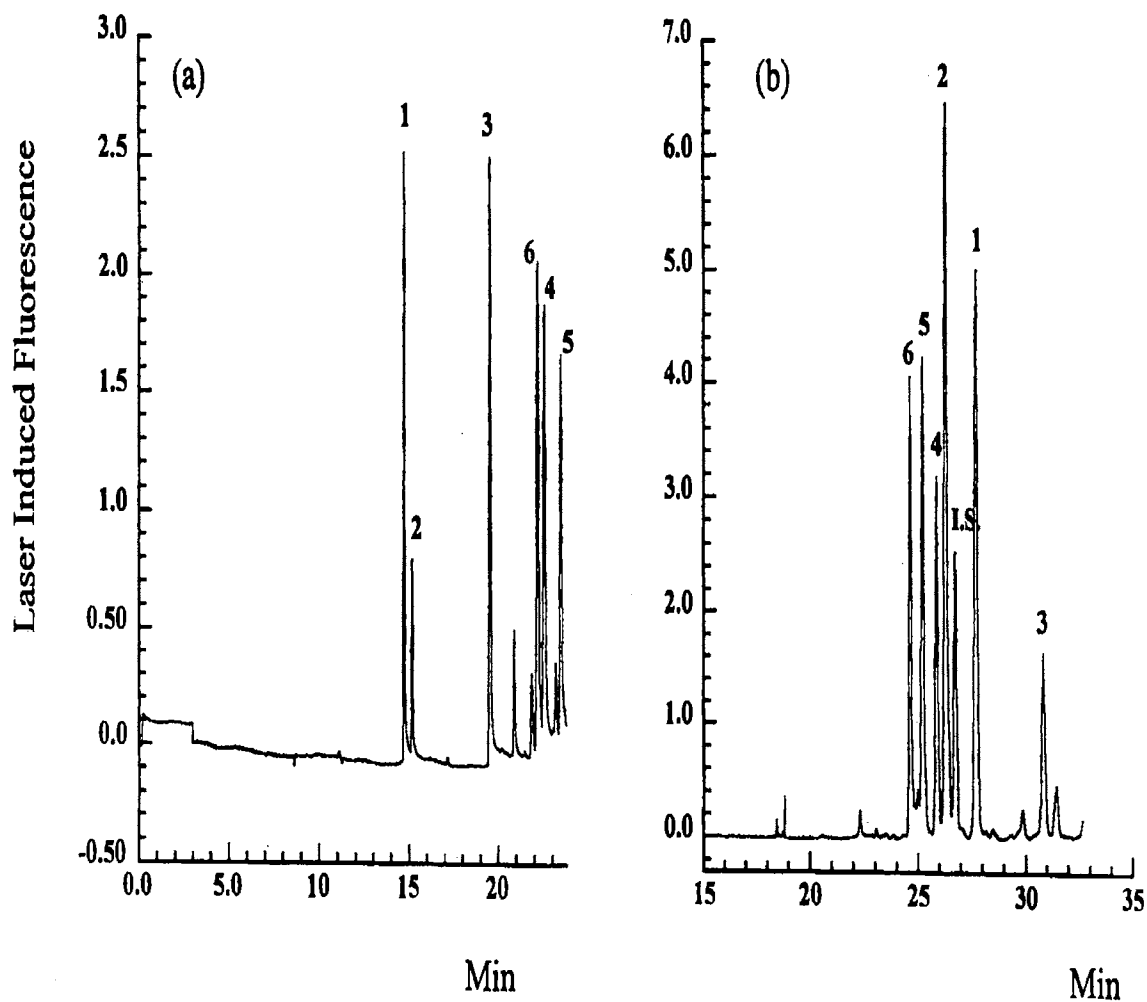
Table II

## PERCENT DERIVATIZATION OF THE AMINES WITH Dns-Cl AND FITC

Analytes	% labeling with Dns-Cl	% labeling with FITC
benzylamine	71	88
phenethylamine	77	84
4-methoxyphenyl amine	78	89
3-(methylsulfinyl) propylamine	75	92
4-(methylsulfinyl) butylamine	80	94

not only does the overall hydrophobicity of the solutes control retention but also polar interactions and steric effects contribute to retention. Since the Dns-amine derivatives are more hydrophobic than the parent isothiocyanates, their separation required the replacement of the NG micelle by the OG micelle which has one methylene group fewer in its alkyl tail than in the alkyl tail of NG. As with the isothiocyanates, the separation of the Dns-amine derivatives is still difficult due to the wide differences in polarity. To separate the sulfinyl derivatives, a higher OG micellar concentration is required than what is needed for the optimum separation of the remaining derivatives. Consequently, the separation is difficult to produce.

The standard amines labeled with FITC (FITC-amines) exhibited a change in the migration order when compared to that of the Dns-amines (Figure 5b). The negative



**Figure 5.** Separation of the standard amines labeled with Dns-Cl (a) or with FITC (b). Electrolyte: 400 mM borate, pH 9.5, containing 50 mM OG in (a) and 650 mM sodium borate, pH 9.05, containing 30 mM OG in (b). Other conditions as described in the legend to Figure 3. Solutes: I.S., internal standard; Dns-Cl (a) or FITC (b) derivatives of the amines corresponding to the isothiocyanates listed in Figure 1.

charge of the FITC function produced electrostatic repulsion between the FITC-amine derivatives and the OG-borate micelle complexes. The net result is a weak interaction with the OG micelle, and consequently the separation is also based on differences in charge-to-mass ratios among the analytes.

The Dns-Cl reaction scheme requires more experimental time than the FITC reaction (Figure 2). It also produces more side products than what is produced with the FITC labeling. These by-products produce a major problem when trying to analyze a complex mixture as encountered with the analysis of plant extracts. The standard amines labeled with FITC shows a much cleaner electropherogram with only a few side-products.

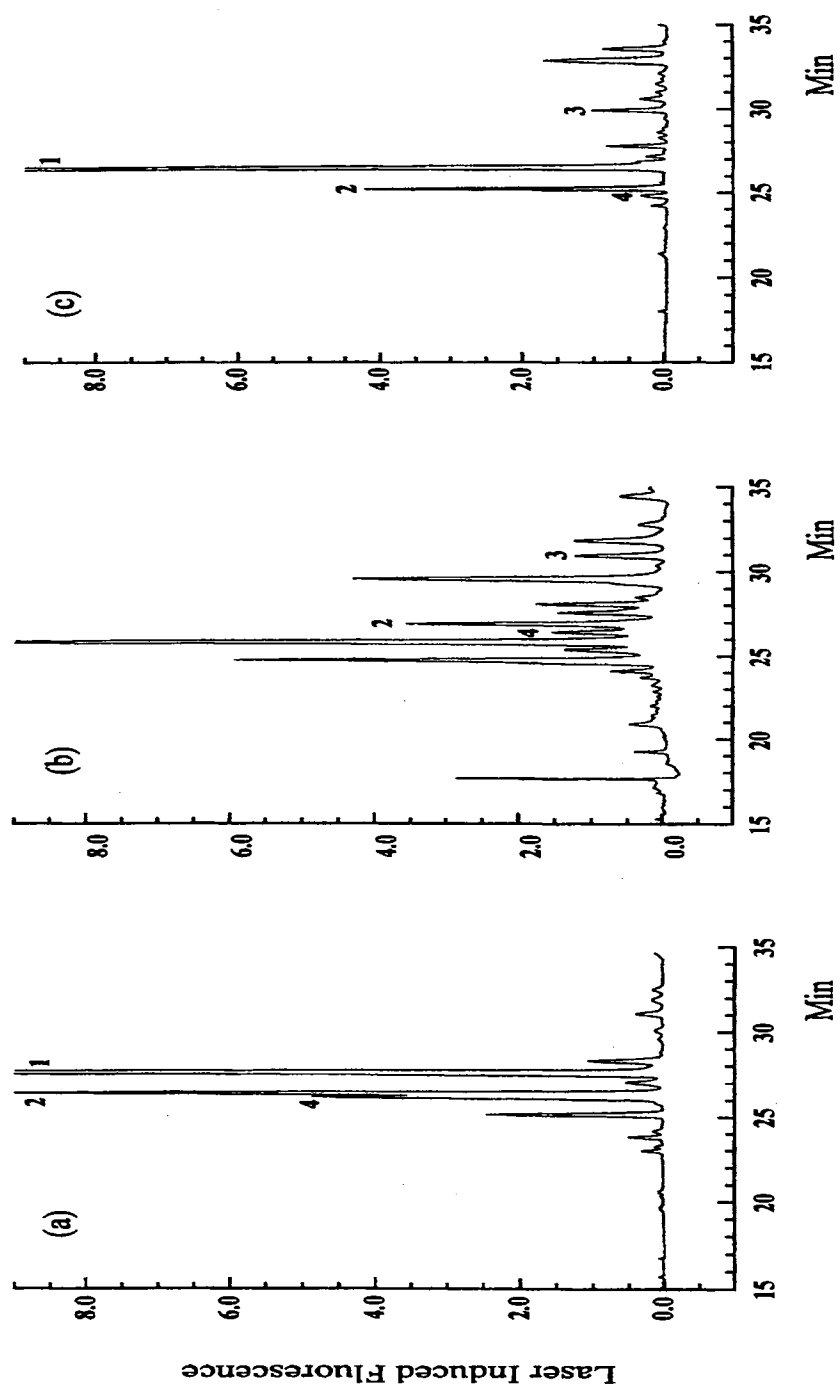
Finally, the Dns-Cl molecule has a limited solubility in an aqueous buffer. In most of the applications of this derivatization procedure (e.g., labeling of amino acids), the analytes of interest are hydrophilic and exhibit a good solubility in aqueous solutions (9). In our study, the analytes are quite nonpolar having low solubilities in aqueous solutions, thus making their dansyl derivatives to be even less soluble. Therefore, low concentrations of these derivatives must be used to adjust for the limited solubility. On the other hand, the FITC derivatives are negatively charged molecules due to the presence of the carboxylic acid group in the FITC moiety. Thus, upon derivatization with FITC, the resulting derivatives show a dramatic increase in solubility in alkaline aqueous solutions (pH>7.5). Also, the negative charge introduces mobility into the analytes, a fact that explains that the separation of the FITC-amines is achieved through differences in mobility of the analytes (charge-to-mass-ratio) as well as via hydrophobic interactions with the micelle. In contrast, and based solely on the hydrophobicity of the derivatives,

FITC-benzylamine should have eluted before the FITC-phenethylamine, and the FITC-3-(methylsulfinyl)propylamine before FITC-4-(methylsulfinyl)butylamine.

#### Quantitative Analysis of the GS Content in the Rapeseed Leaves and Roots, and White Cabbage

Based on the above results, the FITC-amine derivatives were selected to be used in the indirect qualitative and quantitative determination of the individual GS's. As shown in Figure 5b, the optimum conditions for the MECC separation of the FITC-amine standards were reached when using 30 mM OG, 650 mM borate, pH 9.05. With this high ionic strength, it was necessary to cool the capillary cartridge to 17.5 °C to reduce the amount of current and to dissipate the joule heat. A four-point calibration curve was generated for each of the six FITC-amines. In generating the calibration curves, all data points were an average of at least three trials. From the linear fit of these curves, the R values were 0.996, 0.996, 0.992, 0.997, 0.996 and 0.999 for FITC-p-methoxyphenylamine, FITC-phenethylamine, FITC-benzylamine, FITC-allylamine, FITC-3-(methylsulfinyl)propylamine and FITC-4-(methylsulfinyl)butylamine, respectively.

The profiling of the FITC-amines derived from rapeseed leaves is shown in Figure 6a. Through spiking, the FITC-amines identified corresponded to the parent isothiocyanate aglycones found in the rapeseed leaves shown in Figure 4a. As can be seen in Table 3, the amounts of GS's as derived from the calibration curves of their FITC-amine derivatives, whose structures are reflective of the individual GS's, were found to be 464, 19377 and 3221 µg/gm dry weight of leaves for glucotropaeolin (from FITC-



**Figure 6.** Profiling of the FITC labeled amines from the glucosinolates in rapeseed leaves (a), rapeseed roots (b) and white cabbage (c). Other conditions as described in the legend to Fig. 5.

benzylamine), glucoiberin (from FITC-3-(methylsulfinyl)propylamine) and glucoraphanin (from FITC-4-(methylsulfinyl)butylamine), respectively. In our previous report dealing with total GS quantitation, we reported almost 39,000  $\mu\text{g}$  total GS's/gm of rapeseed leaves (8). Thus, the three identified glucosinolates contribute over half of the total amount of GS's present in the rapeseed leaves. Also, this quantitative data closely parallels the profiling of the free isothiocyanates (Figure 4a). By inspecting Figure 4a, it is noticeable that the major constituent present in the leaves is glucoiberin. Of course the peak height ratios in Figure 6a should not match exactly the quantitative data obtained from the standard calibration curves. This can be explained by the different fluorescent properties of the individual analytes. Not all of the analytes will exhibit a maximum emission at 520 nm. Blue or red shifts can be observed when labeling the analytes with a fluorescent tag. Also, from Figure 4a, the peak heights of the benzyl-NCS and sulphoraphane are close in height, but the reported concentrations are far apart. Again, this can be explained in terms of molar absorptivities. Benzyl-NCS has a much higher molar absorptivity when compared to that of sulphoraphane.

The separation of the FITC labeled amines in the rapeseed roots is shown in Figure 6b. Again, the identifiable FITC-amines agree with those profiled from the free isothiocyanates. Table 3 lists the individual GS content as 6226, 373, 2726  $\mu\text{g}/\text{gm}$  dry weight of roots for glucotropaeolin (from FITC-benzylamine), glucoiberin (from FITC-3-(methylsulfinyl)propylamine) and sinigrin (from FITC-allylamine), respectively. From this data, the difference in the GS content of the roots and the leaves is quite noticeable. In the roots, the amount of glucoiberin is drastically lower than in the leaves. Also, sinigrin is found in the roots but in the case of the leaves, sinigrin might exist but only in

extremely minute amounts. The identifiable GS's correspond to over half of the total amount of GS's found in the roots (~10,900 mg/gm), which we reported previously (8).

The electropherogram of the FITC labeled amines in white cabbage is shown in Figure 6c. The amounts found for the individual glucosinolates were 1.39, 189, 27.8 and 25.9  $\mu\text{g/gm}$  dry weight of cabbage for glucotropaeolin, glucoiberin, glucoraphanin and sinigrin, respectively. The fluorescent detection of the labeled amines allowed for the identification of glucotropaeolin. The aglycone (benzyl-NCS) was not detected by UV in the profiling of the free isothiocyanates (Figure 4c). Thus, the laser-induced fluorescence (LIF) detection allows for the trace detection of glucosinolates not detected in the UV. As with the GS's found in the rapeseed leaves and roots, the ones found in the cabbage account for a majority of the total amount (822  $\mu\text{g/gm}$ ). In almost all previously reported data for white cabbage, glucoiberin is the most abundant GS, followed by lesser concentrations of sinigrin and glucoraphanin and minute amounts of glucotropaeolin (17). Any quantitative comparisons with previously reported data are not very relevant since a host of factors have been reported to alter the GS content in cabbage. For instance, size of the cabbage head, growing conditions, amount of pesticide used and length of storage are among many other factors that all affect glucosinolate content. These factors play a strong influence on precise reporting of quantitative data (3). Furthermore, in previous reports by others (18,19), standard deviations were extremely high amongst individual GS's may be due to additional parameters such as the methods used.



Table III

AMOUNTS OF SOME INDIVIDUAL GS'S IN EXTRACTS FROM WHITE  
CABBAGE, RAPESEED ROOTS AND RAPESEED LEAVES  
DETERMINED VIA THEIR CORRESPONDING  
AMINE COMPOUNDS.

sample type	structure of R side chain	corresponding GS	Amount of GS $\mu\text{g/gm}$
white cabbage	$\text{C}_6\text{H}_5\text{-CH}_2$	Glucotropaeolin	1.39
	$\text{H}_3\text{C-SO-(CH}_2)_3$	Glucoiberin	189
	$\text{H}_3\text{C-SO-(CH}_2)_4$	Glucoraphanin	27.8
	$\text{H}_2\text{C=CH-CH}_2$	Sinigrin	25.9
rapeseed roots	$\text{C}_6\text{H}_5\text{-CH}_2$	Glucotropaeolin	6226
	$\text{H}_3\text{C-SO-(CH}_2)_4$	Glucoraphanin	373
	$\text{H}_2\text{C=CH-CH}_2$	Sinigrin	2726
rapeseed leaves	$\text{C}_6\text{H}_5\text{-CH}_2$	Glucotropaeolin	464
	$\text{H}_3\text{C-SO-(CH}_2)_3$	Glucoiberin	19377
	$\text{H}_3\text{C-SO-(CH}_2)_4$	Glucoraphanin	3221

### Conclusions

We have shown that capillary electrophoresis (CE) is a useful tool for the profiling and determination of individual GS's via their isothiocyanate degradation products upon myrosinase digestion. This method, which involved the separation and

detection of the isothiocyanates by CE-LIF, was successfully applied to the determination of GS's in white cabbage, rapeseed leaves and rapeseed roots.

## References

1. Bertelli, D.; Plessi, M.; Braghiroli D.; Monzani, A., *Food Chem.*, **1998**, 63, 417-421.
2. Cai, J.; El Rassi, Z., *J. Chromatogr.*, **1992**, 608, 31-45.
3. Fenwick, G. R.; Heaney, R. K.; Mullin, W. J., *CRC Crit. Rev. Food Sci. Nutrition*, **1983**, 18, 123-201.
4. Geerdink, R., *J. Chromatogr. A*, **1988**, 445, 273-281.
5. Heaney, R. K.; Fenwick, G. R. Glucosinolates. In *Methods of Enzymatic Analysis*; Bergmeyer, H. U. Ed.; VCH: Weinheim, **1984**; pp. 208-219.
6. Heaney, R. K., Fenwick, G. R. Identifying toxins and their effects: Glucosinolates. In *Natural Toxicants in Food, Progress and Prospects*; Watson, D. H. Ed.; VCH: Weinheim, **1987**; pp. 76-109.
7. Karcher, A.; El Rassi, Z., *J. Liq. Chrom. & Rel. Technol.*, **1998**, 21, 1411-1432.
8. Karcher, A.; El Rassi, Z., *Anal. Biochem.*, **1999**, 267, 92-99.
9. Lawrence, J. F.; Frei, R. W. *Chemical Derivatization in Liquid Chromatography*. Elsevier Science: Amsterdam, **1976**.
10. March, J. *Advanced Organic Chemistry* (3rd ed.). John Wiley and Sons, New York, **1985**.
11. Mechref, Y.; Smith, J. T.; El Rassi, Z., *J. Liq. Chromatogr.*, **1995**, 18, 3769-3786.
12. Rodriguez, I.; Lee, H. K.; Li, S. F. Y., *J. Chromatogr. A*, **1996**, 745, 255-262.
13. Shibamoto, T.; Bjeldanes, L. F. *Introduction to Food Toxicology* ; Academic Press: San Diego, **1993**.
14. Smith, J. T.; Nashabeh, W.; El Rassi, Z., *Anal. Chem.*, **1994**, 66, 1119-1133.

15. Tookey, H. L.; VanEtten, C. H.; Daxenbichler, M. E. Glucosinolates. In *Toxic Constituents of Plant Foodstuffs*; Liener, I. E., Ed.; Academic Press: New York, **1980**; pp. 103-142.
16. Van Etten, C.H.; Tookey, H.L. Glucosinolates. In *Handbook of Naturally Occuring Food Toxins*, Rechcigl, M.J., Ed.; CRC Press: Boca Raton, **1983**; pp. 15-30.
17. Van Etten, C. H.; Tookey, H. L. "Chemistry and biological effects of glucosinolates." in *Herbivores. Their Interactions with Secondary Metabolites*; Rosenthal, G. A.; Janzen, D. H., Eds.; Academic Press: New York, **1979**; pp. 471-500.
18. VanEtten, C. H.; Daxenbichler, M. E.; Tookey, H. L.; Kwolek, W. F.; Williams, P. H.; Yoder, O. C., *J. Amer. Soc. Hort. Sci.*, **1980**, 105, 710-714.
19. VanEtten, C. H.; Daxenbichler, M. E.; Williams, P. H.; Kwolek, W. F., *J. Agric. Food Chem.*, **1976**, 24, 452-455.
20. Yu, J.; El Rassi, Z., *J. Liq. Chromatogr.*, **1993**, 16, 2931-2959.
21. Zhang, Y.; Cho, C.-G.; Posner, G.; Talalay, P., *Anal. Biochem.*, **1992**, 205, 100-107.
22. Zhang, Y.; Wade, K.; Prestera, T.; Talalay, P., *Anal. Biochem.*, **1996**, 239, 160-167.

## CHAPTER VII

### DETERMINATION OF TOTAL GLUCOSINOLATES IN CABBAGE AND RAPESEED BY CAPILLARY ELECTROPHORESIS VIA THE ENZYMATICALLY RELEASED GLUCOSE\*

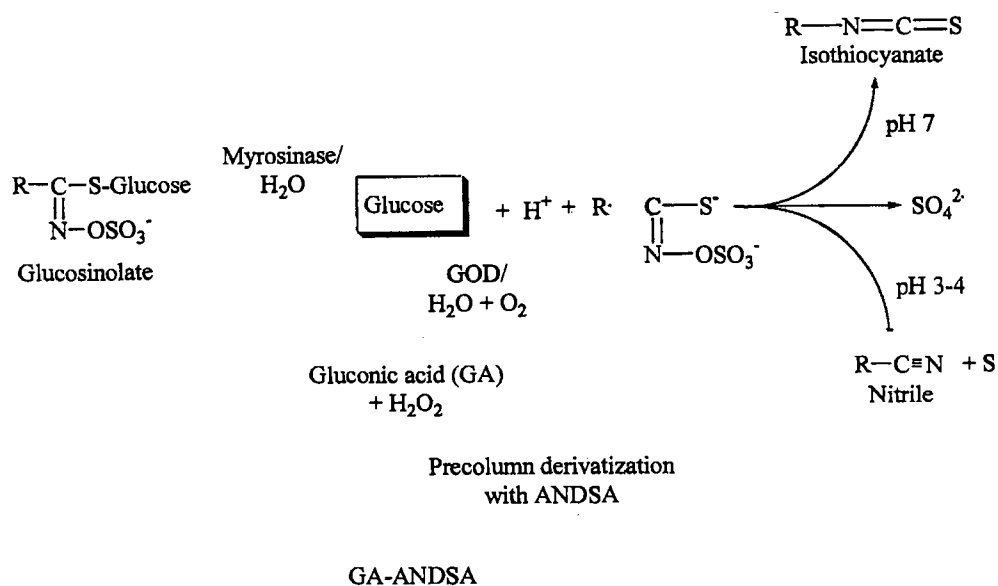
#### Introduction

Glucosinolates (GS's) are naturally occurring thioglucosides (for GS general structure, see Fig. 1) found throughout the roots, stems, leaves, and seeds of plants in the Cruciferae family (1, 2, 3, 4, 5). The structural variations of the GS's are attributed to the nature of the R-group (see Fig. 1), and there are more than 100 known glucosinolates(2). The R group can be alkyl, alkenyl, arylalkyl, methylthioalkyl, methylsulfinylalkyl, methylsulfonylalkyl, indolylalkyl, etc.. The great number of individual GS's produce a large range of flavors as well as toxic effects upon consumption (5).

In this chapter, we selected rapeseed and cabbage to develop a method for the determination of total GS's by CE. Cabbage and rapeseed are good sources of GS's. In addition, cabbage is consumed throughout the world in very large quantities. Also, rapeseed derived from *Brassica* is one of the major oilseeds of commerce(3); its world production amounts to several million metric tons. Usually, the seed meal remaining

---

\* Published in *Anal. Biochem.*, 1999, 267, 92-99



**Figure 1.** General structure and enzymatic degradation of glucosinolates as well as enzymatic conversion of released glucose to GA followed by precolumn derivatization of GA with ANDSA.

after oil extraction can be fed to livestock, but in limited amounts because it contains toxic substances including GS's(3). Varieties of rapeseed have been developed with low amounts of GS's while other varieties contain relatively large amounts of GS's. Thus, there is much interest associated with the development of analytical methods for the quantitative determination of total GS's present in a given plant species.

Some of the early detection approaches of total GS's targeted released glucose from the action of myrosinase(6, 7), see Fig. 1. GS's are accompanied within the same plant by myrosinase, which is released when the plant tissues are crushed or masticated or when autolysis within the plants occurs (3, 4). Under these circumstances, myrosinase and GS's enter into intimate contact which allows the myrosinase to hydrolyze GS's to D-glucose, sulfate, sulfur and aglycones (3, 4). A few approaches have been developed for the detection of glucose. Specific test-paper which was originally developed by Comer (8) for the determination of glucose in urine, was later used for the detection of glucose released from GS's by the action of myrosinase. In the test-paper, hydrogen peroxide, produced from glucose by the action of glucose oxidase, reacts with a chromogen, o-tolidine, in the presence of peroxidase and F.D.C. Yellow No.5 dye to turn the paper from yellow to green. Although the test-paper is rapid, it only gives the approximate GS level in plant tissues and seeds. Björkman (9) has used glucose oxidase, peroxidase and the chromogen, o-dianisidine, to colorimetrically estimate in solution the quantity of GS's in plant extracts. In both the test-paper and the colorimetric method, the results did not compensate for phenolic compounds, which inhibited color development. Inhibition could be overcome by treating the extracts with charcoal before colorimetric analysis or, when using test paper, by separating the inhibiting substances from glucose through

capillary action of the plant extract up a strip of a test paper(10). Also, in these approaches, the results did not account for free glucose in the extract, and any attempt at removing free glucose after crushing or grinding the plant tissues would have immediately promoted endogenous myrosinase activity which releases glucose from GS's. To correct for free glucose, the GS's were separated from free glucose by adsorption on to anion exchange resin (11, 12). In this approach, myrosinase hydrolysis is effected while the intact GS's are retained on the resin and then subsequent colorimetric glucose measurement is carried out on the column effluent. Iori et al. described a polarographic method for the determination of both free and enzymatically released glucose(13) based on the polarographic determination of oxygen uptake of free glucose by a system of double coupled-enzymes, such as myrosinase-glucose oxidase. More recently, Koshy et al. (14) introduced an enzyme biosensor for the analysis of GS's via enzymatically released glucose. This biosensor is based on amperometric detection by a glucose electrode having glucose oxidase or myrosinase-glucose oxidase immobilized on a platinized carbon base. Although electrochemical methods are rapid and sensitive, the fact that the GS extracts from plant tissues or seeds are complex mixtures containing electroactive compounds may lower the accuracy of these methods.

In this chapter, which is a continuation to our previous investigation on high performance liquid phase separation of glycosides (15, 16), we are concerned with the introduction of a capillary electrophoresis (CE) method for the determination of total GS's via the myrosinase released glucose. The released glucose can be readily converted to gluconic acid (GA) upon treatment with glucose oxidase(17). The resulting GA can be readily labeled with a fluorescent tag (see Fig. 1), namely 7-aminonaphthalene-1,3-



disulfonic acid (ANDSA), according to our previously reported precolumn derivatization schemes(18, 19, 20, 21, 22). Glucose can be directly labeled at its reducing end via reductive amination with a UV absorbing or fluorescing tag (23), and the resulting derivative can be readily detected by CE (24, 25). However, due to the fact that all other sugars in glucosinolate samples extracted from plants will be equally tagged, the reductive amination approach is non selective for the determination of glucose and in turn total GS's. On this basis, subjecting a given glucosinolate extract to reductive amination for tagging the enzymatically released glucose will introduce interferences in the measurement, a fact that makes the assay for total GS's via glucose rather complex involving extensive sample clean-up and preparation, and eventually a separation step for glucosinolates in order to avoid other carbohydrates in the sample. In the work described here, we overcame the problem of the non selectivity of reductive amination toward glucose by using glucose oxidase to convert glucose to gluconic acid which can be readily and selectively tagged with ANDSA producing a highly fluorescent derivative GA-ANDSA. In addition, the fluorescent GA-ANDSA derivative is negatively charged over a wide range of pH, thus facilitating the optimization of the separation conditions using an applied voltage of negative polarity at pH 3.0, where molecules migrate by charge-to-mass ratios. Since these conditions allow for only those compounds that are negatively charged to migrate to the detection point, the analyte of interest can in principle be determined in complex matrices with virtually no sample clean-up. In fact, and as will be shown in this chapter, the amount of total GS's in real sample matrices can be selectively and sensitively determined by CE-laser induced fluorescence (LIF) detection.

## Experimental

### Reagents and Materials

The enzymes used in this study were myrosinase (thioglucosidase, EC 3.2.3.1) and glucose oxidase (EC 1.1.3.4), and they were purchased from Sigma (St. Louis, MO, USA). D-(+)-Glucose and D-gluconic acid (GA) as a potassium salt were obtained from Aldrich (Milwaukee, WI, USA). Octyl-  $\beta$ -D-glucopyranoside (OG) was purchased from Anatrace (Mumee, OH, USA). 1-Ethyl-3-(3-dimethylaminopropyl) carbodiimide (EDAC) was from Sigma. The derivatizing agent 7-aminonaphthalene-1,3-disulfonic acid (ANDSA) was purchased from TCI America Inc. (Portland, OR, USA). The internal standard *N*-acetylneuraminic acid (NANA) was obtained from Sigma and then labeled with ANDSA according to our previously reported procedures (18, 19, 20).

### Capillary Electrophoresis Instrument and Capillaries

A Beckman P/ACE model 5510 instrument (Fullerton, CA, USA) was used. It was equipped with a diode array detector and an Omnicrome (Chino, CA, USA) Model 3056-8M He-Cd laser multimode, 8 mW at 325 nm. Utilizing the thermostating ability of the instrument, the temperature of the capillary was held constant at 25 °C for all experiments. The P/ACE Station software and data handling were controlled by a personal computer. The detection of the intact glucosinolates was performed at 228 nm. For LIF detection of the ANDSA derivatives, a fluorescence emission band-pass filter of  $380 \pm 2$  nm was purchased from Corion (Holliston, MA, USA). A 360 nm cut-on filter purchased from Corion was used to reject the laser beam. All of the experiments were

performed in fused-silica capillaries obtained from Polymicro Technology (Phoenix, AZ, USA). The dimensions of the capillaries were 50  $\mu\text{m}$  internal diameter and 365  $\mu\text{m}$  outer diameter. Samples were pressure injected at 0.034 bar (i.e. 3.5 kPa) for various lengths of time. In between runs, the capillary was rinsed with 0.1 M NaOH, distilled water, and running electrolyte for two, three and one minute, respectively.

#### Sources of GS's

The GS standard was sinigrin, which was purchased from Sigma. The white cabbage was bought at a local grocery outlet. Dr. H.A. Melouk, USDA-ARS, Department of Entomology and Plant Pathology, Oklahoma State University, supplied the rapeseed seeds and grew the rapeseed plants in the USDA-ARS greenhouse in Stillwater, OK (Dwarf Essex). At the time of harvesting, the rapeseed plants were approximately ten inches tall and have been growing for 102 days.

#### Procedures

Extraction of intact GS's from white cabbage. Extraction of the intact GS's from white cabbage was performed through modification of previously reported procedures (15, 26). Approximately 85 g of the white cabbage was cut from a section of a cabbage head containing mostly leaf materials and small amounts of large stems. This fresh weight of cabbage was placed into liquid nitrogen until frozen. The frozen vegetation was then ground to a fine powder in a Regal Coffee Grinder (Kewaskum, WI, USA). In the frozen state, endogenous myrosinase can not hydrolyze the GS's. The ground cabbage was quickly transferred into a beaker containing approximately 200 ml of hot

methanol, and the resulting mixture was heated at 70 °C for 3 min. In addition to extracting the GS's, the hot methanol deactivates the endogenous myrosinase. After cooling to room temperature, the mixture was filtered through a Whatman # 1 filter. The methanol in the filtrate was removed by a rotary evaporator and the remaining liquid was reconstituted with a 50% (v/v) methanolic aqueous solution in a 100 ml volumetric flask. Three milliliters of this solution were pipetted into individual vials, dried via speed vacuum, and frozen until analysis by CE.

Extraction of intact GS's from rapeseed. Approximately 15 cm x 60 cm portion of fresh rapeseed plants was removed from the flats, dipped into water to remove excess soil and carefully cut to separate the leaves from the roots. The roots required further cleaning and soaking in distilled water to remove all traces of soil, sand, and decayed dead leaves. The weights were then recorded separately for both the rapeseed roots and leaves. The GS's contained in the two plant tissues were then extracted by the same procedure as that for the white cabbage, except the final volume was 50 ml.

The seeds of the rapeseed plants were weighed and extracted by the above mentioned procedure for the white cabbage with a minor adjustment. After grinding, the seeds were placed in a boiling solution containing 70% methanol. This modified step was to ensure the solubility of the GS's in the solution. The seeds did not contain as much water as the fresh plant tissues used in this study, therefore, constituting the need for additional water. The final volume was 50 ml.

Strategy for determining total GS content via enzymatically released gluconic acid labeled with ANDSA. The content of one vial (6% of the extract for rapeseed and

3% for cabbage) that had been previously dried were sufficient for a single analysis. One milliliter of water was added to this vial to dissolve the GS's. Each sample was filtered through a 0.2  $\mu\text{m}$  Titan syringe filter (Scientific Resources Inc., Eatontown, NJ, USA) to remove any insoluble material. Two hundred microliters of sample were pipetted into a new vial, and a known amount of exogenous myrosinase, usually 1.0 mg (0.83 units), was then added in the solid form. This was stirred magnetically for 30 min. Myrosinase converts the GS's to glucose and other products, see Fig. 1. After that time, approximately 0.5 mg of solid glucose oxidase (114 units) was added and stirred for another 30 min converting the enzymatically released glucose as well as any free glucose in the samples to gluconic acid, see Fig. 1. These two enzymatic steps were allowed sufficient time to permit the complete conversion of the GS's into gluconic acid (GA). Approximately, 0.5 mg of glucose oxidase was added to 200  $\mu\text{L}$  of the same GS sample to measure the free glucose in the sample. Any free glucose in the sample was consequently converted to GA, and the GS's were not enzymatically hydrolyzed. The water was removed by speed vac.

The samples were labeled with the ANDSA derivatizing agent according to our previously published procedure (18, 19, 20, 21, 22), see Fig. 1. 100  $\mu\text{L}$  of a solution containing the appropriate concentration of EDAC were pipetted into each vial followed by 100  $\mu\text{L}$  of a ten fold increase in concentration over EDAC of the labeling agent ANDSA. The vials were capped under nitrogen and allowed to react overnight and later analyzed by CE. The amount of free glucose was determined from the peak area of GA-ANDSA in the extract that was treated only with glucose oxidase. This area count was subtracted from the peak area of the GA-ANDSA corresponding to both the free glucose

in the sample and the enzymatically released glucose from the GS's in that sample (i.e., the sample treated consecutively with myrosinase first and then with glucose oxidase). This difference in the peak areas of the GA-ANDSA corresponds to the total amount of GS's in the plant extract.

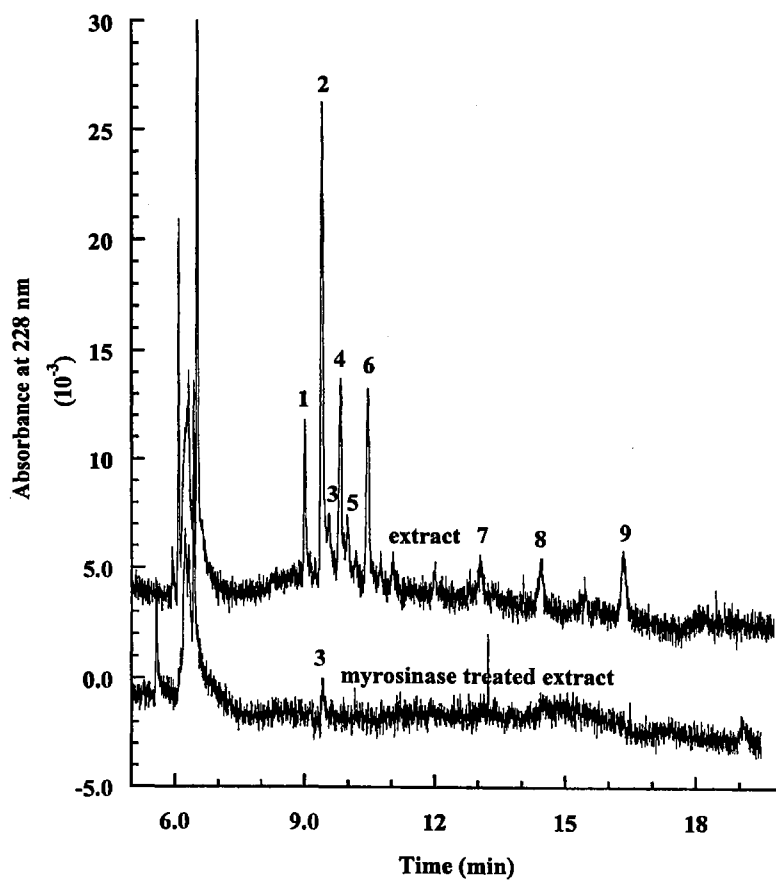
$$\text{Peak area of GA-ANDSA corresponding to total GS's} = (\text{Peak area of GA-ANDSA derived from free and bound glucose in the sample}) - (\text{Peak area of GA-ANDSA derived from free glucose in the sample})$$

In the precolumn derivatization of GA with ANDSA in the presence of a water soluble carbodiimide (e.g., EDAC), a condensation reaction between the amino group of ANDSA and the carboxylic acid group of GA takes place producing a stable amide bond with virtually undetectable side products (18, 19, 20, 21, 22).

## Results and Discussion

### Profiling of Intact GS's in White Cabbage

To assess the effectiveness of the extraction procedure of glucosinolates from various plant tissues and seeds, a small plug representative of each plant extract was analyzed by CE. Figure 2 shows the electropherograms of the white cabbage before and after the enzymatic hydrolysis by myrosinase. In order to achieve the optimum separation conditions, it was necessary to add a neutral micelle to the separation electrolyte, since the GS's are not completely separated based on charge-to-mass ratios (15). The optimum composition for the running electrolyte were determined to be 100 mM OG, 150 mM phosphate, pH 6.5. As can be seen in Fig. 2, by choosing a neutral



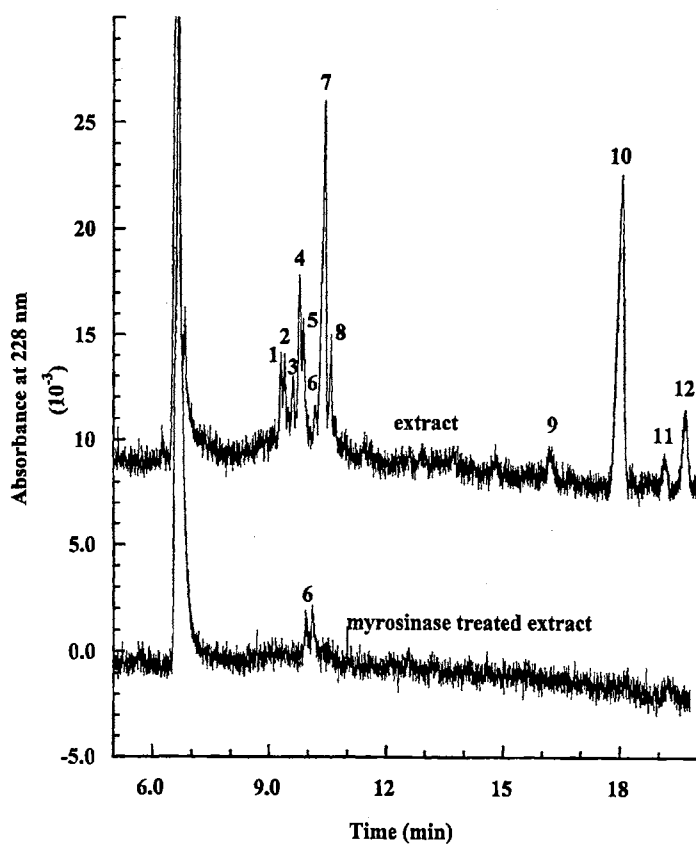
**Figure 2.** Profiling of GS's in a white cabbage extract by HPCE-UV before and after myrosinase treatment. Electrolyte: 150 mM phosphate, pH = 6.5, containing 100 mM OG; 18 kV; 25 °C; capillary, fused-silica, l = 50 cm, L = 57 cm, 50 mm i.d.

micelle, only those compounds that are negatively charged (e.g., GS's) underwent differential migration while all neutral compounds (e.g., matrix interferences) eluted at  $t_0$ , the time of the EOF. Thus, this electrophoretic system is ideal for the analysis of GS samples originating from plants, which are complex mixtures. Before the addition of myrosinase, several peaks eluted after eight minutes. With the exception of one peak (peak #3), all the other peaks disappeared after sample treatment by myrosinase, indicating the presence of at least eight different GS's assuming that no coelution of components occurs. As can be seen in Fig. 2, among the eight possible GS's, four are major and four are minor components. Recently, and with another batch of white cabbage, we found a total of 6 GS peaks with two of them are major components (15). Considerable variation was reported to occur in both individual and total GS content due to genetic origin and nature of the growing plant as well as the age, the cultural and environmental factors associated with the growth of a particular plant (27).

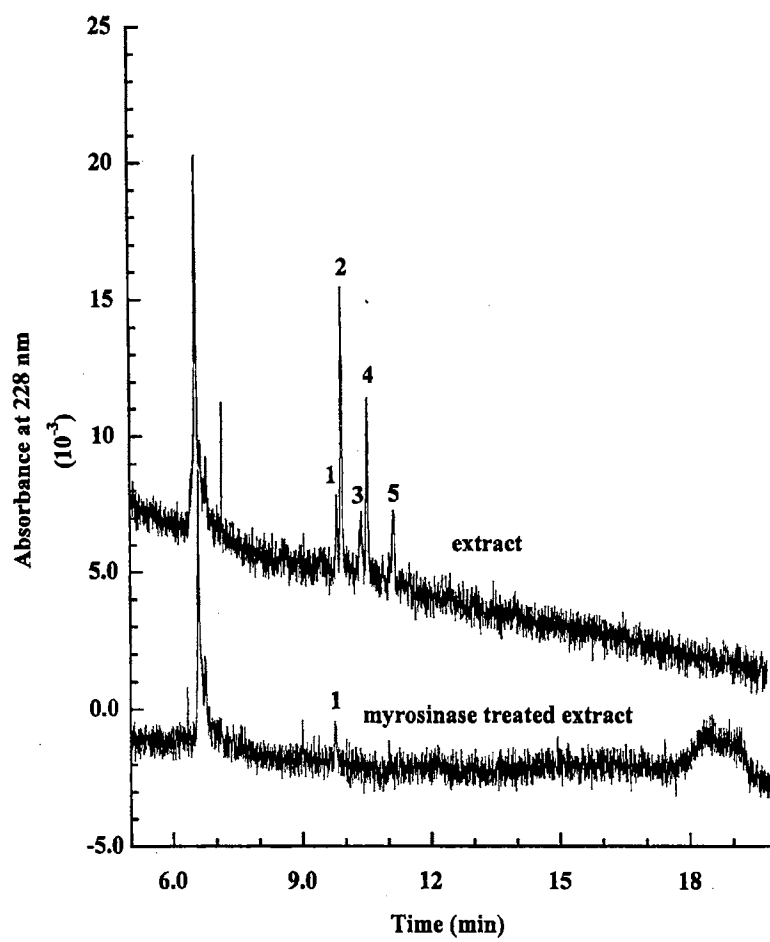
#### Profiling of Intact GS's in Fresh Rapeseed Leaves and Roots

Figures 3 and 4 show the electropherograms of the extracts of rapeseed leaves and roots, respectively, before and after digestion with myrosinase. The separation conditions used in Figs 3 and 4 are the same as those used for the separation of the intact GS's in the cabbage sample, Fig. 2. From Fig. 3, the total number of intact GS's was determined to be at least eleven assuming that all the GS's were resolved from one another. Again, one peak labeled 6, is present in both intact and myrosinase treated sample and is a non-GS compound. There are at least two GS's in the leaves that are present in high amounts.





**Figure 3.** Profiling of GS's in rapeseed leaves extract by HPCE-UV before and after myrosinase treatment. Other conditions as in Fig. 2.



**Figure 4.** Profiling of GS's in rapeseed roots extract by HPCE-UV before and after myrosinase treatment. Other conditions as in Fig. 2.

These are peaks labeled 7 and 10. As with the cabbage, several of the GS's are present in small quantities, or they lack adequate chromophores needed for UV detection.

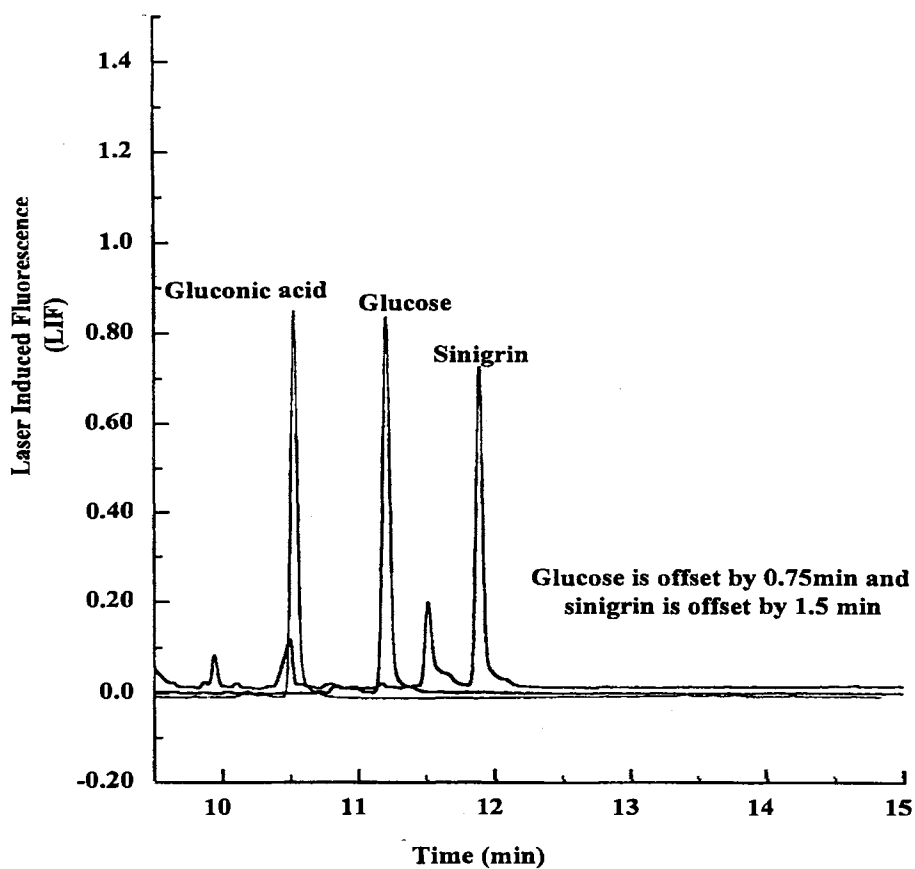
The GS's contained within the rapeseed roots are shown in Fig. 4. From the analysis of the electropherograms in Fig. 4, before and after the addition of myrosinase, the number of intact GS's in the roots was determined to be at least five assuming complete component separation. After the addition of myrosinase, a minor peak labeled 1 is present but in a much smaller amount. This peak is also seen in the electropherogram before the addition of myrosinase. This could be explained by either a non-GS compound co-eluting with a GS or inadequate time was allowed for the enzyme to completely hydrolyze the GS's contained in the sample. Using the detection wavelength of 228 nm one can actually detect only GS's; indicating that the extraction procedure is highly efficient in the crude isolation of GS's. The roots contain less glucosinolates than the leaves both in number and total amount (see later).

The extract from rapeseed seeds was also analyzed by CE. Due to the relatively low sensitivity of CE-UV, only one peak corresponding to GS could be seen in the electropherogram. This is not surprising since the majority of GS's in the seeds (e.g., 3-butenyl-GS, 4-pentenyl-GS, 5-methylthiopentyl-GS) possess chromophoric groups of low molar absorptivities. These GS's, which contain R groups with more than 4 carbon atoms, are relatively hydrophobic to be able to exist in the seed fatty medium. However, and upon digestion of the seed extract with myrosinase, the same kind of hazy solutions was obtained as with the cabbage and rapeseed leaves and roots. The haziness is an indication of the liberation of the very slightly water soluble isothiocyanates from GS digestion with myrosinase.

### Determination of Total GS Concentration via Enzymatically Released Glucose

A six-point calibration curve was constructed using the standard GA which was derivatized with ANDSA (i.e., GA-ANDSA). The curve was prepared in the concentration ranges expected in the plant tissues and seeds. The curve was linear in the concentration range of interest (i.e., from 0.05 mM to 5.0 mM) with an intercept of  $-1.85 \times 10^{-4}$  and an  $R = 0.998$ . An internal standard, i.e., NANA-ANDSA, was used to correct for bias in the injection volume. NANA was chosen as the internal standard for three obvious reasons: (i) NANA possesses in its structure a carboxylic acid group, and therefore it is a carboxylated sugar as GA, (ii) NANA can be readily tagged with ANDSA (18, 19) to yield a fluorescent tag that can be detected by the same LIF detection system as GA-ANDSA, and (iii) NANA is not present in plant extracts. In fact, NANA is part of the oligosaccharide moieties of glycoproteins and glycolipids, and as a free sugar, NANA is excreted in the urine of animal and man via several pathological states (28).

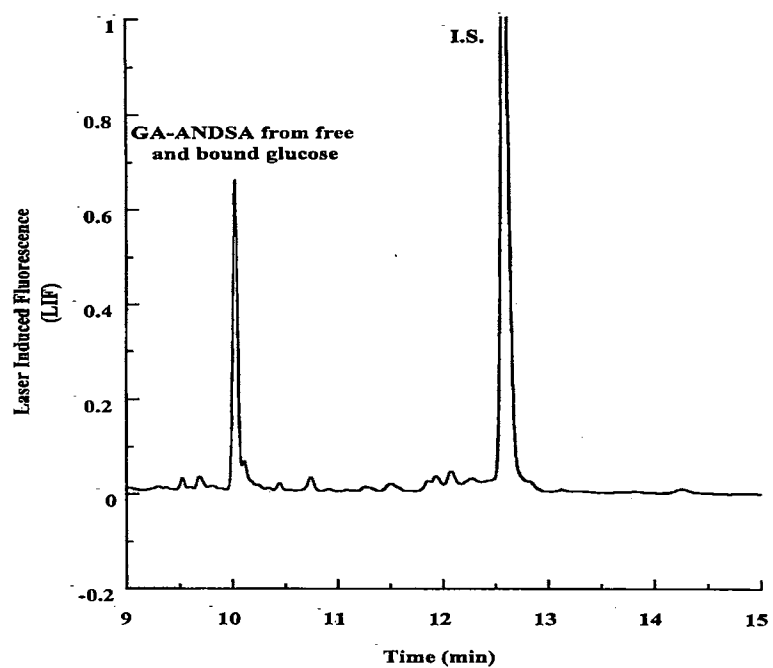
To establish the procedure concerning the determination of total GS's via the enzymatically released glucose in real world samples, it was first necessary to compare the peak area obtained from standard GA-ANDSA with the peak areas from (i) the conversion of a standard GS to GA-ANDSA via successive treatment of the GS with myrosinase and glucose oxidase followed by the labeling of the produced GA with ANDSA, and (ii) from the conversion of standard glucose to GA-ANDSA via treatment with glucose oxidase and labeling the resulting GA with ANDSA.. Figure 5 shows the results based on 1.0 mM concentration. First, 1.0 mM of standard GA was labeled with ANDSA and analyzed. Also, a 1.0 mM standard solution of glucose was first converted



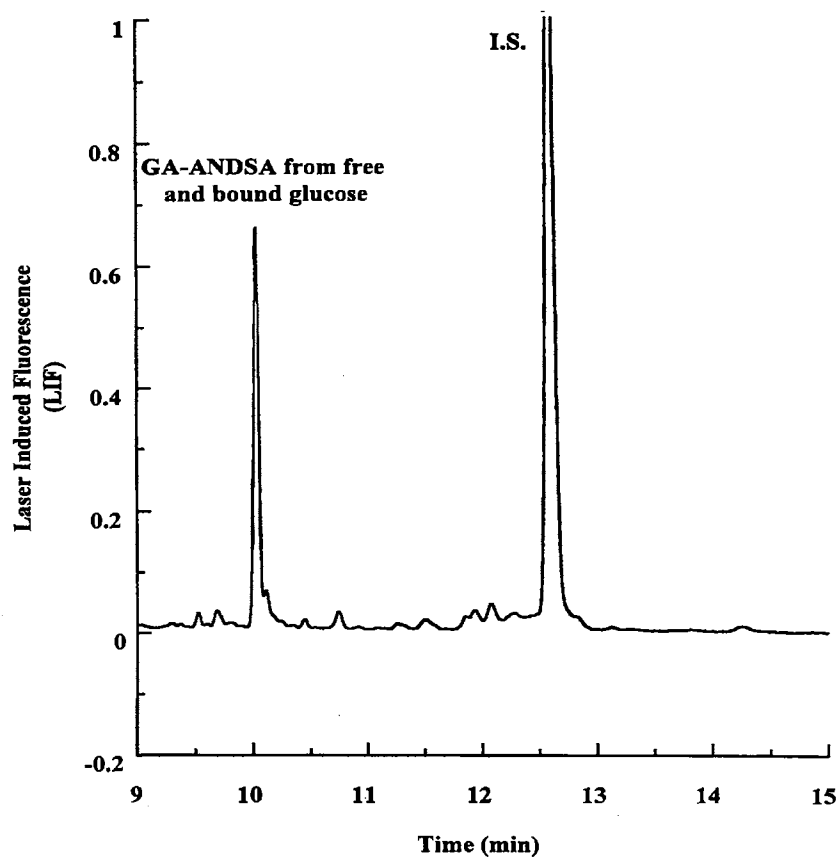
**Figure 5.** Electropherograms of the ANDSA derivatives of sinigrin, glucose and gluconic acid obtained by LIF detection. Electrolyte: 50 mM sodium phosphate, pH = 3.0; -25 kV. Other conditions as in Fig. 2.

to GA via glucose oxidase and then tagged with ANDSA. The resulting peak area of the GA-ANDSA derived from standard glucose compared favorably with the peak area of GA-ANDSA derived from the standard GA, and corresponded to 1.13 mM. This means that glucose oxidase converts quantitatively glucose to GA and that the derivatization with ANDSA proceeds similarly regardless of the matrix interferences. Sinigrin containing the same concentration (i.e., 1 mM) was subjected to both myrosinase and glucose oxidase, and then the resulting GA was labeled with ANDSA. The peak area of GA-ANDSA derived from sinigrin was compared to the peak area of GA-ANDSA derived from standard GA. This conversion was found to be 1.08 mM. From these results, it was concluded that the enzymatic conversion of the solutes proceeded quantitatively, and did not interfere with the labeling process.

The above same system was applied to real GS samples from cabbage, and rapeseed seeds, leaves and roots. Two derivatizations with ANDSA were required for the determination of total GS's. One derivatization was used to determine the amount of free glucose in the sample. The other derivatization was aimed at estimating the free glucose, and the glucose released by myrosinase from the GS's contained within the sample. The electropherograms corresponding to the free glucose and to both free glucose and myrosinase released glucose are shown for the rapeseed leaves in Fig. 6 and 7, respectively. The difference between the areas of the two peaks in Fig. 6 and 7 gave the amount of total GS's contained within the sample. In all cases, the peak areas were used for calculations and normalized by the use of an internal standard (i.e., NANA-ANDSA). Table 1 shows the results obtained when analyzing the real world samples with the above mentioned procedure. White cabbage contained 822  $\mu\text{g}$  of GS's per gram



**Figure 6.** Electropherogram of GA-ANDSA obtained for rapeseed leaves after glucose oxidase treatment diluted ten fold. Solute: I.S., internal standard. Other conditions as in Fig. 5.



**Figure 7.** Electropherogram of GA-ANDSA obtained for rapeseed leaves after treatment with myrosinase and glucose oxidase diluted 100 fold. Other conditions as in Fig. 6.



of fresh cabbage. This relates very well with the data found in the literature (27). Next, the rapeseed leaves contained 38799  $\mu\text{g}$  per gram while the roots contained 10922  $\mu\text{g}$  per gram of wet vegetable. The seeds of the rapeseed plant contained a moderate amount of 17138  $\mu\text{g}$  per gram.

TABLE 1.

TOTAL GLUCOSINOLATE CONTENT IN THE  
SAMPLE MATRICES IN THIS STUDY

Sample media	Total GS content ( $\mu\text{g}$ GS/g sample)	Values reported in literature ( $\mu\text{g}$ GS/g sample)
Rapeseed roots	10922 $\pm$ 119	
Rapeseed seeds	17138 $\pm$ 50 <sup>a</sup>	14818-54014 <sup>b</sup>
Rapeseed leaves	38799 $\pm$ 45.7	
White cabbage leaves	822 $\pm$ 150.8	300-1070 <sup>c</sup>

a) Defatted dry weight value

b) Literature values for other genotypes (29)

c) Literature values (27).

Derivatization and enzyme %RSD = 3.46%, (from reaction-to-reaction) for rapeseed roots and leaves.

## References

1. Heaney, R. K. and Fenwick, G. R., in *Methods of Enzymatic Analysis* (Bergmeyer, H. U., Ed.), VCH, Weinheim, **1984**, 6, 208-219.
2. Heaney, R. K. and Fenwick, G. R., in *Natural Toxicants in Food, Progress and Prospects* (Watson, D. H., Ed.), VCH, Weinheim, **1987**, 76-109.
3. Tookey, H. L., VanEtten, C. H. and Daxenbichler, M. E., in *Toxic Constituents of Plant Foodstuffs* (Liener, I. E., Ed.), Academic Press, New York, **1980**, 103-142.
4. Van Etten, C. H. and Tookey, H. L., in *Herbivores, Their Interaction with Secondary Plant Metabolites* (Rosenthal, G. A. and Janzen, D. H., Eds), Academic Press, New York, **1979**, 471-500.
5. Shibamoto, T. and Bjeldanes, L. F., in *Introduction to Food Toxicology*. Academic press, San Diego, **1993**.
6. Lein, K. A., *Z. Pflanzenzuecht.*, **1970**, 63, 137-154 .
7. Lein, K. A. and Schon, W. J., *Angew. Bot.*, **1969**, 43, 87-92.
8. Comer, J. P., *Anal. Chem.*, **1956**, 28, 1748-1750.
9. Björkman, R., *Acta Chem. Scand.*, **1972**, 26, 1111-1116.
10. Van Etten, C. H., McGrew, C. E. and Daxenbichler, M. E., *J. Agric. Food Chem.*, **1974**, 22, 483-487.
11. Haeney, R. K. and Fenwick, G. R., *Z. Pflanzenzuecht.*, **1981**, 87, 89-95.
12. Van Etten, C. H. and Daxenbichler, M. E., *J. Assoc. Off. Anal. Chem.*, **1977**, 60, 946-949.
13. Iori, R., Leoni, O. and Palmieri, S., *Anal. Biochem.*, **1983**, 134, 195-198.

14. Koshy, A., Bennetto, H.P., Delaney, G.M., MacLeod, A.J., Mason, J.R., Stirling, J.L. and Thurston, C.F., *Anal. Lett.*, **1988**, *21*, 2177-2194.
15. Karcher, A. and El Rassi, Z., *J. Liq. Chrom. & Rel. Technol.*, **1998**, *21*, 1411-1432.
16. Wasserkrug, K. and El Rassi, Z., *J. Liq. Chrom. & Rel. Technol.*, **1997**, *20*, 335-349.
17. Bentley, R., in *The Enzymes* (Boyer, P. D., Ed.), Academic Press, New York, **1963**, *7*, 567-586.
18. Mechref, Y. and El Rassi, Z., *Electrophoresis*, **1994**, *15*, 627-634.
19. Mechref, Y., Ostrander, G. K. and El Rassi, Z., *J. Chromatogr. A*, **1995**, *695*, 83-95.
20. Mechref, Y., Ostrander, G. K. and El Rassi, Z., *Electrophoresis*, **1995**, *16*, 1499-1504.
21. Mechref, Y. and El Rassi, Z., *Anal. Chem.*, **1996**, *68*, 1771-1777.
22. El Rassi, Z., Postlewait, J., Mechref, Y. and Ostrander, G. K., *Anal. Biochem.*, **1997**, *244*, 283-290 .
23. Hase, S., in *Carbohydrate Analysis: High Performance Liquid Chromatography and Capillary Electrophoresis* (El Rassi, Z., Ed.), Elsevier, Amsterdam, **1995**, 555-575.
24. El Rassi, Z. and Mechref, Y., *Electrophoresis*, **1996**, *17*, 275-301.
25. El Rassi, Z. and Mechref, Y., in *Capillary Electrophoresis: Theory and Practice* (Camilleri, P.), Ed., CRC Press, Boca Raton, **1998**, 273-362.

26. McGregor, D. L., Mullin, W. J. and Fenwick, G. R., *J. Assoc. Off. Anal. Chem.*, **1983**, *66*, 825-849.
27. Fenwick, G. R., Heaney, R. K. and Mullin, W. J., *CRC Crit. Rev. Food Sci. Nutrition*, **1983**, *18*, 123-201.
28. Schauer, R., *Methods Enzymol.*, **1987**, *138*, 132-161.
29. Smith, C. and Dacombe, C., *J. Sci. Food Agric.*, **1987**, *38*, 141-150.

VITA

Arron Lee Karcher 

Candidate for the Degree Of

Doctorate of Philosophy

Thesis: NOVEL DETECTION APPROACHES FOR CAPILLARY  
ELECTROPHORESIS OF POLLUTANTS AND TOXICANTS

Major Field: Chemistry

Biographical:

Personal Data: Born in Perry, Oklahoma, On July 21, 1972, the son of Jerry and Carol Karcher.

Education: Graduated from Perry High School, Perry, Oklahoma in May 1990; received Bachelor of Science degree in Chemistry from the University of Central Oklahoma, Edmond, Oklahoma in December 1994. Completed the requirements for the Doctorate of Philosophy with a major in Chemistry at Oklahoma State University, May 2000.

Experience: Worked two years for Techrad Environmental as an undergraduate; employed by Oklahoma State University, Department of Chemistry as a graduate student; employed by the Environmental Institute at Oklahoma State University as a graduate research assistant, July 1998 to January 2000.

Professional Memberships: Phi Lambda Epsilon, American Chemical Society